Engineering advances are continually changing medical practice. Therefore, it is incumbent upon us all not only to be aware of the latest developments, but to be part of the development of improved treatments for our patients. The Engineering and Urology Society (EUS) is a venue to present and discuss the latest tools and techniques to diagnose and treat urologic pathology. It also serves as a forum where individuals from academia, industry and clinical practice can discuss challenges and formulate ideas for new approaches and tools.

The EUS holds its 24th annual meeting on Saturday, April 25th, 2009 in Chicago, IL. Program Chair are Dr. Manoj Monga and Dr. Hessel Wijkstra, who put together numerous informative and innovative sessions.

The main body of the program includes two sessions on 'what a urologists needs to know about Novel Engineering' with an emphasis on advanced imaging and minimal invasive treatments. The outline of this program is fueled by the rapid change in the paradigm of treatment of oncologic urological diseases and especially in renal and prostate carcinoma. With the increasing number of early detected cancers, the treatment shifts from radical curative treatment to curative organ preserving treatment. This year's contribution of the European society ESUT is related to 'Endoscopic Training'. High profile cases of medical and surgical errors have sensitized the public and the medical professionals all over the world while an extraordinary development of Minimally Invasive Technologies has taken place. These two facts, mainly, have lead to a serious questioning of the classical surgical training program and the search for new formulas to be implemented in the 'old' training programs. In the current urological scenario conventional open surgery coexists with endoscopy, laparoscopy and more recently with robot assisted laparoscopic surgery. Many procedures are nowadays performed while looking at a monitor and the ability to see and feel tissues directly has been lost. Besides this degradation of the senses, the loss of joints dexterity, the counter-intuitive movement of the instrument due to the fulcrum effect of the abdominal wall, and the necessary acquisition of hand-eye coordination take more time to be learned compared to open surgery. This longer learning curve has presented a challenge to most urologists often hindering the incorporation of endourology or laparoscopy into everyday practice. Different training models have become available including ex-vivo models for training in BPH, endourology and laparoscopy.

The new kids on the block will also be introduced: presentations will address the use of Single Incision Laparoscopy and NOTES. In the afternoon the NOTES working group will meet and discuss in more detail the present and future position of this technology.

The review of the abstracts for the poster sessions was performed online by a group of precisely 100 reviewers from around the world. Each paper received between 18 and 20 independent reviews. We would like to thank the reviewers, listed at the end of this program book, for their constructive comments and essential contribution to the quality of the meeting.

The Best Paper Award was selected for the abstract with the highest review score average. The award goes to Dr. Misop Han and his colleagues for the paper entitled "Tandem-Robot Assisted Laparoscopic Radical Prostatectomy: Clinical Feasibility Study for Neurovascular Bundle Visualization". Because the science reported this year has been overwhelmingly novel and significant, in addition the society presents Outstanding Paper awards for the top 10 ranked abstracts to Drs. Shadie Badaan, David Finley, Timothy Hall, John Kefer, Michael Louie, Pierre Mozer, Richard Pollock, Vijay Rajagopal, Jong Yoon, Dinusha Zbyszewski and their coauthors.

We gratefully thank all reviewers for their hard work, objective scoring, and contribution to the success of the meeting. The society presents Best Reviewer Awards for the online review process, based on the scoring performance and the number of reviews performed. The Best Reviewer Awards are presented to Drs. Ernesto Arada, Mahesh Desai, Brian Eisner, Michael Gong, Hrishikesh Joshi, Kazumi Kamoi, Thomas Lawson, and, for the 3rd consecutive year to Dr. Kevin Zorn.

We congratulate all award winners and welcome all urologists, engineers, and scientists to join us for this unique multi and interdisciplinary experience. As always, we are grateful to Dr. George Nagamatsu, the founder and first president of the society for setting the foundations based upon which we meet. May his memory remain a blessing and inspire us to continued innovations in Engineering and Urology.

Please visit the web site of the EUS, http://engineering-urology.org for a complete version of this program including the abstracts presented, which will also be published in the Journal of Endourology. Last two years abstracts were published in the issues January 2008 pages 159-212, and November 2008 pages 2583-2640.

Thank you for your continued scientific support,

Jean de la Rossette
Dan Stoianovici

CONTINUING MEDICAL EDUCATION

Method of Participation and Instructions for Claiming Credits
Please be sure to swipe your Expo card when attending any activity for CME credit.

Disclosure Policy
As a provider accredited by the ACCME, and the American Urological Association Education and Research, Inc., must insure balance, independence, objectivity and scientific rigor in all its activities.

All faculty participating in an educational activity provided by the American Urological Association Education and Research, Inc., are required to disclose to the audience any relevant financial relationships with any commercial interest to the provider. The intent of this disclosure is not to prevent faculty with relevant financial relationships from serving as faculty, but rather to provide members of the audience with information on which they can make their own judgments. The Program Planners and Scientific Planning Committee must resolve any conflicts of interest prior to the commencement of the educational activity. It remains for the audience to determine if the faculty's relationships may influence the educational content with regard to exposition or conclusion. When unlabeled or unapproved uses are discussed, these are also indicated.

Learning Objectives
At the conclusion of this medical education activity participants should be able to:
- Discuss novel technology to treat urologic pathology.
- Assess new urologic techniques and equipment.

Credit Designation
The American Urological Association Education and Research, Inc. designates this educational activity for a maximum of **8.25** ***AMA PRA Category 1 Credit(s)***^{TM}. Physicians should only claim credit commensurate with the extent of their participation in the activity.

Accreditation Statement
The American Urological Association Education and Research, Inc. is accredited by the Accreditation Council for Continuing Medical Education (ACCME) to provide continuing medical education for physicians. The American Urological Association takes responsibility for the content, quality, and scientific integrity of the CME activity.

Unlabeled or Unapproved Use of Drugs or Devices
The audience is advised that one or more presentations in this continuing medical education activity may contain reference(s) to unlabeled or unapproved uses of drugs or devices. Please consult the prescribing information for full disclosure of approved uses. Faculty and speakers are advised to disclose unlabeled or unapproved use of drugs or devices before their presentation or discussion during this activity.

Acknowledgement
The American Urological Association Education and Research, Inc. and the Engineering and Urology Society thanks the following companies for their support of this course: C.R. Bard, Inc., Percutaneous Systems, Inc., GYRUS ACMI, Astellas, Cook Urological

CONTINUING MEDICAL EDUCATION

FACULTY DISCLOSURES:

Abbou, Clement-Claude: Nothing to disclose
Angermeier, Kenneth Wayne: American Medical Systems: Consultant or Advisor
Bischof, John C.: American Medical Systems: Investigator; Sanarus Medical : Consultant or Advisor
Box, Geoffrey N.: Nothing to disclose
Breda, Guglielmo: Nothing to disclose
Cadeddu, Jeffrey Anthony: Ethicon Endosurgery, Inc: Scientific Study or Trial; MedTrials, Inc: Consultant or Advisor
Cleveland, Robin: Nothing to disclose
de la Rosette, Jean: AMS: Consultant or Advisor; BSC: Consultant or Advisor; Galil: Consultant or Advisor
Desai, Mahesh Ramanlal: Nothing to disclose
Desai, Mihir Mahesh: Baxter Inc: Consultant or Advisor; Hansen Medical: Consultant or Advisor
Ebbini, Emad: Nothing to disclose
Fogarty, Thomas: Nothing to disclose
Frede, Thomas: Nothing to disclose
Gettman, Matthew Thomas: Nothing to disclose
Gill, Inderbir Singh: Hansen Medical: Investment Interest
Haber M.D., Georges Pascal: Nothing to disclose
Harisinghani, Mukesh: Nothing to disclose
Joyce, Adrian D.: Nothing to disclose
Kaouk, Jihad H.: Endocare: Meeting Participant or Lecturer; Intuitive surgical: Other: proctoring surgery
Klingler, Christoph H: Nothing to disclose
Laguna Pes, Pilar Maria: Galil: Consultant or Advisor
Liatsikos, Evangelos N.: Nothing to disclose
Lima, Estevao Augusto Rodrigues: Nothing to disclose
McDougall, Elspeth Marguerita: Astellas: Other: Grant funding; Endocare: Other: Unrestricted Grant; Ethicon Endo-Surgery: Other: Equip Support-MIS Educ Center @UCI; Intuitive Surgical: Other: Equip Support-MIS Educ Center @UCI; LapED : Other: Co-Founder/Stock holder; METI, Inc.: Scientific Study or Trial; Simbionix: Other: Equip Support-MIS Educ Center @UCI; Storz Endoscopy: Other: Equip Support-MIS Educ Center @UCI
Michel, Maurice Stephan: No financial compensation: Meeting Participant or Lecturer; University Hospital Mannheim, Germany, Dept. of Urology, University Heidelberg: Meeting Participant or Lecturer
Monga, Manoj: Boehringer-Ingelheim: Meeting Participant or Lecturer; Sanofi-Aventis: Investigator; Stryker: Investigator
Muschter, Rolf: GSK, Starmedtech, AMS, Biolightech, Misonix: Meeting Participant or Lecturer
Piechaud, Thierry: Nothing to disclose
Ponsky, Lee Evan: Accuray: Scientific Study or Trial
Raman, Jay D.: Nothing to disclose
Rane, Abhay: COVIDIEN: Consultant or Advisor
Rao, Pradeep Prabhakar: Nothing to disclose
Rassweiler, Jens: Nothing to disclose
Roberts III, William Woodruff: Terumo Cardiovascular Systems: Consultant or Advisor
Stoianovici, Dan: Nothing to disclose
Timm, Gerald: American Medical Systems: Investment Interest; Amgen: Investment Interest; Boston Scientific: Investment Interest; GT Urological, LLC: Owner; Medtronic: Investment Interest; Pfizer: Investment Interest; Synovus: Investment Interest; Uroplasty: Investment Interest
Trabulsi, Edouard John: Intuitive Surgical: Meeting Participant or Lecturer
van Velthoven, Roland F.P.: Nothing to disclose
Wijkstra, Hessel: Nothing to disclose

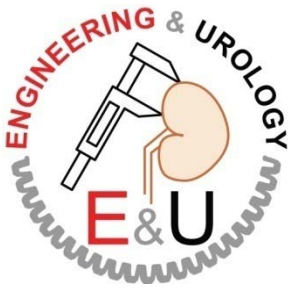

24th Annual Meeting

Saturday, April 25th, 2009
Monroe Ballroom, Palmer House Hilton
Chicago, IL

Program Chair: Manoj Monga, Hessel Wijkstra

7:00 AM	**Registration**	
7:30 – 9:30	**Novel Engineering: What a Urologist Needs to Know**	Christoph Klingler Manoj Monga
7:30 AM	Innovative Urology	Gerry Timm
7:45 AM	HIFU – How It Functions, Urology	Emad Ebbini
8:00 AM	Cryo Bio	John Bischof
8:15 AM	Taking the Mystery out of Histotripsy	William Roberts, III
8:30 AM	SWL – Science with Lithotripsy	Robin Cleveland
8:45 AM	NOTES I: Single Incision Laparoscopy	Jeffrey Cadeddu
9:00 AM	NOTES II: Notes, Novel Technology	Matthew Gettman
9:15 AM	State of the Art: Stents	Evangelos Liatsikos
9:30 – 10:35	**ESUT Session – Endoscopic Training in Europe**	Roland van Velthoven Jean de la Rosette Jens Rassweiler
9:30 AM	Adaption of Training after Introduction of New Technology - A European Survey	Claude Abbou
9:40 AM	Integration of Skills Acquisition in the Curriculum of Urologic Training	Pilar Laguna Adrian Joyce
9:48 AM	Virtual and Augmented Reality in Training	Thierry Piechaud
9:56 AM	Ex-Vivo Models for Training in Endourology	Guglielmo Breda
10:04 AM	Ex-Vivo Models for Management of BPH	Rolf Muschter
10:12 AM	Ex-Vivo Models for Training in Laparoscopy	Thomas Frede
10:20 AM	High versus Low Fidelity Training Models (Counter Debate)	Elspeth McDougall Maurice-Stephan Michel
10:35–11:45	**Novel Engineering: What's Hot?**	Pilar Laguna Hessel Wijkstra
10:35 AM	Innovations in the Ultrasound Detection of Prostate Cancer	Edouard Trabulsi
10:50 AM	Functional Ultrasound Imaging in Follow-up of Minimal Invasive Therapies	Jean de la Rosette
11:05 AM	Endourological Imaging	Mahesh Desai
11:20 AM	Needle Ablative Techniques: Prostate & Kidney	Inderbir Gill
11:35 AM	Reflections	
11:45–12:00	**Awards Presentation**	Dan Stoianovici
11:50AM	Tandem-Robot Assisted Laparoscopic Radical Prostatectomy: Clinical Feasibility Study for Neurovascular Bundle Visualization	Misop Han

12:00–1:00PM	**Lunch** (Adams Ballroom) *Key Note Lecture*: Challenge in Medical Innovation–Bringing Creativity to Practice	 Thomas J. Fogarty
1:00–4:30PM	**Single Port Laparoscopy and NOTES**	Jihad Kaouk Matthew Gettman
1:00PM	*Key Note Lecture*: Minimally Invasive Surgery: The Past, Present and Future	 Ralph Clayman
1:20PM	LESSCAR Consortium	Inderbir Gill
1:30PM	Training for Single Site Surgery	Jay Raman
1:40PM	Robotic Applications for Single Port Surgery	Jihad Kaouk
1:50PM	Transvesical Single Port Surgery	Mihir Desai
2:00PM	Round Table Discussion on Instrumentation for Single Port Surgery: - Scopes - Magnets/Retractors - Ports - Robotics - Needlescopic - Flexible Instruments	 Estevao Rodrigues de Lima Jay Raman Pradeep Rao Georges-Pascal Haber Lee Ponsky Abhay Rane
2:30PM	Point-Counter-Point: Standard Laparoscopy vs. Single Port: - Standard Laparoscopy - Single Port	 Arieh Shalhav Abhey Rane
3:00PM	NOTES: - Current Status of Future Directions - Workshops and Training for NOTES	 Geoff Box Lee Ponsky
3:30PM	Urology NOTES Working Group Business Meeting	

POSTER SESSIONS:

1:00–2:30PM	**Poster Session 1**	– Session 1A (Grant Park Parlor Room)	Misop Han Pierre Mozer
		– Session 1B (Hancock Parlor Room)	Mohamed Allaf Kevin Zorn
3:00–4:30PM	**Poster Session 2**	– Session 2A (Grant Park Parlor Room)	Li-Ming Su Thomas Polascik
		– Session 2B (Hancock Parlor Room)	William Roberts Peter Pinto

POSTER SESSION 1A

1:00 PM – 2:30 PM
Grant Park Parlor Room

Misop Han
Pierre Mozer

No.	Title	Presenting Author
1	TISSUE EFFECTS OF GREENLIGHT HPS™ and EVOLVE SLV™ LASERS ON CANINE PROSTATES: AN ACUTE *IN VIVO* MODEL	Massimiliano Spaliviero
2	SOLIDFLEX NEW TECHNOLOGY ENDOSCOPE. ENGINEERING FEATURES AND PRELIMINARY PROTOTYPE RESULTS	J. A. Campos
3	PROSTATE HISTOTRIPSY IN AN ACUTE ANTICOAGULATED CANINE MODEL	Jeffery C. Wheat
4	METABOLIC STONES: HOW RELIABLE ARE STONE ANALYSIS RESULTS?	Amy E. Krambeck
5	THREE-PORT ROBOTIC UROLOGIC SURGERY WITHOUT A LAPAROSCOPIC BEDSIDE ASSISTANT	Gregory Lowe
6	COMPARATIVE EFFECTS OF HISTOTRIPSY ON CANINE AND HUMAN PROSTATE TISSUE	Jeffery C. Wheat
7	NOTES (Natural Orifice Translumenal Endoscopic Surgery) RENAL CRYOABLATION IN THE PORCINE MODEL	Sebastien Crouzet
8	PRESSURE MODULATION WITHIN A FLUID STORAGE MODEL TO ATTENUATE PRESSURE PULSES	Jeffrey A. Snyder
9	2-D SEGMENTATION OF OCT PROSTATE IMAGES	Shahab Chitchian
10	ROBOTIC ASSISTED MICROSURGICAL VARICOCELECTOMY	Larry Yeung
11	TANDEM-ROBOT ASSISTED LAPAROSCOPIC RADICAL PROSTATECTOMY: CLINICAL FEASIBILITY STUDY FOR NEUROVASCULAR BUNDLE VISUALIZATION	Misop Han **Best Paper Award**

12	PERIURETHRAL NEUROMUSCULATURE STIMULATION IN REDUCING VOIDING FREQUENCY: A RAT STUDY	Yingchun Zhang
13	MODELING AND SIMULATION FOR FLEXIBLE URETEROSCOPY	Vijay Rajagopa **Outstanding Paper Award**
14	SINGLE-PORT LAPAROSCOPIC PARTIAL NEPHRECTOMY	Ricardo Brandina
15	NOTES™ TRANSVAGINAL NEPHRECTOMY USING A NOVEL QUAD-PORT AND LAPAROSCOPIC INSTRUMENT	Monish Aron
16	THE Wii™ TRANSRECTAL ULTRASONOGRAPHY SIMULATOR	Yunhe Shen
17	PROSPECTIVE COMPARISON OF NOVEL BACKLOADING AND STANDARD BIOPSY DEVICES FOR THE DIAGNOSIS OF UPPER TRACT TRANSITIONAL CELL CARCINOMA	Rhonda Walsh
18	AN ACUTE *IN VIVO* PORCINE STUDY TO CHARACTERIZE THE OCCLUSION OF A NOVEL METAL URETERAL STENT	Michael K. Louie
19	*IN VITRO, EX VIVO,* AND *IN VIVO* ISOTHERMS FOR RENAL CRYOTHERAPY	J.L. Young
20	A NOVEL PROXIMITY-SENSING STENT TO ASSIST NON-UROLOGICAL SURGEONS WITH INTRAOPERATIVE IDENTIFICATION OF THE URETER	John C. Kefer **Outstanding Paper Award**

POSTER SESSION 1B

1:00 PM – 2:30 PM
Hancock Parlor Room

Mohamed Allaf
Kevin Zorn

21	A NOVEL MEANS OF LOW COST, OFFICE-BASED ENDOSCOPY	Nicholas J. Hellenthal
22	NEPHRON-SPARING SURGERY USING THE AQUAMANTYS 6.0 BIPOLAR SEALER	Jason Kim
23	IS ULTRASOUND IMAGING HELPFUL IN PREDICTING EXTRACAPSULAR PENETRATION IN PROSTATE CANCER?	Charalampos Mamoulakis
24	THE SIGNIFICANCE OF ACCURATE SHOCK WAVE COUPLING IN EXTRACORPOREAL SHOCK WAVE LITHOTRIPSY	Thorsten Bergsdorf
25	INCREASED ESWL FRAGMENTATION OF STONES WITH THE USE OF THE ACCORDION DEVICE: *In Vitro* and *Ex Vivo* RESULTS	Joseph V. Di Trolio
26	PUBO-URETHRAL PEXY FACILITATES AND IMPROVES RESULTS IN RADICAL ROBOTIC PROSTATECTOMIES	Joseph V. Di Trolio
27	DEVICE AND METHOD FOR MINIMALLY INVASIVE URODYNAMIC ASSESSMENT IN MEN	João C.M. de Almeida
28	METHOD FOR URETER LOCALIZATION IN MINIMALLY INVASIVE SURGERY	David M. Kwartowitz
29	ARE MULTIPLE CRYOPROBES ADDITIVE OR SYNERGISTIC IN RENAL CRYOTHERAPY?	J.L. Young
30	NOTES AND SINGLE PORT SURGERY: WHAT DO PATIENTS WANT?	David Canes
31	DOES NEEDLE SPINNING IMPROVE TARGETING PRECISION?	Shadie Badaan **Outstanding Paper Award**
32	IDENTIFICATION OF OPTIMAL LASER FIBER MOVEMENT FOR PHOTO-SELECTIVE VAPORIZATION OF THE PROSTATE IN AN *EX VIVO* ANIMAL MODEL	Eric C Kauffman

33	ROBOTIC LAPAROENDOSCOPIC SINGLE SITE SURGERY USING GELPORT AS THE ACCESS PLATFORM	Robert J. Stein
34	PRELIMINARY INVESTIGATIONS OF IRREVERSIBLE ELECTROPORATION (IRE) IN *IN VIVO* PORCINE KIDNEYS: ABLATION WITHOUT HEAT	Raymond J. Leveillee
35	A COMPARATIVE STUDY BETWEEN NOVEL AIR-CUSHION PROBE AND WHEELED PROBE FOR MIS	Dinusha Zbyszewski **Outstanding Paper Award**
36	ENZYMATIC DISSOLUTION OF CALCIUM AND STRUVITE CRYSTALS: AN *IN VITRO* EVALUATION OF BIOCHEMICAL REQUIREMENTS	Nabil K. Thalji
37	STEREOTACTIC PERCUTANEOUS CRYOABLATION FOR RENAL TUMOR: INITIAL CLINICAL EXPERIENCE	Georges-Pascal Haber
38	ROBOTIC VERSUS LAPAROSCOPIC PARTIAL NEPHRECTOMY: A SINGLE SURGEON MATCHED COMPARISON OF 100 CASES	Georges-Pascal Haber
39	LAPAROENDOSCOPIC SINGLE SITE (LESS) SURGICAL TOOLBOX: INSTRUMENTS, SCOPES, AND PORTS	Georges-Pascal Haber
40	*IN VITRO* TEST OF AN AUTOMATED CYSTOSCOPIC PROCEDURE FOR BLADDER SURVEILLANCE	W. Jong Yoon **Outstanding Paper Award**

POSTER SESSION 2A

3:00 PM – 4:30 PM
Grant Park Parlor Room

Li-Ming Su
Thomas Polascik

41	A THERM-SENSITIVE REMOVABLE METALLIC PROSTATE STENT FOR THE MANAGEMENT OF BLADDER OUTFLOW OBSTRUCTION (BOO)—EXPERENCE FROM THREE CENTERS IN TWO COUNTRIES	A.G. Papatsoris
42	ROBOTIC INSTRUMENT INSULATION FAILURE: INITIAL REPORT OF A POTENTIAL SOURCE FOR PATIENT INJURY	Adam C. Mues
43	MICROFABRICATION OF HEAT-SENSITIVE MICROBUBBLES FOR ABLATION MARGIN ASSESSMENT	Jiwei Huang
44	ICE BURN: PROTECTING THE FLANK DURING RENAL CRYOTHERAPY	Jennifer L. Young
45	ANALYSIS OF INFECTIOUS STONES: VARIABILITY OF LABORATORY ANALYSIS	Amy E. Krambeck
46	DRILLING THROUGH THE IMPACTION: POSSIBLE USE OF AN ATHERECTOMY DRILLING DEVICE FOR UROLITHIASIS	David A. Lifshitz
47	SHOCK WAVE ADMINISTRATION RATE – IS SLOWER REALLY BETTER?	Thorsten Bergsdorf
48	BOVINE SERUM ALBUMIN GLUTARALDEHYDE FOR COMPLETELY SUTURELESS LAPAROSCOPIC PARTIAL NEPHRECTOMY IN A UNIQUE SURVIVAL PORCINE MODEL	Michael K. Louie
49	INTRAVESICAL PROSTHETIC MATERIALS: *IN VITRO* AND *IN VIVO* (RABBIT) ENCRUSTATION AND BIOCOMPATIBILITY	D. Pick
50	VESICAL MICTURITION MODIFIED CYSTOMETRY: AN INNOVATIVE WAY TO DECREASE PAIN ON CATHETER REMOVAL	Michael Eufemio Macalalag
51	ULTRASOUND TO FACILITATE CLEARANCE OF RESIDUAL STONES	Anup Shah
52	PRIMARY FIXATION OF MINI SLINGS: A COMPARATIVE STUDY *IN VIVO*	Paulo Palma

53	SINGLE-PORT VERSUS STANDARD LAPAROSCOPIC DONOR NEPHRECTOMY: MATCHED-PAIR COMPARISON	David Canes
54	USE OF A NOVEL ANTIRETROPULSION DEVICE REDUCES STONE FRAGMENT MIGRATION AND SIGNIFICANTLY INCREASES THE EFFICIENCY OF PNEUMATIC LITHOTRIPSY: AN *IN VITRO* STUDY	Brian H. Eisner
55	IS ROBOTIC PROSTATECTOMY SAFE IN ASIAN ELDERLY PERSONS OVER 75 YEARS OLD? COMPARISION OF PERIOPERATIVE DATA	Wooju Jeong
56	FUTURE PROSPECTS IN PERCUTANEOUS ABLATIVE TARGETING: COMPARISON OF A ROBOTIC AND COMPUTER-ASSISTED NAVIGATION	Richard Pollock **Outstanding Paper Award**
57	LAPARO-ENDOSCOPIC SINGLE SITE (LESS) SURGERY: FIRST 100 CASES	Mihir Desai
58	THE IMPACT OF A URETERAL STENT AND A FOLEY CATHETER ON RENAL PELVIC PRESSURES IN THE *IN VIVO* PORCINE MODEL	Michael K Louie **Outstanding Paper Award**
59	AirSeal™ VALVE-LESS TROCAR FOR UROLOGIC LAPAROSCOPY: AN INITIAL EVALUATION	Amin S. Herati
60	REGIONAL HYPOTHERMIA DURING ROBOTIC RADICAL PROSTATECTOMY USING AN ENDORECTAL COOLING BALLOON TO IMPROVE URINARY CONTINENCE	David S. Finley **Outstanding Paper Award**

POSTER SESSION 2B

3:00 PM – 4:30 PM
Hancock Parlor Room

William Roberts
Peter Pinto

61	IMPACT OF PNEUMOPERITONEUM ON ICEBALL SIZE IN RENAL CRYOTHERAPY	Jennifer L. Young
62	THE NEW Invisio® DUR-D "chip-on-the-tip" URETEROSCOPES—EVALUATION OF CHANGES IN PHYSICAL PROPERTIES OVER TIME	T. El-Husseiny
63	ACOUSTIC RADIATION FORCE IMPULSE (ARFI) IMAGING OF HUMAN PROSTATE *IN VIVO*	Vladimir Mouraviev
64	MOLECULAR IMAGING OF PROSTATE CANCER *IN VIVO* USING A TARGETED CONTRAST AGENT IN INTERMOLECULAR MULTIPLE-QUANTUM COHERENCES MRI EXPERIMENTS	Vladimir Mouraviev
65	ANTI-RETROPULSION DEVICES INCREASE STONE FRAGMENTATION EFFICIENCY WITH HOLMIUM:YAG LASER LITHOTRIPSY	Lee M. Jonat
66	*IN VIVO* URETERAL AND VESSEL SEALING ACHIEVED WITH ENERGY BASED SEALING DEVICES IN THE ACUTE PORCINE MODEL	Michael K Louie
67	SEMI-AUTOMATIC SEGMENTATION OF PROSTATE ULTRASOUND IMAGES USING SHAPE PRIORS	Kevin Dowlut
68	SYRINGE WITH SPIRAL TIP USED IN BOTULINUM TOXIN A INJENCTON FOR TREATING LOWER URINARY TRACT DYSFUNCTION	Chung Cheng Wang
69	LAPAROSCOPIC VERSUS PERCUTANEOUS RENAL CRYOABLATION	Sebastien Crouzet
70	SINGLE PORT – SINGLE SURGEON ROBOTIC-ASSISTED LAPAROSCOPIC UROLOGIC SURGERY	Sebastien Crouzet
71	3D ULTRASOUND IMAGE GUIDED FIXED PLATFORM TRANS-RECTAL PROSTATE BIOPSY	Sijo J. Parekattil
72	ANALYSIS OF ACOUSTIC ACCESS TO THE PROSTATE THROUGH THE PERINEUM FOR NON-INVASIVE HISTOTRIPSY THERAPY	Timothy Hall **Outstanding Paper Award**

73	PHYSICAL CHARACTERISTICS OF FOLEY CATHETERS	Kari Hendlin
74	ROBOTIC ASSISTED MICROSURGICAL DENERVATION OF THE SPERMATIC CORD	Sijo J. Parekattil
75	6-DOF HAPTIC MASTER FOR ROBOTIC LAPAROSCOPIC SURGERY	Felix Schäfer
76	*IN VITRO* EVALUATION OF THE EFFECT OF COLOR ON IDENTIFICATION OF URINARY TRACT CATHETERS IN A HEMORRHAGIC ENVIRONMENT	Zhamshid Okhunov
77	THE SOLO-SURGEON VAMS DONOR NEPHRECTOMY	Young Seung Lee
78	ROBOTIC RADICAL PROSTATECTOMY: TRANSVESICAL APPROACH	Andre Berger
79	A NOVEL UNIFIED SPATIAL FORMULATION METHOD FOR MODELING 1/2/3-DIMENSIONAL OBJECTS IN REAL TIME FOR SURGICAL SIMULATION	Nan Zhang
80	FREE HAND 3D-TRUS PROSTATE BIOPSY MAPPING	Pierre Mozer **Outstanding Paper Award**

ABSTRACT 1

TISSUE EFFECTS OF GREENLIGHT HPS™ and EVOLVE SLV™ LASERS ON CANINE PROSTATES: AN ACUTE *IN VIVO* MODEL

Massimiliano Spaliviero, Roman Wolf, Stanley Kosanke,
Marie Chavez-Suarez, Fred Broach, Motoo Araki, Carson Wong

University of Oklahoma Health Sciences Center, Oklahoma City, OK, USA

Introduction: We evaluate the tissue effects and efficacy of the GreenLight HPS™ and Evolve SLV™ lasers for prostate vaporization in living dogs.

Methods: Prostate vaporization was performed either with GreenLight HPS™ (Group I) or Evolve SLV™ (Group II) systems. 40 kJ of energy were delivered with both systems on canine prostates. Dogs were euthanized 2 hours following completion of prostate vaporization and prostates were excised *en bloc*. The volume of vaporized tissue was determined by taking multiple measurements of the 3-dimensional cavity. Prostates were then sectioned (3-5 mm) and stained with triphenyltetrazolium chloride (TTC) and nitroblue tetrazolium (NBT) to establish the thickness of necrotic and healthy tissue zones.

Results: 5 (I) and 5 (II) consecutive mongrel dogs underwent prostate vaporization. Mean age (I: 9±1, II: 8±1 years) and weight (I: 25±1, II: 28±3 kg) were similar between the two groups. Despite similar energy utilization (I: 40.0±0.4, II: 40.0±0.1 kJ), laser time was shorter in Group II (I: 359±19, II: 269±1 seconds, $p<0.001$). Measurement of the vaporization cavity revealed it to be comparable (I: 3.06±1.52, II: 1.73±0.41 mL, $p=0.18$). However, the depth of thermal necrosis was thicker in Group II (TTC: I: 2.1±0.4, II: 5.8±0.8 mm, $p=0.0002$; NBT: I: 2.6±0.8, II: 3.9±1.0 mm, $p=0.07$) prostate specimens.

Conclusion: Despite the formation of a comparable vaporization cavity, the depth of thermal necrosis was thinner in Group I. This factor may have implications in the clinical outcomes of prostate vaporization in human subjects.

ABSTRACT 2

SOLIDFLEX NEW TECHNOLOGY ENDOSCOPE: ENGINEERING FEATURES AND PRELIMINARY PROTOTYPE RESULTS

J. A. CAMPOS

Hospital Angeles de las Lomas MEXICO

Introduction: The next generation of endoscopy has been designed, incorporating novel features to create a coherent, intuitive and ergonomic exploratory instrument for the obscured portions of the human cavities.

Methods: This new teaching's shaft, has three different elastic properties along with the same diameter; a first proximal rigid or semirrigid section, connected to an intermediate passive flexible and subsequently to a distal active flexible segment. In the instrument's resting position, a rotor over an ergonomic handle directs the more distal segment towards right or left which is the same orientation of the intrarrenal urinary system, while the patient is in a decubitus position during exploration (Fig 1, 2). This coherent motion during instrumentation provides intuitiveness (instinctive perception).

Results: Manufacturing of the endoscope is state of the art in design and engineering, it allows the surgeon to be comfortably seated, it weights half the average of a flexible ureteroscope or a cystoscope (Fig 2), it also accommodates easily inside the urinary system allowing one hand simple reach of every area in the urinary system including the lower pole of the kidney (Fig. 3). The surgeon alone controls both instrument and operating accessories such as the nytinol basket for stone retrieval. The prototype has been utilized in 9 patients and 11 renal units with outstanding results.

Conclusion: This revolutionary development can also be utilized in a cystoscope, nephroscope, robotics, and natural orifice transluminal endoscopic surgery (NOTES). Full HD videos and mechanical drawings will be shown.

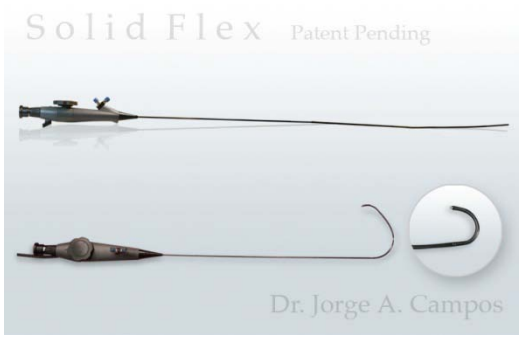

Fig. 1

Fig. 2

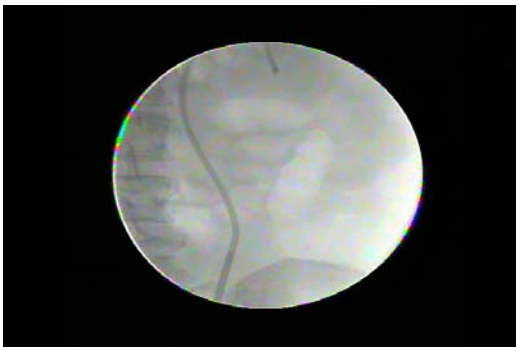

Fig. 3

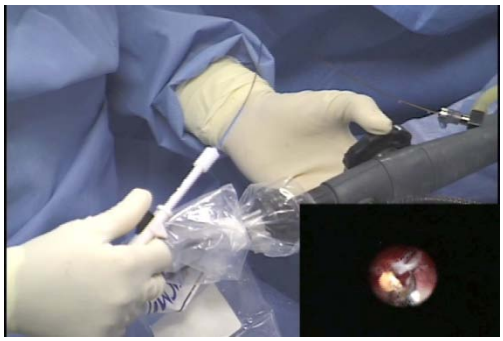

Fig. 4

ABSTRACT 3

PROSTATE HISTOTRIPSY IN AN ACUTE ANTICOAGULATED CANINE MODEL

Jeffery C. Wheat[1], Timothy L. Hall[1], Christopher R. Hempel[1], William W. Roberts[1,2]
Departments of Urology[1] and Biomedical Engineering[2], University of Michigan

Introduction: Histotripsy is a non-invasive ultrasound technology which produces microbubbles (cavitation) causing mechanical tissue fractionation. Early canine models noted minimal hematuria despite significant prostatic debulking. In the current study, we seek to evaluate the safety of prostate histotripsy in an anticoagulated canine model.

Methods: Histotripsy was performed in vivo on 9 canine subjects pre-treated with 6 mg of oral warfarin for 3-5 days using an extracorporeal 750 kHz therapeutic ultrasound transducer delivering acoustic pulses to the prostatic urethra and periurethral parenchyma. A 12 French urinary catheter was removed 1 day following treatment. After 7-28 days, the subjects were euthanized, transrectal prostate ultrasound was performed and the prostate was harvested. Serum hemoglobin and International Normalization Ratio (INR) were measured immediately prior to histotripsy treatment and at euthanasia.

Results: Mean treatment INR was 4.6 (median 2.4, range 1.2 to 11.3) with 2 of 9 subjects failing to achieve therapeutic levels. There was no overall change in hemoglobin at euthanasia compared to baseline. At harvest, gross sections revealed a large cavity corresponding to the planned treatment volume incorporating the prostatic urethra and parenchyma in all subjects (Figure 1). Urine was clear within 2 days of treatment and no clots were seen in any of the subjects.

Conclusion: Despite supratherapeutic oral anticoagulation, no clinically significant blood loss was noted with fractionation of the prostatic urethra and parenchyma. Future research is planned to explore the mechanism of hemostasis seen with histotripsy.

Figure 1: Gross and microscopic photographs of prostate 7 days after histotripsy treatment in a subject whose INR was 11.3 at the time of treatment. Necrotic debris in the urethral cavity and a small amount of parenchymal hematoma are noted.

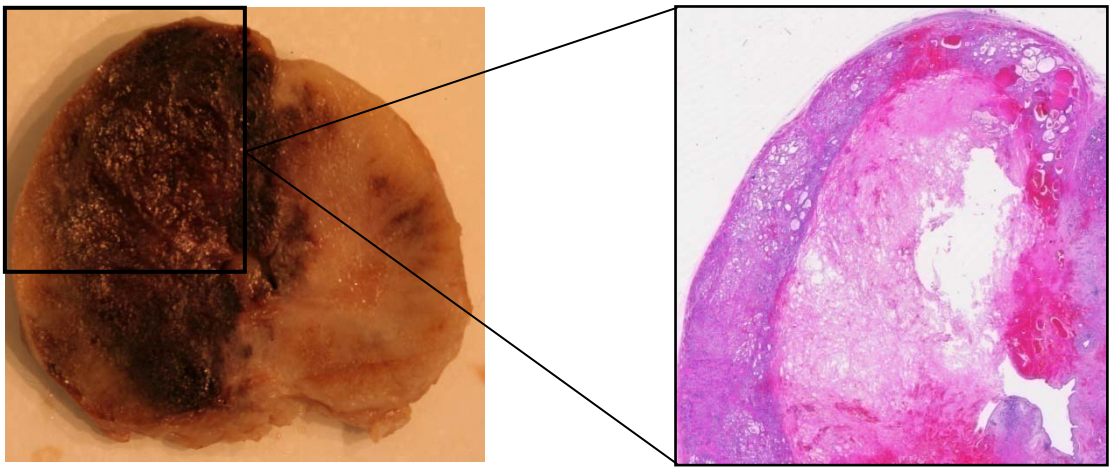

ABSTRACT 4

METABOLIC STONES: HOW RELIABLE ARE STONE ANALYSIS RESULTS?

Amy E. Krambeck[1], Naseem F. Khan[2], Molly E. Jackson[2], James E. Lingeman[1], James C. Williams, Jr.[2]

[1]Methodist Hospital Institute for Kidney Stone Disease [2]Indiana University School of Medicine Indianapolis, Indiana

Introduction: The accuracy of stone composition analysis is not only important in guiding clinical treatment decisions, but also for research that assesses the association of stone composition with pathophysiology of stone disease, treatment outcomes, and long-term disease progression. The goal of this study was to determine the accuracy of stone composition analysis by major commercial laboratories.

Methods: Forty-six human renal stones with known compositions determined by infrared spectroscopy (IR) were hand fragmented into six aliquots and studied with micro computed tomography (CT) to ensure similar fragment compositions. Only 26 stones had fragments similar enough to be considered identical. The identical fragments were submitted to 1 research and 5 commercial laboratories for blinded analysis.

Results: All labs agreed on stone composition for the 2 pure uric acid (UA) and 2 cystine stones. For 2 brushite stones all labs reported brushite as the primary component; however, 4 labs also reported secondary components [carbonate apatite (CA), hydroxyapatite (HA), calcium oxalate (CaOx) monohydrate (COM), or calcium oxalate dehydrate (COD)], that did not agree. For the 9 stones composed primarily of CaOx, 3 (33%) stones were not reported as CaOx by a lab; instead they were reported as HA. Of these 9 stones, all labs agreed on the secondary component in only 2 stones, and in only 1 stone was the proportion of COM to COD agreed upon by all labs. For both of 2 mixed UA with COM stones the labs did not agree on the primary or secondary components. For 4 apatite stones, all labs agreed on the primary component in only 1 stone and for 3 stones some, but not all, of the labs reported struvite, ammonium acid urate, and COM as components. Nomenclature for the different forms of apatite differed among labs, with one lab reporting all apatite as CA and never reporting HA, another lab never reporting CA and always reporting HA, and a third lab reporting CA as a percentage of apatite mixed with calcium carbonate.

Conclusion: Commercial laboratories can reliably diagnose pure calculi; however, there is enough variability in both qualitative and quantitative results of mixed calculi to suggest a problem with reproducibility of stone analysis results. Furthermore, there is a lack of standardization of nomenclature used by laboratories. It is difficult to determine the significance of stone components on pathophysiology, as well as for clinical and surgical therapy outcomes, if reported stone compositions can differ according to the laboratory performing the analysis.

ABSTRACT 5

THREE-PORT ROBOTIC UROLOGIC SURGERY WITHOUT A LAPAROSCOPIC BEDSIDE ASSISTANT

GREGORY LOWE, RONNEY ABAZA

Ohio State University Medical Center, Columbus, Ohio

Objective: The role of robotics for renal and upper tract urologic surgery has been called into question in part due to the perceived need for additional bedside-assistant ports beyond those used for laparoscopy and the perceived need for an experienced laparoscopist as the bedside assistant. We review our experience with three-port robotic renal, adrenal and upper tract reconstructive surgery.

Methods: A total of 32 procedures were performed between June 2008 and January 2009 that were accomplished using three ports, including a 12mm robotic scope port and two 8mm robotic instrument ports. No assistant port was placed, nor was a bedside assistant needed beyond the scrub technician. Procedures included four robotic simple nephrectomies with morcellation through the 12mm port site, 14 pyeloplasties, two ureteral reimplantations, one ureteral reconstruction, two adrenalectomies, and nine radical nephrectomies with an extraction incision.

Results: Mean operative times from incision to dressing were 106min for simple nephrectomy, 159min for pyeloplasty, 122min for ureteral reimplantation, 180min for ureteral reconstruction, 70min for adrenalectomy, and 170min for radical nephrectomy with lymphadenectomy. During the same time period four radical nephrectomies were performed with a four port approach. These were due to a 19 cm renal mass requiring retraction with the robotic fourth arm in one, liver retraction in one, one planned partial nephrectomy, and one needed for retraction of intra-abdominal fat. Four patients were discharged on the day of surgery and all others the day after surgery. Mean estimated blood loss was 19 mL but was difficult to measure in most cases as no suction was routinely used during the procedures.

Conclusions: Three-port robotic urologic surgery is feasible. The ability to perform robotic renal surgery without a bedside assistant experienced in laparoscopy is encouraging, particularly as single-port or natural-orifice robotic surgery becomes possible. Three port robotic surgeries may facilitate a transition to NOTES or single port procedures that limit an assistant. We demonstrate that pyeloplasties, adrenalectomies, ureteral reimplantation and ureteral reconstruction can all be done without an assistant. In the majority of cases, robotic assisted radical nephrectomy may also be accomplished without an assistant port; however some intra-operative techniques are beneficial to improve this approach. We routinely place the patient in 90 degree flank position and have learned to retract the liver utilizing the working robotic arm. The cost benefit of assistant-less robotic surgery may make robotic surgery more profitable and cost-effective for both hospitals and physicians. Further studies are needed to define which radical nephrectomy cases may benefit from the presence of an accomplished assistant.

ABSTRACT 6

COMPARATIVE EFFECTS OF HISTOTRIPSY ON CANINE AND HUMAN PROSTATE TISSUE

Jeffery C. Wheat[1]; Timothy L. Hall[1]; Charles Cain[2]; Zhen Xu[2]; William W. Roberts[1,2]
Departments of Urology[1] and Biomedical Engineering[2], University of Michigan

Introduction: Histotripsy is a non-invasive ultrasound technology which produces non-thermal, mechanical fractionation of biologic tissues. We have previously shown that histotripsy can produce significant prostate debulking in a canine model. In the current study, we compared the differential effects of histotripsy on canine and human ex vivo prostate tissue to evaluate the feasibility of future human trials.

Methods: All prostate tissues were stored fresh at 4°C in 0.9% normal saline until histotripsy treatment was performed within 48 hours of harvest. Treatment consisted of a fixed dose of 200,000 pulses delivered to a 1x1 cm rectangular grid centered in the right prostate lobe and encompassing the urethra. The left lobe was left untreated. After treatment the tissue was fixed in formalin for one week and then sectioned for histologic analysis.

Results: A total of three human (ages 29, 47 and 76) and two canine prostates were treated. The human prostates all had more stromal elements whereas the canine prostates were more glandular. In the treated region, a clear area of cellular destruction (including both stromal and glandular elements) was noted in both human and canine tissues (Fig).

Conclusions: Histotripsy is a promising technology which produced significant tissue debulking in pre-clinical studies. In the current study we have shown that the effects of histotripsy are comparable between human and canine tissues despite significant differences in the histologic composition of the glands. Further study is needed to determine whether histotripsy is safe and effective for treatment of BPH in human subjects.

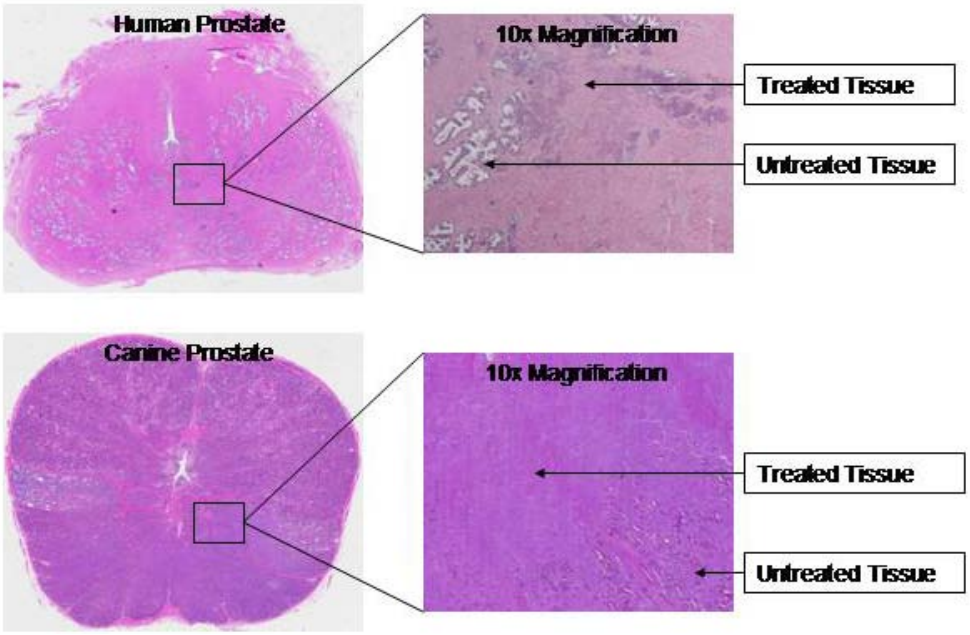

ABSTRACT 7

NOTES (Natural Orifice Translumenal Endoscopic Surgery) RENAL CRYOABLATION IN THE PORCINE MODEL

Sebastien Crouzet, Georges-Pascal Haber, Kazumi Kamoi, Stacy Brethauer, Patrick Gatmaitan, Jihad Kaouk

Section of Laparoscopic and Robotic Surgery, Glickman Urological and Kidney Institute
Cleveland Clinic, Cleveland, Ohio

Introduction: We present our initial laboratory experience with natural orifice translumenal endoscopic surgery (NOTES) renal cryoablation.

Methods: In 2 female farm pigs, we performed 4 NOTES renal cryoablation. In each animal we performed 1 transgastric approach and 1 transvaginal approach. The animal is placed in the flank position and pneumoperitoneum obtained using a transabdominal Veress® needle. In the first animal, we started on the left kidney with a transgastric approach: a dual-channel video gastroscope (Olympus, Tokyo, Japan) was used, the stomach wall was punctured using a needle-knife, a guide wire was passed into the abdominal cavity and the access dilated using a controlled radial expansion balloon. The bowel was mobilized medially and the Gerota's fascia overlying the upper pole was dissected. Under direct endoscopic vision, a cryoablation probe was introduced percutaneously into the anterior upper pole of the kidney. Then the animal is flipped and a transvaginal approach is used for the right side: the gastroscope is introduced through the posterior fornix of the vagina in a similar transgastric fashion and the procedure was performed. For the second animal, we performed initially a transgastric right side cryoablation then a transvaginal left side cryoablation: as described in the first animal.

Results: All 4 procedures were performed successfully. No intraoperative complication was observed. No additional laparoscopic port or open conversions were necessary. The vision of the kidney and the ice-ball were excellent. Mean operative time was 82.75 min. The stomach closure was watertight, and no abdominal or pelvic injuries were found at autopsy.

Conclusion: NOTES can provide adequate minimal surgical dissection for safe and effective percutaneous renal cryoablation under direct videoscopic monitoring at kidney locations otherwise not accessible percutaneously. Both transgastric and transvaginal approaches can be used effectively to perform renal cryoablation providing a minimally-invasive scarless surgery.

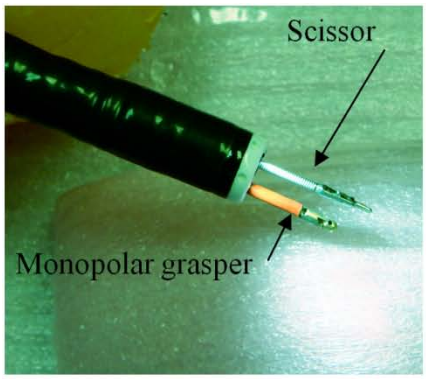

Figure 1: Endoscopic instruments

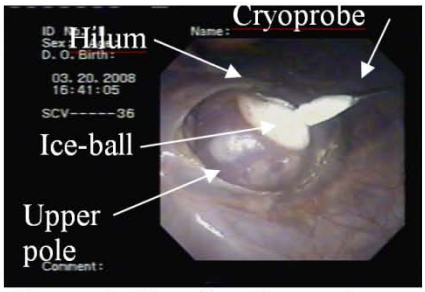

Figure 2: First freezing cycle

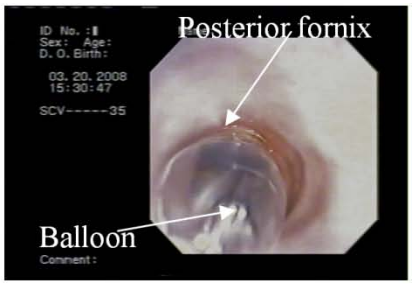

Figure 3: dilatation with a controlled radial expansion balloon

ABSTRACT 8

PRESSURE MODULATION WITHIN A FLUID STORAGE MODEL TO ATTENUATE PRESSURE PULSES

Jeffrey A. Snyder[1], Peter L. Dayton[2]

[1]*Genitourinary Surgical Consultants, Denver, CO,* [2]*Solace Therapeutic, Inc. Newton, MA*

Introduction Stress urinary incontinence (SUI) is a pervasive problem amongst women. Treatment options run the gamut from non-invasive therapies to surgeries. SUI consists of the involuntary loss of urine that occurs as a result of activity that increases pressure within the bladder. To date, most therapies increase the urethral outlet resistance. An alternative therapy is to increase the effective bladder compliance to reduce pressure spikes during activity. We have developed a novel experimental model to demonstrate attenuation of pulse spikes within the storage component of a fluid filled device.

Theory By placing a detachable balloon device filled with a compressible gas within a storage vessel filled with an incompressible liquid, we will demonstrate the attenuation of pressure during a short phase pressure pulse.

Method A controlled water-filled chamber was subjected to 80 millisecond pulse pressure spikes of 141 cm H_2O (2 psi). A gas-filled balloon was inserted into the chamber and was challenged by the same pulse pressure. Repetitive controlled trials were performed with balloons filled with 0ml, 5ml, 10ml, 15ml, 20ml, and 25ml of gas.

Results As demonstrated in Figure 1, the reduction in peak pressure is proportional to the volume of the compressible gas in the balloon. Incremental increases in the absolute volume of a compressible gas within a liquid environment caused a measurable and reproducible attenuation of reservoir pressure during these short duration, high intensity pressure spikes.

Discussion This laboratory model demonstrates pressure modulation within a fluid filled reservoir similar to a human bladder. By adding a gas-filled balloon, we have shown attenuation of extrinsic pressure spikes as a result of the shock absorber property of the balloon. It is proposed that in the analogous human model, although the bladder is a distensible storage vessel with its own inherent compliance, that a gas-filled balloon will further attenuate pressure spikes exerted on it by coughing, sneezing, or other extrinsic pressures thereby reducing leakage as observed with SUI. A prospective randomized controlled clinical trial is currently in progress.

The experiment was funded by Solace Therapeutics, Inc.

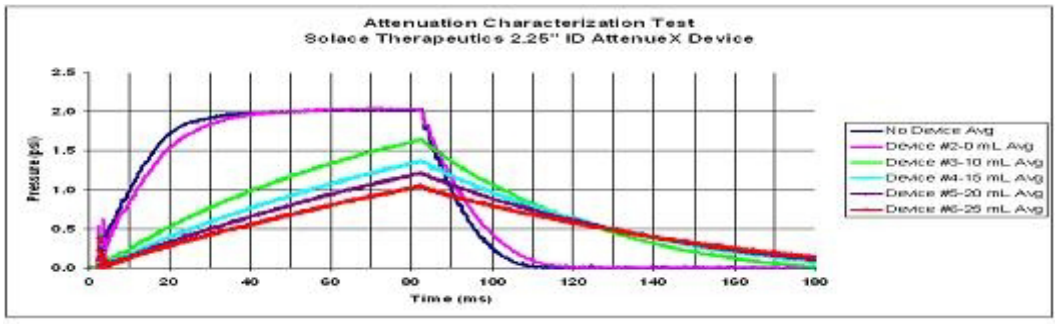

ABSTRACT 9

2-D SEGMENTATION OF OCT PROSTATE IMAGES

Shahab Chitchian[1], Thomas P. Weldon[2], and Nathaniel M. Fried[1,3]

[1] *Department of Physics and Optical Science, University of North Carolina, Charlotte, NC*
[2] *Department of Electrical and Computer Engineering, University of North Carolina, Charlotte, NC*
[3]*Department of Urology, Johns Hopkins Medical Institutions, Baltimore, MD*

Introduction: The cavernous nerves, which are responsible for erectile function, course along the prostate surface and vary in size and location among patients, making identification and preservation of the nerves difficult during surgical removal of a cancerous prostate gland. Optical coherence tomography (OCT) has recently been tested for high-resolution *in vivo* imaging of the cavernous nerves in both rat and human prostates. However, improvements in the quality of OCT images are necessary before this new technology is suitable for clinical use. In this study, two-dimensional (2D) image segmentation is investigated to differentiate the nerves from the prostate gland.

Methods: 2-D rat prostate images acquired with a clinical endoscopic OCT system are segmented into three regions or classes: background, nerve, and prostate gland. To detect these classes, three image features were employed: Gabor filter, Daubechies wavelet, and Laws filter. The Gabor feature is applied with different standard deviations in the x and y directions. In the Daubechies wavelet feature, 8-tap Daubechies orthonormal wavelet is implemented, and the low pass sub-band is chosen as filtered image. Finally, Laws feature extraction is applied to the images. The features are segmented using a nearest-neighbor classifier. N-ary morphological post-processing is used to remove small voids.

Results: The cavernous nerves were differentiated from the prostate gland using this segmentation algorithm. The overall error rate measured only 0.058 and was obtained by manually creating a segmented image and comparing it to the automatic segmentation.

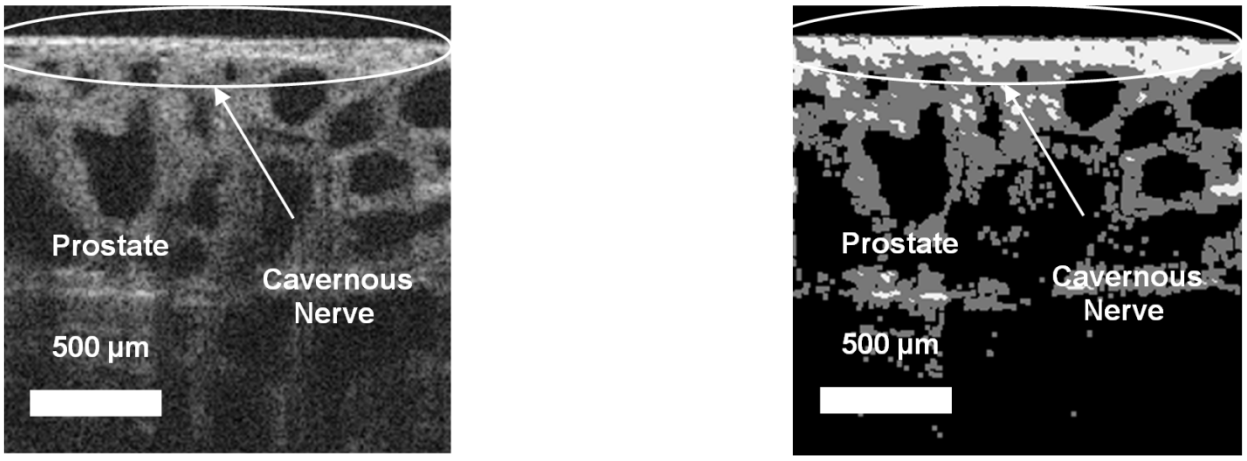

Figure 1. Representative OCT image of the rat cavernous nerve: (a) before; (b) after segmentation, showing the cavernous nerve in white, prostate tissue in gray, and background in black.

Conclusion: This algorithm for image segmentation of the prostate nerves may prove useful for implementation in clinical endoscopic OCT systems currently being explored for potential use in laparoscopic and robotic nerve-sparing prostate cancer surgery.

Acknowledgments: *This work was supported by an Idea Development Award from the Department of Defense Prostate Cancer Research Program, Grant #PC073709.*

ABSTRACT 10

ROBOTIC ASSISTED MICROSURGICAL VARICOCELECTOMY

Larry Yeung, Drew Palmer, Danielle Holland, Nabeel Thalji, Hany Atalah, Benjamin Canales, Marc S. Cohen, Johannes W. Vieweg and Sijo J. Parekattil.
University of Florida, Gainesville, FL

Introduction: Previous studies have shown that robotic assistance may provide technical advantages in microsurgery. Our goal was to compare standard microsurgical varicocelectomy (MVV) to robotic assisted varicocelectomy (RAVx) and present our initial human results.

Methods: A prospective randomized control trial of MVV to RAVx was performed in a canine varicocele model by an experienced surgeon and 4 surgeons of varying training level. Each surgeon performed 10 vein ligations, randomized into 2 arms (5-MVV, 5-RAVx). Procedure duration, vessel injury, knot failure and surgeons' preference for MVV or RAVx for specific tasks were recorded. 16 human RAVx cases from Jun'08-Feb'09 are presented (follow up 1-8 months: mean 3).

Results: There was no significant difference in procedure duration between MVV and RAVx. There were more knot failures in the MVV cases than the RAVx cases. No vessel injury occurred in any case. The learning curve was steeper in the RAVx cases for 3 surgeons (MVV had a steeper curve for the other 2 surgeons). For vessel dissection, 3 of 5 surgeons preferred MVV (since the robotic instruments were not as fine). For knot tying, 3 of 5 surgeons preferred RAVx. In the human series (figure below), mean duration for the RAVx on each side was 42 mins (25-80). 4 cases were bilateral and 11 unilateral. No complications occurred. Indications for the procedures were: 3 patients with azoospermia, 11 with oligospermia and 2 with testicular pain. Sufficient follow up (3 months) is available for 5 patients: 3 with preop oligospermia had significant improvement in sperm counts (one of these achieved a pregnancy), one patient with preop oligospermia has a decrease in count at 3 months post-op and one patient with preoperative azoospermia remains azoospermic. The testicular pain patients both responded to the procedure – one patient had complete resolution of pain, the other only a 50% reduction in pain. The 4th robotic arm allowed the surgeon to control one additional instrument (Potts scissors or Doppler probe for arterial localization) during the cases. This enabled improved surgeon efficiency and less reliance on the microsurgical assistant.

Conclusion: Robotic assisted microsurgical varicocelectomy appears to be a safe procedure. It requires a unique skill set different from microsurgery. There appear to be two types of surgeons: a) a group that learns faster on the robot, ties knots better with the robot and prefers this approach, and b) a group that learns faster on the microscope and prefers this approach. The preliminary human results appear promising. Further evaluation and follow up is needed.

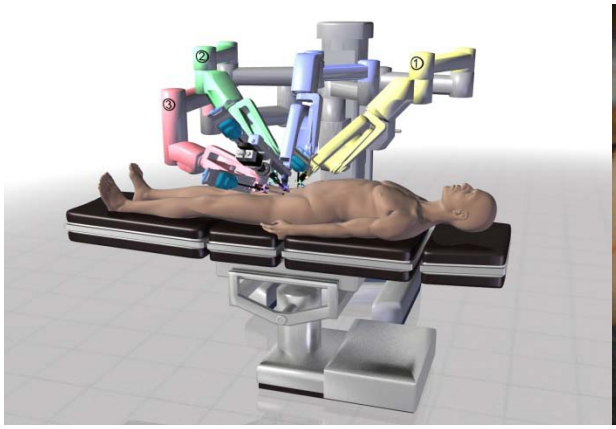

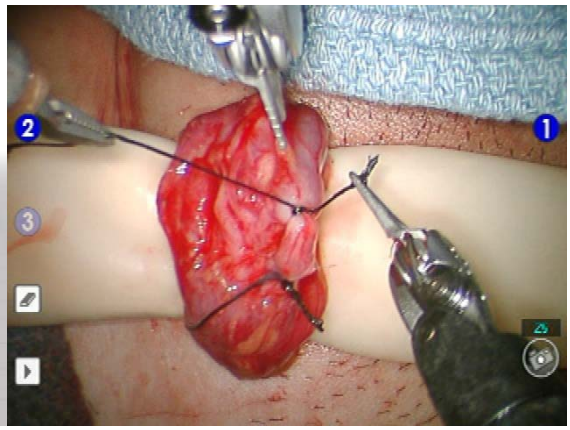

ABSTRACT 11 **BEST PAPER AWARD**

TANDEM-ROBOT ASSISTED LAPAROSCOPIC RADICAL PROSTATECTOMY: CLINICAL FEASIBILITY STUDY FOR NEUROVASCULAR BUNDLE VISUALIZATION

Misop Han, Chunwoo Kim, Pierre Mozer, Shadie Badaan, Bogdan Vigaru, Felix Schäfer,
Kenneth Tseng, Doru Petrisor, Bruce Trock, Dan Stoianovici
Robotics Lab, Urology Department, Johns Hopkins Medicine, Baltimore, MD
http://urobotics.urology.jhu.edu/

Introduction: Robot-assisted laparoscopic radical prostatectomy (RALP) using daVinci® surgical robot system (Intuitive Surgical) is a commonly performed operation for the treatment of clinically localized prostate cancer. The preservation of the neurovascular bundle (NVB) including cavernous nerves during the surgery improves the postoperative recovery of sexual potency. However, NVB visualization can be challenging due to the periprostatic connective tissue and intraoperative hemorrhage. The accompanying blood vessels in the NVB, which are visible with Doppler ultrasound, can serve as a macroscopic landmark to localize the microscopic cavernous nerves in the NVB. Herein, a novel robotic transrectal ultrasound probe manipulator (TRUS Robot) was used concurrently with the daVinci® in a tandem robot approach (T-RALP) to intraoperatively image the prostate and NVB.

Methods: The TRUS Robot was developed to provide a steady holding of the TRUS probe and allow remote manipulation using a joystick located next to the daVinci® console (Figure 1). Manual TRUS handling discards position data. But when the TRUS probe is manipulated by the robot then its positional data is readily available. This allows for recording image-position data pairs for robot control and 3-D reconstruction. The robot scans the prostate volume by rotating the TRUS probe about its axis (lateral imaging). Special imaging algorithms were developed for the rotary scan, because typically 3-D reconstruction is based on parallel slices. The scope of this first study was to determine the feasibility of the T-RALP approach by recording images during the surgical case. The objective of the T-RALP approach is to use TRUS images for guiding the surgeon. The Food and Drug Administration (FDA) and the Institutional Review Board (IRB) approvals were obtained and T-RALP was performed on three patients.

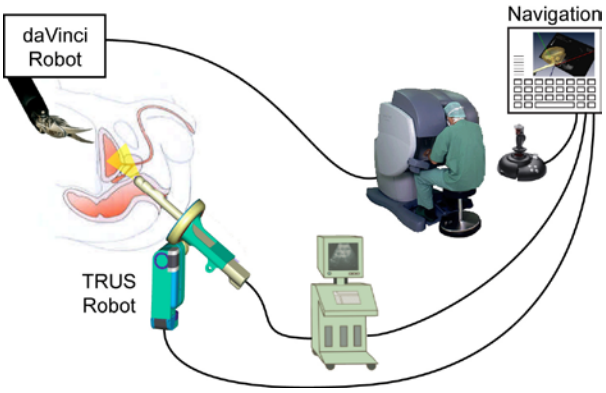

Figure 1: T-RALP Setup

Results: After informed consent was obtained three subjects underwent T-RALP. Figure 2 shows the TRUS robot in place before docking the daVinci®, as there is a limited space between the patient's perineum and the daVinci®. With the TRUS robot, the surgeon was able to directly and remotely control the TRUS probe. During T-RALP, the daVinci® instruments were clearly visible in the TRUS images as hyperechoic marks, especially with motion. The prostate could be scanned with the TRUS and Doppler activity was observed for the NVB. Images were recorded and analyzed subsequently. Ultrasound image slices were recorded while rotating the probe in one direction, from one lateral side to the other, and Doppler images were recorded in the opposite direction. The image sets were automatically registered to the same reference frame held by the robot. Figure 3 in the Appendix below, is a 3-D model of a prostate, urethra, and NVBs of a patient. No interference with the functionality of daVinci® was observed. No complications or patient discomfort were associated with the use of the TRUS robot.

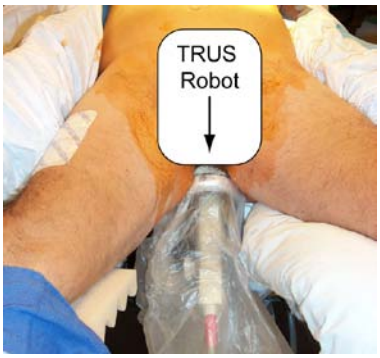

Figure 2: TRUS Robot in place before docking the daVinci®

Conclusion: We developed a robot for TRUS probe manipulation and performed a pilot feasibility study for T-RALP. The approach is feasible and has a potential clinical utility as it may provide important information about the location of the NVBs to a surgeon during RALP. Next steps will address, the refinement of Doppler visualization, improved image processing, image-guided navigation software developments and tests, and finally clinical research studies of TRUS guided RALP and clinical significance trials.

Appendix: The figure below is a **3D Model** that can be interactively scaled and reoriented. It is best viewed if this PDF document is opened with *Adobe Acobat 9* (free download). Other recent versions may show lower image quality and may not display the 3D labels, which are shown under the Default view.

Click on the image, wait for the 3D commands, and then adjust the view using the mouse as desired.

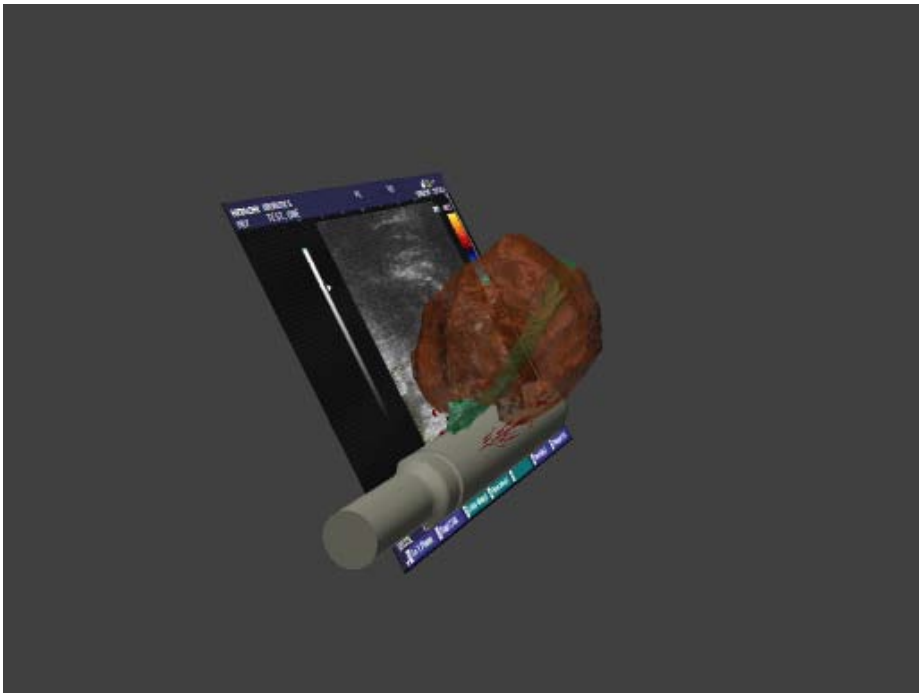

Figure 3: 3D reconstruction of a prostate, urethra (green), and NVB (red) constructed of images recorded in a T-RALP case. Volumes are rendered by spinning the lateral-fire TRUS probe about its axis with the TRUS robot.

Acknowledgement: This study was supported in part by the Johns Hopkins Institute for Clinical and Translational Research. The Doppler ultrasound used in the study was provided by Hitachi Medical Systems.

ABSTRACT 12

PERIURETHRAL NEUROMUSCULATURE STIMULATION IN REDUCING VOIDING FREQUENCY: A RAT STUDY

Yingchun Zhang[1], Angela J Forrest[2], Gerald W. Timm[1]
[1]*Department of Urologic Surgery*
[2]*Department of Biomedical Engineering at the University of Minnesota, Minneapolis MN*

Introduction: Pelvic floor stimulation has been delivered on nerves or muscles of the urinary tract to treat urinary incontinence (UI), studies in patients have shown that pelvic floor stimulation is effective in treating voiding dysfunction, but the mechanisms by which it works are unknown. With a goal towards evaluation of the utility of periurethral neuromusculature stimulation (PUNS) in reducing voiding frequency, the effects of PUNS on the cystometry were investigated in rats.

Methods: Ten Female Sprague Dawley rats were anesthetized and the bladder was catheterized through a small incision in the bladder dome and sealed with a suture. Inner bladder pressure was monitored while continuously infusing the bladder with warm saline. Continuous filling of the bladder triggers repeated cycles of voiding which can be identified through bladder pressure increases and visual urination. The pubic symphysis bone was then cut to expose the urethra, and a stimulating electrode was placed in the periurethral region. The PUNS procedure used in the present study is shown in Fig. 1.

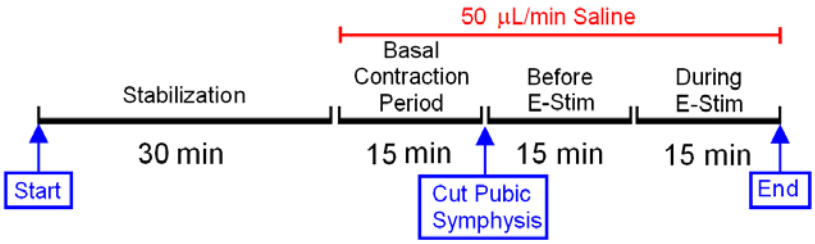

Fig. 1: Schematic diagram of the periurethral electrical stimulating procedure in the study.

Results: The typical intra-bladder pressure recordings without/with PUNS in a rat were shown in Fig. 2. The comparison clearly shows that the periurethral electrical stimulation increased the inter-contraction interval (ICI) and decreased the voiding frequency of the rat. Statistically, the rats with and without PUNS have an average ICI of 97.2 sec (+/-43.0 sec) and 63.1 sec (+/-31.3 sec) respectively. The results indicate that the PUNS caused 54.0% increase in average ICI. T-test result (p=0.001) further confirmed that the average ICIs without/with PUNS have significant difference. Correspondingly, rats with and without PUNS have an average voiding volume of 0.088 ml (+/- 0.043 ml) and 0.063 ml (+/- 0.041 ml) respectively. The results indicate that the PUNS caused 40% increase in average voiding volume. T-test result (p=0.02) also confirmed that the average voiding volumes without/with PUNS have significant difference, which is consistent with the ICI analysis above.

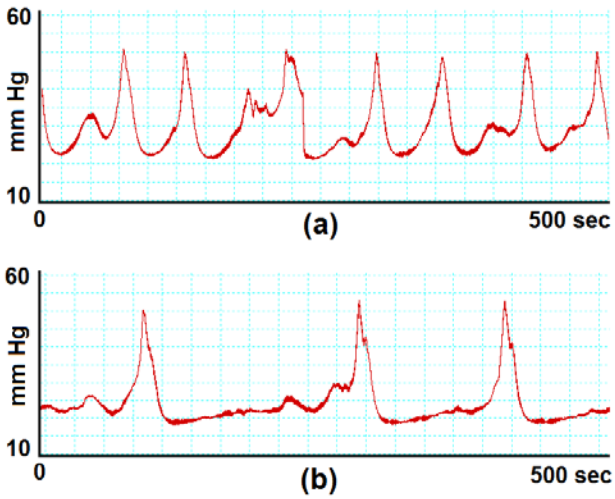

Fig. 2 Intra-bladder pressure recordings, (a) without PUNS and (b) with PUNS.

Conclusion: Periurethral neuromusculature stimulation significantly increased the inter-contraction interval and voiding volume, and reduced the voiding frequency of the rats. These results support periurethral neuromusculature stimulation as an alternative to spinal nerve stimulation for the treatment of bladder over activity.

ABSTRACT 13 **OUTSTANDING PAPER AWARD**

MODELING AND SIMULATION FOR FLEXIBLE URETEROSCOPY

Vijay Rajagopal[1], Ravi Janardan[1], Ricardo Miyaoka[2], Manoj Monga[2], Robert M. Sweet[2]
[1]*Computer Science & Engineering, University of Minnesota, Minneapolis MN 55455*
[2]*Urologic Surgery, University of Minnesota, Minneapolis, MN 55455*

Introduction: The flexible ureteroscope is a small caliber endoscope that serves as an important tool for diagnosing and treating stones, scar tissue and tumors in the ureter and collecting system of the kidney. Presently, surgical planning decisions (e.g., understanding patient-specific calyceal anatomy, identifying the size and location of stones, and scope selection and manipulation) are based on imaging data taken externally via X-Ray fluoroscopy and CT, and internally by a fiber-optics-based system at the tip of the scope. Presently, synthesis of these different (essentially 2D) data modalities into a common mental model is done by the individual practitioner, with no opportunities for patient-specific procedural rehearsal. We report on preliminary work aimed at improving the efficacy of the surgical decisions made by the urologist by using a combination of physical and virtual prototyping in 3D. Specifically, 3D-printing techniques are used to generate, from CT scan data, a physical model of the collecting system (calyces) on which scope manipulations can be practiced. A computer-based interface and associated algorithms are under development to facilitate simulation studies and interaction with a virtual model.

Methods: We used MIMICS software (www.materialise.com/mimics) to extract a 3D surface mesh of the collecting system from contrast-CT data. This included thresholding (identifying regions of interest based on pixel intensity), region-growing (connecting identified regions), and model creation (stitching the regions into a 3D model). The threshold parameter (pixel intensity) that best captured the details of the collecting system was found by trial and error and was aided by the presence of contrast. The output was in STL format, as a set of unordered triangles and their outer normals (30,552 triangles). The mesh surface was thickened by 2mm for structural integrity, the model was split into two halves by a plane (to allow stone placement), and rectangular alignment tabs were added. The model was then sliced into layers and fabricated by the PolyJet process (www.solidconcepts.com), which prints the layers successively, using a UV-curable photopolymer resin (TangoPlus). The model was tested in a saline bath with a DUR8E ureteroscope, single-action pump navigability, and stone extraction capability.

In parallel work on the virtual prototype, we have developed an efficient algorithm to convert the STL format to the more informative DCEL format for better downstream processing, written functions for viewing and manipulation (clip, zoom, pan, rotate, fly-through), and designed a basic graphical user interface, all in JAVA. Work is underway on developing efficient geometric algorithms to compute appropriate motion parameters for the scope relative to target stones.

Results: The physical model was soft and flexible, had a flesh-like feel, and captured faithfully the relevant features of the calyceal anatomy (left and middle figures). The tactile feedback was realistic, as was the view through the eyepiece. Despite leakage of saline outside of the collecting system, it was possible to snare stones in the renal pelvis (but not in the calyces). More simulations are planned.

Conclusion: The development of a patient-specific physical prototype of the collecting system is feasible and, with proper validation, may prove beneficial in training residents in flexible ureteroscopy.



Acknowledgement: Thanks to Andy Beeson for help with the STL file. This work was supported, in part, by the National Science Foundation under Grant CCF-0514950.

ABSTRACT 14

SINGLE-PORT LAPAROSCOPIC PARTIAL NEPHRECTOMY

Ricardo Brandina, Andre Berger, Monish Aron, Brian Irwin, Robert Stein, David Canes,
Mihir Desai, Inderbir Gill
Department of Urology, Glickman Urological and Kidney Institute, Cleveland Clinic, Cleveland, Ohio, USA

Objective: To present the initial experience with laparoscopic partial nephrectomy (LPN) performed through a trans-umbilical single port.

Methods: Between 11/2007 and 04/2008, 5 selected patients underwent single-port LPN for renal tumor. All procedures were performed through a single intra-umbilical multi-channel laparoscopic port. A 2 mm grasper was inserted through a 2 mm Veres needle-port in the anterior axillary line to aid in tissue retraction and sutured renal reconstruction. The technique of standard multi-port LPN was replicated, with the renal hilum clamped.

Results: Single-port LPN was successfully completed in 4 patients, while additional 5-mm port was required in 1 patient. Tumor size ranged from 1-5.9 cm (median 3 cm). Median operating time was 270 minutes (range 240-345 minutes), blood loss was 150 ml (range 100-600 ml). Median warm ischemia time was 20 minutes (range 11-29 minutes). Median length of the umbilical incision was 2.5 cm (range 2.5-4 cm). Median hospital stay was 3 days (range 3-22). No intra-operative complications occurred. All surgical margins were negative for tumor. There were no postoperative complications in 4 patients. One patient had post-operative bleed and pulmonary embolism.

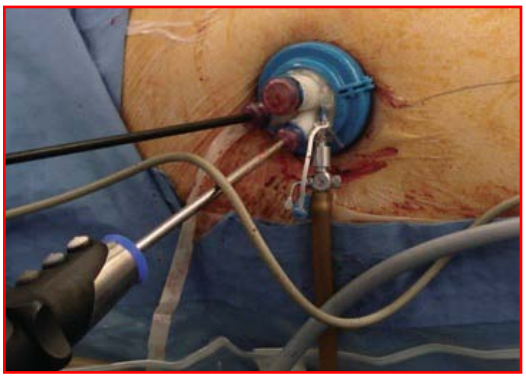

Figure 1. R-Port

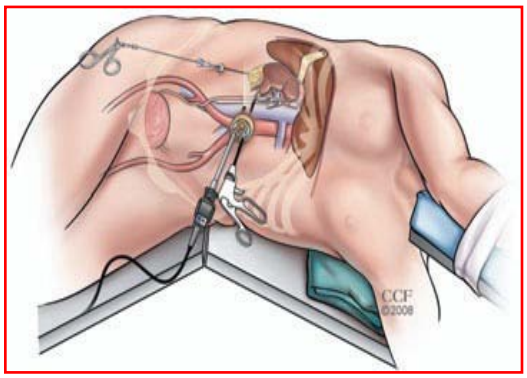

Figure 2. Ilustration: Port and 2mm grasper

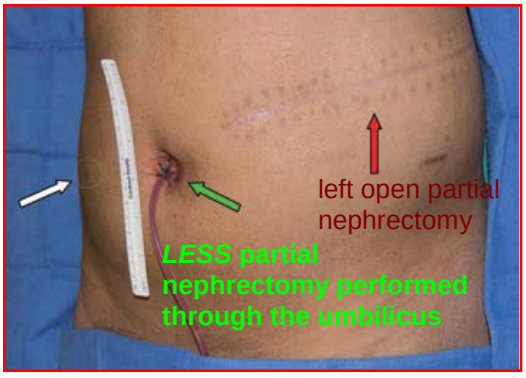

Figure 3. Patient with bilateral renal Tumors

Figure 4. Late Post operative picture

Conclusions: Single-port LPN is technically feasible, albeit more challenging than conventional LPN. Proper case selection is essential. Advances in single-port specific instrumentation are needed before these procedures can become a part of mainstream urological laparoscopy.

ABSTRACT 15

NOTES™ TRANSVAGINAL NEPHRECTOMY USING A NOVEL QUAD-PORT AND LAPAROSCOPIC INSTRUMENTS

Monish Aron, Andre Berger, Ricardo Brandina, Kazumi Kamoi, Sebastien Crouzet, David Canes, Brian Irwin, Robert Stein, Inderbir Gill, Mihir Desai
Department of Urology, Glickman Urological and Kidney Institute, Cleveland Clinic, Cleveland, Ohio, USA

Objective: To determine whether a novel Quad-Port can facilitate NOTES® transvaginal nephrectomy, using standard and articulating laparoscopic instruments.

Methods: Four fresh female cadavers were used in this feasibility study with a plan to perform two right sided and two left sided transvaginal nephrectomies. Exclusion criteria were history of nephrectomy and height taller than 6 feet. The cadaver was placed in lithotomy position with the target side up 30-45 degrees. A 3 channel R-port was placed in the umbilicus to monitor the transvaginal procedure. A 4-channel Quad-Port was placed through the posterior fornix into the peritoneal cavity. Regular laparoscopic instruments were used transvaginally to mobilize the colon, dissect the ureter, identify and divide the renal artery between clips, and divide the renal vein with a laparoscopic stapler. Remaining attachments of the kidney were divided and the specimen entrapped in a plastic bag prior to transvaginal extraction.

Results: Three (2 right and 1 left sided) nephrectomies were successfully performed. One left sided procedure was aborted in the last cadaver due to dense pelvic adhesions from prior pelvic surgery. In the first two cadavers we required assistance from the umbilical port only to divide attachments between the upper pole of the kidney and the diaphragm supero-posteriorly. In the third case we were able to perform this dissection completely transvaginally using a flexible gastroscope.

Figure 1. QUAD-Port placed in the vagina

Figure 2. Animation: Port + instruments

Figure 3. Medial mobilization of the cecum and ascending colon

Figure 4. Exposure of the vena Cava

Figure 5. Division of the renal artery using endoshears introduced through the vaginal port

Figure 6. Extraction of the intact specimen

Conclusions: Completely NOTES® transvaginal nephrectomy in humans is challenging. Robust laparoscopic instruments have the requisite tensile strength when deployed through a large caliber; secure, multi-channel transvaginal port. Extra-long laparoscopic instruments are helpful. The cephalad aspect of the hilum and the upper pole attachments are difficult areas. Novel flexible instruments still need to be developed.

ABSTRACT 16

THE Wii™ TRANSRECTAL ULTRASONOGRAPHY SIMULATOR

Yunhe Shen[1], Pat Fulgham[2], Xiangmin Zhou[1], Daniel Burke[1], Robert Sweet[1]
[1]Department of Urologic Surgery, University of Minnesota Medical School [2] Urology Clinics of North Texas

Introduction: Hands-on training is important for learning ultrasound skills. Only with interactive models and realistic images is a learner able to transfer the physical principles of ultrasound diagnosis from the didactic setting to practice and grasp the nuance of the technique. Live models have been used to achieve these requirements in minimally invasive, low risk examinations, such as renal and scrotal ultrasound. Transrectal ultrasound is invasive and poses a challenge to training using live models. Virtual reality (VR) models can provide objective learning data and feedback, and further relieve concerns of subject discomfort or injury during training. We have developed a high-fidelity, low-cost prototype VR simulator intended to train the skills necessary in order to perform transrectal Ultrasonography (TRUS) of the prostate.

Methods: Actual ultrasound images have been acquired in the sagittal and axial views, and then registered in virtual space. We use several infrared and accelerometer sensors in a commercial gaming interface, the Wii™ set, to track motions for each degree of freedom (DoF). One programmable Wii™ remote is mounted on a dummy probe, and the second is deployed laterally to the probe. The simulation software program reads and translates the outputs of the tracking sensors, calculates the orientation of the hand-held probe, registers its scanning plane with the pre-built ultrasound data model, processes and manipulates the pixels on the plane, and accordingly updates the images on the monitor as the final visual output. A rubber rectum with lubrication serves to provide the appropriate force-feedback. Wii™ buttons are utilized to simulate ultrasound transducer probe features.

Results: Figure 1 is the screen capture of the TRUS simulation. Figure 2 shows the hardware peripherals and the mannequin setup.

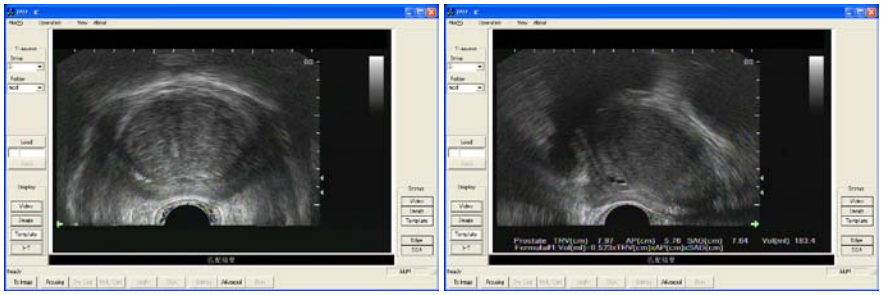

Figure 1. TRUS simulation – axial and sagittal views

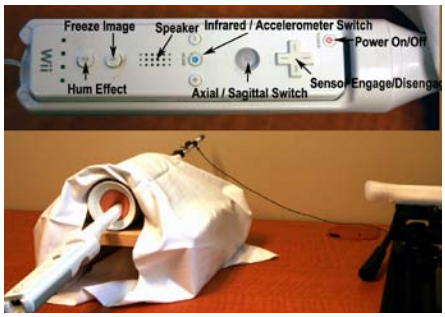

Figure 2. Hardware interface

The trainer successfully simulates the ultrasound imaging, tracks and registers the spatial DoFs necessary to perform TRUS. Buttons on the Wii remote are programmed to successfully control sagittal vs. axial views, freeze frame, set tracking modes and an on/off function with the "hum" felt during real TRUS.

Conclusion and Future Work: Using the Wii™ interface, integrated with our virtual TRUS software, we have built a high-fidelity basic simulator with force-feedback for transrectal ultrasound. Currently, a limitation exists if the scanning plane of probe is manipulated out of the volume of the virtual model, with only part of the ultrasound image being represented. The creation of a curriculum along with the capability for more complex procedures such as biopsy that require model deformation and penetration will transform this simulator into a robust trainer worthy of clinical validation studies.

ABSTRACT 17

PROSPECTIVE COMPARISON OF NOVEL BACKLOADING AND STANDARD BIOPSY DEVICES FOR THE DIAGNOSIS OF UPPER TRACT TRANSITIONAL CELL CARCINOMA

Rhonda Walsh, Preston Sprenkle, Dan Lee, Maria Ordonez, Mantu Gupta

Columbia University Medical Center, New York, NY

Introduction: Increasingly, endoscopic upper urinary tract diagnosis and treatment is being employed for diseases including transitional cell carcinoma. Due to the diminutive nature of existing endoscopes and traditional biopsy devices, biopsy of upper tract lesions has been difficult and tissue yields have been poor. The Bigopsy (Cook Medical) is a novel biopsy forceps with large cups which is backloaded through a ureteroscope. We compared the Bigopsy to a standard biopsy device in a an IRB approved prospective trial.

Methods: Six patients with upper tract lesions were enrolled in this study and complete data was available on four (*lamina propria* and epithelium measurements are absent for 2 patients). Each patient had a ureteroscopic biopsy with both the Piranha biopsy forceps (Boston Scientific) and the Bigopsy device. Surgeons rated the two devices on a scale of 1-5 for ease of opening, force needed to open, depth of bite, stiffness of grasper, limitation of ureteroscope deflection, limitation of irrigant inflow, ease in advancing scope, and visibility. The pathology results were also compared for size of specimen, amount of epithelium and lamina propria present, and whether or not the specimen was crushed. The pathology was reviewed by a single pathologist.

Results: No complications or adverse events occurred in this study. There were no significant differences in size of specimens or amount of epithelium or lamina propria between the two groups. There were also no significant differences in any of the surgeon ratings, except for "depth of biopsy" which was felt to be better with the Bigopsy ($p=0.02$). Biopsy results were the same in 4/6 cases; in one discrepancy the Bigopsy did not allow the scope to reach the lesion and so it was non-diagnostic, and in the other the Piranha was non-diagnostic.

Conclusions: In this pilot study, the Bigopsy appears to be a viable option for biopsy of large, exophytic, easily approached urothelial lesions. It may be less useful for procedures which require deflection of the ureteroscope or when the lesion is small or flat. Our completed study should answer these questions in the future.

ABSTRACT 18

AN ACUTE *IN VIVO* PORCINE STUDY TO CHARACTERIZE THE OCCLUSION OF A NOVEL METAL URETERAL STENT

Michael K Louie, Aldrin J Gamboa, Hung P Truong, Rachelle J Lin, Victor B Huynh, Kevin Sohn, Reza Alipanah, Lorena A Andrade, Cervando G Ortiz, Elspeth M McDougall, Ralph V Clayman
University of California, Irvine Medical Center, Orange, CA

Introduction: The Resonance® stent (Cook Medical Inc., Bloomington, IN) is a novel metal ureteral stent designed for long term ureteral stinting of ureteral strictures or extrinsic obstructions. Prior in vitro and in vivo animal data has suggested that the Resonance® stent is not able to be occluded. Recently, there have been several instances in our clinical experience where a patient treated with a Resonance® stent developed increasing hydronephrosis and flank pain afterwards. Our study objective is to confirm the flow characteristics of the Resonance® stent and to determine if indeed the stent cannot be occluded.

Methods: 6 Yucatan pigs underwent bilateral laparoscopic ligation of the renal hilar vessels to stop urine production. A gravity cystogram at 40 cm H_2O was performed in all animals to exclude renal units with vesicoureteral reflux. Bilateral retrograde ureteropyelograms were also performed in all animals to exclude those renal units with hydronephrosis. Renal units not excluded underwent placement of a 6 F nephrostomy tube connected to a saline reservoir at 20 cm H_2O and a 16 F Foley catheter placed to measure flow rate. Fluid flow was allowed to calibrate the ureter for 5 min with each change in experimental condition prior to measurement. Fluid flow rates were then measured consecutively 3 times every 3 minutes at baseline with and without a Resonance stent, then with intraluminal flow only, with extraluminal flow only, and lastly with complete occlusion. Complete occlusion was obtained by extraluminal ligation with two separate silk ties separated by 2 cm and intraluminal occlusion with removable plastic cladding developed by the engineers at Cook Medical Inc.

Results: Mean flow rates, standard deviation, and the range of flow rates are shown in the table.

Ureteral Condition:	Mean (ml/3min)	SD (ml/1min)	Range (ml/1min)
No Stent - Right Flow	4.48	1.85	1.73-8.00
No Stent - Left Flow	5.49	1.93	1.83-9.00
Resonance Stent	4.65	1.96	1.60-8.27
Extraluminal Flow	2.22	2.229	0.09-6.10
Intraluminal Flow	1.42	1.78	0-5.77
Complete Occlusion	0.12	0.23	0-0.83

Extraluminal flow compared to intraluminal flow ($p=0.56$) or complete occlusion ($p=0.07$) did not reach statistical significance. Intraluminal flow compared to complete occlusion was not significantly different ($p=0.12$). Baseline ureteral flow rates and the Resonance stent flow rates were not significantly different ($p=0.76$).

Conclusion: Despite our best attempts to occlude the Resonance stent, there was still flow in the complete occlusion model. However, given the severe decrease in flow in this model, there is a functional obstruction of the ureter which likely would be clinically significant.

ABSTRACT 19

IN VITRO, EX VIVO, AND *IN VIVO* ISOTHERMS FOR RENAL CRYOTHERAPY

J. L. Young, S. B. Kolla, D. L. Pick, D. E. Osann, P. Sountoulidis, O. G. Kaufmann, C. G. Ortiz-Vanderdys, A. G. Kaplan, V. B. Huynh, Lorena A. Andrade, E. M. McDougall, R. V. Clayman

University of California, Irvine, USA

Purpose: Preoperative planning for renal cryotherapy is currently based on isotherms mapped in gel. Herein, the gel isotherms are replicated and correlated with *ex vivo* and *in vivo* isotherms in a porcine renal model for two cryosurgerical systems.

Materials and Methods: Endocare 1.7 mm PERC-17 cryoprobes and Galil 1.47 mm IceRods underwent six trials each in gel, *ex vivo* porcine kidney and *in vivo, in situ* porcine kidney. Temperatures were recorded at thirteen predetermined locations using three 4 point MultiThermal Sensors (MTS) probes and one single point temperature sensor (TS).

Results: At the cryoprobe, temperatures are not statistically significantly different along the probe ($p= 0.0947$ to 0.9609) for either cryosurgical system. However at 10 and 20 mm away, ex vivo and *in vivo* trials had warmer temperatures towards the distal end of the cryoprobe for both systems with statistical significance values ranging from 0.2141 to 0.0003. The temperature did not differ between sites 10 mm to either side of the probe ($p=0.1232$ to 0.9819) with the one exception for Endocare in gel ($p<0.0005$). The 10 mm peripheral sites were significantly colder than the 20 mm peripheral sites after adjusting for sensor differences for both systems ($p<0.0005$). Temperatures were consistently colder with Endocare than Galil in gel ($p<0.00005$), *ex vivo* ($p<0.00005$) and *in vivo* ($p=0.0014$). Endocare temperatures were significantly colder *ex vivo* than in gel ($p=0.0029$). Galil temperatures were not statistically significantly between *ex vivo* and gel ($p=0.4299$). Temperatures were significantly colder in gel than *in vivo* for both Endocare ($p=0.0107$) and Galil ($p<0.00005$). Temperatures were significantly colder in *ex vivo* than *in vivo* at nearly all sites for both Endocare ($p=0.0008$) and Galil ($p<0.00005$).

Conclusions: 10 and 20 mm away from the cryoprobe, temperatures were unevenly distributed such that it was warmer towards the tip of the cryoprobe. Tissue just beyond the tip of the probe did not achieve suitably cold temperatures. Temperatures did not differ 10 mm on either side of the cryoprobe and were significantly colder further from the cryoprobe. The Endocare system consistently produced colder temperatures than the Galil system. Gel and *ex vivo* isotherms were not predictive of the *in vivo* pattern of freezing and thus cannot be used for accurate preoperative planning. MTS probes should always be used to record the actual temperature during renal cryotherapy and we recommend that at least one thermosensor be deployed to increase the accuracy of the procedure.

ABSTRACT 20 **OUTSTANDING PAPER AWARD**

A NOVEL PROXIMITY-SENSING STENT TO ASSIST NON-UROLOGICAL SURGEONS WITH INTRAOPERATIVE IDENTIFICATION OF THE URETER

John C. Kefer, Mihir M. Desai, Monish Aron, Georges Pascal-Haber, Inderbir S. Gill
Glickman Urological and Kidney Institute†, Cleveland Clinic, Cleveland OH

Introduction: Inadvertent ureteric injury by non-urological surgeons remains a significant concern. Temporary ureteric stents may be placed preoperatively to assist in the identification of a difficult ureter, but these stents may not be palpable during laparoscopic surgery, nor visible if surrounded by a bulky mass. Here, we report our design and laboratory experience with a novel intraoperative device incorporating a flexible, magnetic, 7 Fr J-J stent (Fig. 1), combined with a portable, battery-powered, magnetic field-detecting intraoperative wand utilizing a linear output Hall effect transducer (Honeywell Intl. Inc., Morristown, NJ) (Fig.2). When the detector wand nears the stent, an audible warning tone is emitted. As proximity to the stent increases, the frequency of the audible tone increases proportionally.

Methods: Our stent design utilizes rare-earth neodymium-iron-boron cylindrical magnets (OR 0.975 mm, IR 0.53 mm) incorporated into a silicone JJ stent. The cylindrical magnet shape was required to allow guidewire placement and luminal urinary drainage. Detection of the magnetic stent within the ureter was quantified using a portable, battery-powered voltimeter. The stent was placed in 4 pigs (8 renal units), and laparotomy was subsequently performed. The sensor wand was placed near the ureter at varying distances before and after releasing the colon. The magnetic field strength was recorded in all positions.

Results: The intraoperative detector wand reliably registered increasing magnetic field strength from a distance of 2 cm to 0.1 cm from the stent, and also precisely detected the position of the ureter behind the colon. The detected magnetic signal increased proportionally with increasing proximity to the stent from all angles of attack, including perpendicular and parallel to the stent, and reliably produced an audible warning tone when near the ureter.

Conclusion: Our novel stent design allows precise, predictable proximity detection of the ureter during intra-abdominal and pelvic surgeries. This magnetic stent and portable sensor system may serve to decrease the rate of inadvertent ureteral injury, and allows non-urologic surgeons the ability to actively identify the difficult ureter intraoperatively.

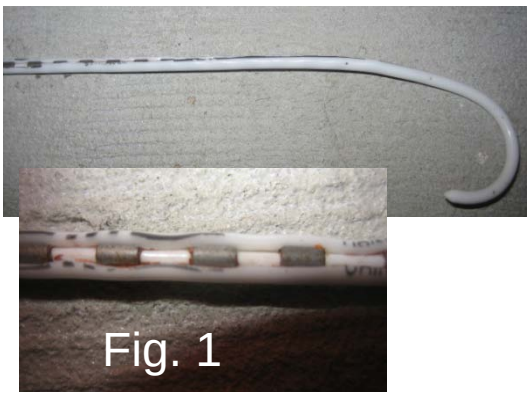
Fig. 1


Fig. 2

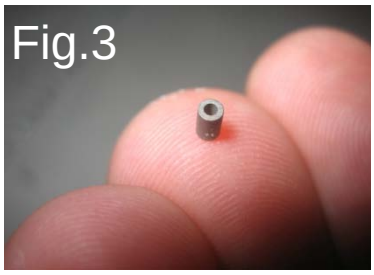
Fig.3

ABSTRACT 21

A NOVEL MEANS OF LOW COST, OFFICE-BASED ENDOSCOPY

Nicholas J. Hellenthal, Lars M. Ellison

University of California, Davis: Sacramento, CA

Introduction: Capture endoscopy in its current practice is an extremely expensive and space prohibitive procedure that has experienced limited integration into electronic medical records systems. Current medical endoscopic camera and tower systems range in price from $10,000 to $40,000, typically employ a dedicated room in a given practice, and produce Polaroid style pictures suitable for paper charts. We sought to develop a simple, cost-effective means of digital capture applicable to most endoscopic procedures.

Methods: We have developed a medical device to allow for the effective integration of off-the-shelf, consumer-grade digital camera technology and office-based endoscopy. The device allows for usage of a consumer-grade digital camera to view and record office-based endoscopic procedures. University rights were obtained, and a prototype was designed and tested.

Results: The device has been trialed in a number of outpatient cystoscopic procedures at multiple institutions. Both patient and physician satisfaction with our protocol device have been excellent. Multiple users have stated that image quality and recording abilities are equal to or better than currently employed multi-component tower systems. A United States patent is currently pending.

Conclusions: Office-based endoscopy in its current form has numerous limitations, including cost, demand for space, and lack of ability for digital integration. Our simple product integrates consumer digital-camera technology and office endoscopy and allows for any trained practitioner to provide high-quality digital imagery and electronic recording capability.

ABSTRACT 22

NEPHRON-SPARING SURGERY USING THE AQUAMANTYS 6.0 BIPOLAR SEALER

Jason Kim[1], Jay Yuan[1], Wayne Waltzer[1], Joseph Ditrolio[2], Rahuldev Bhalla[1]

[1] Stony Brook University Medical Center, Department of Urology [2] UMDNJ-Newark, Department of Urology

Introduction: Nephron-sparing surgery (NSS) has currently evolved as safe alternative renal masses less than 4 cm. Patients undergoing this procedure are at a significant risk of intra-operative blood loss which often necessitates temporary renal artery occlusion. However, this may lead to postischemic renal injury even with surface cooling. The Aquamantys is a novel device that integrates saline and radiofrequency energy to decrease surgical blood loss via remodelling of collagen. In this abstract we describe the initial use of a novel bipolar device for hemastasis during a partial nephrectomy with decreased need for clamping the renal artery.

Methods: We prospectively evaluated 10 patients with newly diagnosed renal masses who underwent open nephron-sparing surgery. The Aquamantys 6.0 bipolar sealer was used in 5 patients and the other 5 had traditional nephron-sparing surgery.

Results: A total of 5 patients underwent planned NSS using the Aquamantys 6.0 bipolar sealer (group 1) and we compared outcomes with the last 5 patients at our institution that underwent NSS without the Aquamantys 6.0 bipolar sealer (group 2). Results are listed in table 1. Group 1 had a larger mean tumor size, decreased intraoperative blood loss, and decreased need for renal hilar clamping, and decreased need for blood transfusions. Average operative time for group 1 was 171 minutes, compared to 186 minutes for group 2. All margins were negative for tumor in both groups. There was one incidence of significant post-operative acute renal failure in group 2 and none in group 1.

Conclusion: The Aquamantys bipolar device is a promising new tool that may have significant benefit while performing NSS. This allows excision of renal tumors without renal artery occlusion and subsequent renal ischemia. The Aquamantys allows for excision of renal masses without significant blood loss. While our results were not statistically significant due to our power, the overall trend is toward reduced intraoperative blood loss, decreased need for renal artery occlusion, and reduced need for blood transfusions. Larger scale studies will need to be performed to confirm this benefit.

Table I.

	Tumor Size (cm)	Blood Loss	Hilum Clamped	Blood Transfusion
Group 1 (Aquamantys)	**2.94**	**225**	**1/5**	**0/5**
Group 2 (No Aquamantys)	**2.4**	**530**	**3/5**	**2/5**

ABSTRACT 23

IS ULTRASOUND IMAGING HELPFUL IN PREDICTING EXTRACAPSULAR PENETRATION IN PROSTATE CANCER?

Charalampos Mamoulakis,[1] Luppo Kuilman,[1] Henk G. van der Poel,[2] Jean J.M.C.H. de la Rosette,[1] Pilar Laguna,[1] Theo M. de Reijke,[1] Hessel Wijkstra,[1]

[1] *Department of Urology, Academic Medical Center, Amsterdam, the Netherlands*

[2] *Department Urology, Netherlands Cancer Institute, Amsterdam, the Netherlands*

Introduction: The aim of the study was to investigate whether transrectal ultrasound (US) imaging modalities, namely high resolution grayscale-, high sensitivity color-Doppler- and contrast-enhanced US can be helpful in predicting local staging of prostate cancer (PCa), i.e. in detecting extracapsular tumor penetration.

Methods: Eighteen patients with histologically proven PCa eligible for laparoscopic radical prostatectomy were retrospectively selected from a collaborative database. Based on pathological specimen results, they were randomly assigned into two groups: group A (extracapsular penetration; n=10) and group B (organ confined disease; n=8). Imaging was performed preoperatively using a high-end US machine (Philips iU22, Bothell, WA, USA) with a transrectal probe (C8-4V). Data were implemented into specifically designed software for the purpose of the study to ensure randomization and blinding of the analysis. One observer reviewed all images. Specificity, sensitivity, negative and positive predictive value of extracapsular penetration was calculated.

Results: Results are summarized in tables 1 and 2. Neither modality nor their combination exhibited a statistically significant clinical performance. However, it should be noted that in this highly selected group of patients up to 61% of PCa cases have been correctly staged.

Table 1. Patients characteristics

	Age (y)	PSA (ng/ml)	pT Stage					
	Mean (SD)	Mean (SD)	T2a	T2c	T3a	T3b	T3c	T4
Group A	61.6 ± 6.5	13.5 ± 7.0	-	-	5	2	2	1
Group B	65.0 ± 4.8	6.2 ± 2.3	1	7	-	-	-	-

Table 2. Clinical performance of US imaging modalities in detecting extracapsular penetration

Modality	Sensitivity	Specificity	PPV	NPV
	(%)	(%)	(%)	(%)
Grayscale US	30.0	75.0	60.0	46.2
Colour Doppler US	30.0	100	100	53.3
Contrast-enhanced US	30.0	75.0	60.0	46.2
Combination (all three)	60.0	62.5	66.7	55.6

Conclusion: The use of US imaging contributes to local staging of PCa supporting the correct indication for radical prostatectomy.

ABSTRACT 24

THE SIGNIFICANCE OF ACCURATE SHOCK WAVE COUPLING IN EXTRACORPOREAL SHOCK WAVE LITHOTRIPSY

Thorsten Bergsdorf, Christian Chaussy, Stefan Thueroff

Department of Urology, Klinikum Harlaching, Munich, Germany

Introduction: The so-called "dry coupling" with a water cushion and ultrasound gel is the preferred method in actual lithotripsy systems, to transfer shock wave energy into the patient's body. This contact area between shock wave source and patient's skin represents a weak spot in lithotripsy, because air bubbles in this acoustic interface can reduce the delivery of shock wave energy considerably**.**

Methods: A transparent test tank with integrated membrane (simulating the patient's skin) for coupling with the shock wave system was mounted on a clinical lithotripter (SIEMENS Lithoskop®). For the evaluation of coupling quality, digital photographs were taken of the coupling area, using ultrasound gels of different composition (low and high viscosity), various volumes of gel and different coupling strategies; the quantity of trapped air pockets served as indicator for coupling quality. In a second setup, artificial stones (AST 0118) fixed in a basket with 2 mm mesh were fragmented in the test equipment with interposition of air bubbles (0 – 3.5 cm) in the coupling area, to assess the quantitative influence of trapped air on stone comminution. The number of shock wave impulses, required for total stone fragmentation with bubbles of specific size (0cm/1.5 cm/2.1 cm/2.6 cm/3.0 cm/3.4 cm) was the criterion for efficacy.

Results: The quantity of trapped air in the coupling area, representing the quality of coupling was varying over a wide range; ultrasound gel of low viscosity, appliance of large volume of gel and manual removal of air bubbles yielded the best results. The disintegration tests showed a statistically proven linear correlation between bubble size and required number of shock wave pulses (regression analysis, CI 95 %, R-Sq (ad) 99.4 %). An air bubble of 2 cm diameter (2 % coverage of the coupling area in our setup) increased the number of shock wave impulses for complete stone fragmentation by factor two.

Conclusion: Our *in vitro* findings suggest, that efficacy of ESWL is significantly correlated to air bubbles within the coupling area. The use of a large volume of low viscous ultrasound gel and the correct application are key measures, to obtain a good coupling quality. The neglecting of these aspects will be a relevant reason for poor disintegration results in shock wave lithotripsy.

ABSTRACT 25

INCREASED ESWL FRAGMENTATION OF STONES WITH THE USE OF THE ACCORDION DEVICE: *In Vitro* and *Ex Vivo* RESULTS

Joseph V Di Trolio[1], Patrick N Ciccone[2], Michael D LaSalle[3], Rahuldev Bhalla[4]
[1] *Department of Urology, UMDNJ/New Jersey Medical School, Newark, New Jersey*
[2, 3] *Department of Urology, St. Barnabas Medical Center, Livingston, New Jersey*
[4] *Department of Urology, Stony Brook University Medical Center, Long Island, New York*

Introduction: Contributing agents in the fragmentation of stones by extracorporeal shockwave lithotripsy (ESWL) are microshocks generated by the collapse of the cavitation bubbles produced by the negative pressure of the shockwaves. The lower success rate of ESWL in ureteral calculi has been attributed to the urothelium coapting to the stone and, so, a lower incidence of fluid adjacent to the stone's surface needed for bubble formation. The objective of this study was to determine whether a stone device (Accordion, PercSys) would improve ESWL effectiveness by tenting the ureter walls away from the stone, thus forming a fluid chamber around the stone and allowing increased cavitation.

Methods: Representative stones were molded from UltraCal-30 for use in the *in vitro* and *ex vivo* models. In the *in vitro* model, a stone 6.5 mm (diameter) by 10 mm (length) was advanced into an artificial ureter and placed in the focusing cup of a Modulith SLX (Storz Medical) filled with deionized water. The ESWL session was standardized to apply energy level 9 for 1000 shocks. The procedure was replicated five times each with either a 10 mm Accordion device immediately distal to the stone or no device present. For the *ex vivo* model, a stone 3 mm (diameter) and 5 mm (length) was advanced within an explanted porcine ureter and then the kidney and ureter were placed upon the treatment head of an ESWL machine (Compact Delta, Dornier), sandwiched between 2 three-liter pouches of saline. The ESWL procedure applied was that typically used in the clinic—120 shocks per minute, starting at power level III and increasing to power level V for a total of 2400 shocks. The procedure was replicated three times each with either a 10 mm Accordion device immediately distal to the stone or no device present. Significance between mean values was determined using Student's *t*-Test.

Results: The mean weight of residual stone fragments contained within the simulated ureter following a single ESWL session was 0.183 g when an Accordion device was positioned distal to the stone versus 0.264 g without use of the device (p=0.04). Use of the Accordion device resulted in a mean weight loss of 63% of the material in contrast to a loss of 47% of the material without the use of such a device (p=0.04). Following a single session of ESWL to stones in the excised porcine ureters found a 0.050 g mean weight of residual stone fragments with the Accordion device versus a mean weight of 0.068 g without use of the device (p=0.008). The mean loss of stone weight was 34% for stones where the Accordion device was used versus only 10% without use of the device (p=0.008).

Conclusion: Tenting tissue away from the stone surface so as to create a fluid interface in both the simulated ureters and excised porcine ureters with the Accordion device significantly increased the efficiency of stone fragmentation with a single ESWL session. Use of the Accordion device distal to the stones in each of these models resulted in significantly higher loss of stone weight than in the non-Accordion controls. Further studies are needed in order to validate these lab results in clinical usage.

ABSTRACT 26

PUBO-URETHRAL PEXY FACILITATES AND IMPROVES RESULTS IN RADICAL ROBOTIC PROSTATECTOMIES

Joseph V DiTrolio[1], Domenico J Savatta[2], Michael D LaSalle[2]

[1] *Department of Urology, UMDNJ/New Jersey Medical School, Newark, New Jersey*
[2] *Department of Urology, St. Barnabas Medical Center, Livingston, New Jersey*

Introduction: Robotic assisted radical prostatectomy has become the standard of care for organ-confined prostate cancer in young males. A retrospective study of our 100 most recent patients with urethral pexing was compared to our last group of 100 patients prior to urethral pexing. Improved surgical techniques are shortening operative time and reducing post-operative management. An immobilizing urethral pexing suture has been evaluated retrospectively for reduction in operative time, better urethrovesicle anastomosis, elimination of intra-operative Jackson Pratt drainage, as well as post-operative cystograms, and less foley catheter drainage time.

Methods: During robotic assisted radical prostatectomy, at the time of transection of the distal prostate from the proximal urethra, a superficial pexing suture of 4-0 prolene is placed on the dorsal surface of the urethra, securing it to the periosteum of the pubic symphysis. Once performed, complete transection of the urethra is accomplished and the urethra fails to migrate distally, facilitating the urethrovesicle anastomosis with double-armed 2-0 PDS (polydioxanone) sutures. In the presence of a tension-free anastomosis, a more water tight suture line is attained, eliminating the need for Jackson Pratt drainage.

Results: Comparison studies with the same surgical team have shown that intra-operative urethral pexing significantly decreases the anastomotic time as there is no distal migration of the urethra and less time is required placing sutures on the urethral side with the proximal urethra held in place. Intra-operative evaluation of the water tight nature of the anastomosis has allowed us to eliminate Jackson Pratt drainage. Post-operative Foley catheter time has been reduced by about 50%, to an average of 5.5 days. Experience has shown us that the cystogram was an unnecessary procedure as we have not been able to document extravasation. Complete continence has been attained in half the time, an average of 15 days in 90% of our patients.

Conclusion: Continued evolution of the robotic assisted prostatectomy has allowed us to streamline surgical intervention, reducing operative time and risk. Reduced post-operative management has allowed the patient to return sooner to a normal quality of life. As surgical techniques improve, patients have less apprehension to utilize this cutting edge technology

ABSTRACT 27

DEVICE AND METHOD FOR MINIMALLY INVASIVE URODYNAMIC ASSESSMENT IN MEN

João C.M. de Almeida[1,2], Rodrigo H. Watanabe[1], David J. Cohen[3], Carlos A.L. D'Ancona[3], José W.M. Bassani[1,2]

[1]School of Electrical and Computer Engineering, [2]Center for Biomedical Engineering,
[3]Division of Urology of School of Medical Sciences, University of Campinas, Campinas, SP, Brazil

Introduction: More than 20% of men presenting lower urinary tract symptoms need prostate surgery. The decision on the treatment of these patients is usually taken with basis on the results of their urodynamic assessment. The conventional urodynamic test is not free of risk of complications (e.g. macroscopic hematuria, urinary tract infection), which are present in about 19% of the cases. In this study, we describe new improvements on a previously developed device for minimally invasive measurement of isometric bladder pressure.

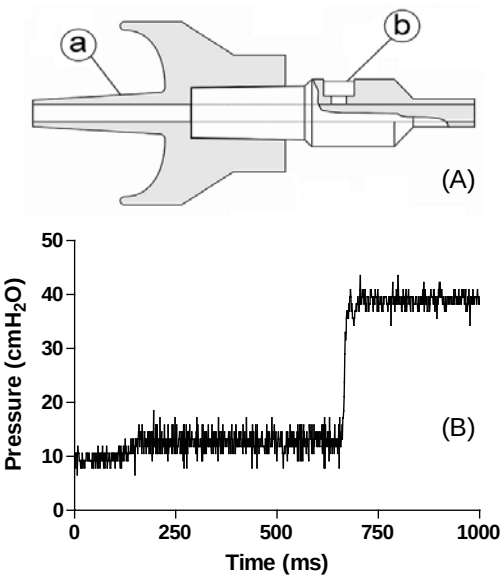

Figure 1 - Urethral connector (UC) and bench test result.

Methods: The developed device, named urethral connector (UC), is made of polyvinyl carbon and polytetrafluoroethylene, and has now an adapter (a in Fig. 1A) provided with a conic tube designed to fit the urethral meatus and fossa navicularis and a built-in pressure transducer (b in Fig.1A, *Freescale* MPX2300DT1). Transducer calibration and dynamic bench-tests were performed with a setup in which pressure gradient was generated by gravity, and the reference pressure values were obtained by manometry. After a few seconds for continuous flow and pressure stabilization, the outlet of the UC was occluded, so that the steady-state static pressure could be recorded. To avoid hydraulic shock, occlusion was not instantaneous. The output voltage of the transducer was fed to a computer via NI USB-6215 interface (*National Instruments Inc.*), in which a *LabView*^{TM} program was used for data acquisition and processing. The UC was tested (immediately after the conventional urodynamic exam) in 8 patients, who signed the consent form. Patients were instructed to manually occlude and release urine flow through the UC. A t-test for paired comparisons was used to compare the pressure obtained with the UC with the conventional urodynamic method.

Results: Bench-tests showed that the device responded linearly, and with high reproducibility, to the applied pressure. The steady-state pressure could be reliably measured in less than 400 ms after non-instantaneous UC occlusion, a period not long enough to cause much discomfort to the patient, but sufficiently long to avoid hydraulic shock (Fig.1B). Preliminary clinical tests indicated that the new device is easy to use and allows shorter examination time. Patients referred no major discomfort. About 75% of the patients considered the minimally invasive test as preferable to the conventional evaluation. Although mean values of pressure were not statistically different with the two methods, present data were insufficient to allow reliable determination of correlation between them.

Conclusion: The UC performed well in bench-tests. Although more clinical testing is required, preliminary application indicated that the UC method is a convenient alternative to the conventional urodynamic test for measurement of static bladder pressure.

ABSTRACT 28

METHOD FOR URETER LOCALIZATION IN MINIMALLY INVASIVE SURGERY

David M. Kwartowitz[1], David R. Holmes III[1], Andrea Mariani[2], Richard A. Robb[1]

[1] *Biomedical Imaging Resource, Mayo Clinic, Rochester, MN*
[2]*Department of Obstetrics-Gynecology, Mayo Clinic, Rochester, MN*

Introduction: The visualization of subsurface structures during minimally invasive surgical techniques is limited by the use of light based laparoscopic video. This video allows the surgeon to survey the surface of the body cavity under study; however subsurface structures which may be of critical importance cannot be adequately visualized. For example in many urologic or gyno-urologic procedures, the location of the ureters is critical. Severing a ureter can lead to loss of function or sepsis.

In minimally invasive surgery, vision of structures like the ureter is often obstructed by fat, blood, or other structures. Locating the ureter by traditional methods can be time consuming and complicated. In this work we present a method of localization and visualization using a chemoluminescent agent with image processing.

Methods: A system was built using the Framework for Image-Guided Navigation Using a Distributed Event-Driven Real-Time Database (FINDER). In FINDER, image guidance tasks are divided into modules, each of which communicates with a centralized database server. These tasks operate independently of each other, using the database only as means of coordinated communication. In this system three PCs are used, two for video capture and display, one for each eye, and one as a database and processing server.

A chemoluminescent agent was injected into the ureter of a pig at the proximal end with distal ligation. This agent was not visible to the laparoscopic camera either with the laparoscopic light source illuminated (light) or not (dark). A video capture program acquired and displayed every frame of laparoscopic video with an applied mask image. The initial mask image was defined as all zeros. This capture server sends dark images to the database to be processed by the processing server. When the processing server receives the images, they are integrated, and segmented. This new segmented image is applied as a revised mask to the newly captured video.

Results: Figure 1 shows a frame of the raw video feed (a) and the same frame with the segmented mask image overlaid (b). This mask image displays clearly the position of the ureter and allows the surgeon to manipulate tissue without risk of ureteral damage. These mask images can be easily updated by presenting dark frames to the capture module.

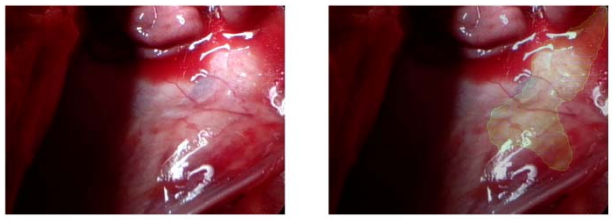

Figure 4: (a) Video frame of ureter obstructed by blood and fat. (b) Contour overlaid in yellow on frame showing ureter's position

Conclusion: We have created a system which allows for easy positional localization of the ureter using a combination of chemoluminescent agents and image processing. This method provides an intuitive visualization of ureter position within the same reference as the live laparoscopic video.

ABSTRACT 29

ARE MULTIPLE CRYOPROBES ADDITIVE OR SYNERGISTIC IN RENAL CRYOTHERAPY?

J. L. Young, D. W. McCormick, S. B. Kolla, C. G. Ortiz-Vanderdys, V. B. Huynh, A. G. Kaplan, N. S. Jain, D. L. Pick, L. A. Andrade, K. E. Osann, Petros Sountoulidis, Oskar G. Kaufmann, Lorena A. Andrade, E. M. McDougall and R. V. Clayman

University of California, Irvine, USA

Objectives: Recently 1.47 mm (17 gauge) cryoprobes have been introduced to the armamentarium of tools for renal cryotherapy. The small size of these probes is thought to be beneficial by allowing the use of multiple probes over a larger area with less risk of bleeding or cracking than the thicker cryoprobes. It is currently unknown if multiple probes work in a simply additive or truly synergistic fashion.

Methods: Laparoscopic-guided cryoablation was performed in the upper and lower renal pole of three farm pigs using three 17 gauge IceRod cryoprobes (Galil Medical Inc., Plymouth Meeting). These twelve cryolesions were compared to twelve cryolesions using a single IceRod cryoprobe in the upper and lower renal pole of farm pigs from a prior study. Each cycle consisted of 2 ten minute freeze cycles separated by a five minute active thaw with pressurized helium gas. At the conclusion of each freeze cycle, the iceball volume was measured with intraoperative ultrasound. After completion of the cryotherapy, the kidneys were harvested and the cryolesion surface area was visually calculated. The lesions were fixed in 10% buffered formalin then excised with a 1 mm margin to obtain a volume measurement using fluid displacement. Statistical analysis compared the single probe results multiplied by three to the multiple probe group.

Results: Iceball volume for the first freeze cycle for the single cryoprobe multiplied by three was 8.55 cm^3 compared to 9.79 cm^3 for the multiple cryoprobe group ($p=0.44$). Iceball volume for the second single probe freeze cycle was 10.01 cm^3 compared to 16.58 cm^3 for the multiple probe group ($p=0.03$). Cryolesion volume was 11.29 cm^3 versus 14.75 cm^3 ($p=0.06$). Gross cryolesion surface area was 13.14 cm^2 compared to 13.89 cm^2 ($p=0.52$) respectively.

Conclusions: The cryolesion created by three simultaneously activated 1.47 mm probes appears to be larger than what one would otherwise expect. The lesions were statistically significantly larger as measured by ultrasound and nearly so by gross cryolesion volume. However, in general this difference is not overly great and as such the use of multitemperature sensing probes is essential when determining the cryolesion's effective area of ablation.

ABSTRACT 30

NOTES AND SINGLE PORT SURGERY: WHAT DO PATIENTS WANT?

David Canes, Andre Berger, Monish Aron, Kazumi Kamoi, Georges-Pascal Haber, Robert J Stein, Steve Campbell, Jihad H. Kaouk, Mihir M. Desai, Inderbir S. Gill

Department of Urology, Glickman Urological and Kidney Institute, Cleveland Clinic, Cleveland, Ohio, USA

Background: Enthusiasm for Natural orifice translumenal endoscopic surgery (NOTES) and Laparo-endoscopic single-site (LESS) surgery continues to escalate. Notably absent are specific insights into patient attitudes towards these techniques, and surgical scars. Our aim was to evaluate patient perceptions of various approaches, determine how scarring impacts patient decision making, determine the preferred orifice-of-entry for NOTES, and understand the demographics of patients interested in these novel approaches.

Materials and Methods: After IRB exemption, beginning July 2008, 608 consecutive patients presenting to urologic, general surgical, and obstetrics/gynecology clinics were asked to complete a 25-item questionnaire. The survey included baseline demographics, medical history, presence and attitudes about preexisting scars, decision making for hypothetical surgeries for benign/malignant indications.

Results: Mean age was 58 and 51% were male. Forty percent were presenting to Cleveland Clinic for surgical indications, and 73%, 46%, 10% had prior open, laparoscopic, or robotic surgery respectively. Fourteen percent were unhappy about the scars.
When presented the hypothetical need for nephrectomy for benign and malignant indication, or cholecystectomy, surgical scars ranked 11th amongst considerations for surgical approach, with reputation of hospital, reputation of doctor and doctor's recommendation accounting for the top three considerations. Majority of patients preferred standard laparoscopic approach for cholecystectomy (34%) and benign nephrectomy (31%). However the preferred approach for nephrectomy for malignancy was open surgery (24%), followed by laparoscopy (21%). LESS was chosen by 13%, 11% and 8%, and NOTES by 2%, 2.5%, and 2%, respectively. When asked to choose between NOTES and LESS, 70% preferred LESS for kidney cancer and 75% preferred LESS for non-kidney cancer surgery. The preferred orifice for NOTES was rectum in males (38%) and vagina in females (43%). On multivariate analysis, only female was an independent predictor for choosing NOTES or LESS for benign indications.

Conclusions: Postoperative scarring ranks low in the hierarchy of patient concerns when given hypothetical surgical scenarios. Patients currently prefer LESS over NOTES. Further research is warranted to determine how best to communicate these novel approaches, which at face value may not be appealing to patients.

ABSTRACT 31 **OUTSTANDING PAPER AWARD**

DOES NEEDLE SPINNING IMPROVE TARGETING PRECISION?

Shadie Badaan[1], Pierre Mozer[1], Chunwoo Kim[1], Doru Petrisor[1], Felix Schäfer[1], Mohamad Allaf[1], Kevin Cleary[2], Dan Stoianovici[1]

[1]*Urology Robotics, Department of Urology, Johns Hopkins Medicine, Baltimore, MD*
[2]*ISIS Center, Georgetown University, Washington, DC*
http://urobotics.urology.jhu.edu/

Introduction: When the point of a needle advances through the skin there is significant uncertainty of its path, as limited means of transcutaneous imaging are available for real time three-dimensional (3D) visualization. Needle bending and soft tissue deflections have a significant influence on the precision of targeting in percutaneous procedures. In image-guided procedures these are a component of the overall targeting accuracy. Needle delivery errors may have a direct influence on the final treatment outcome of the procedure. Several mechanisms have been proposed for preventing deflections or steering the needle. We developed a Revolving Needle Driver (RND) to spin the needle during insertion. This is used with our AcuBot robot for image-guided interventions. Experiments show that spinning prevents lateral deviations and target deflections.

Methods: A narrow glass box was made and filled with gelatin (Figure 1). Line markers are used to help observe deflections. A first experiment was setup to asses lateral needle deflections. Several 18-G needles with diamond or beveled points were inserted with or without spinning. The speed of needle insertion was maintained constant at 50 mm/sec. A second experiment evaluated the displacement of a silicone rubber target (10mm dia. x 15mm long) suspended in the softer gelatin base when targeted with a needle. Several 18-G needles were inserted with and without spinning. Experiments were video recorded to evaluate the displacement of the target.

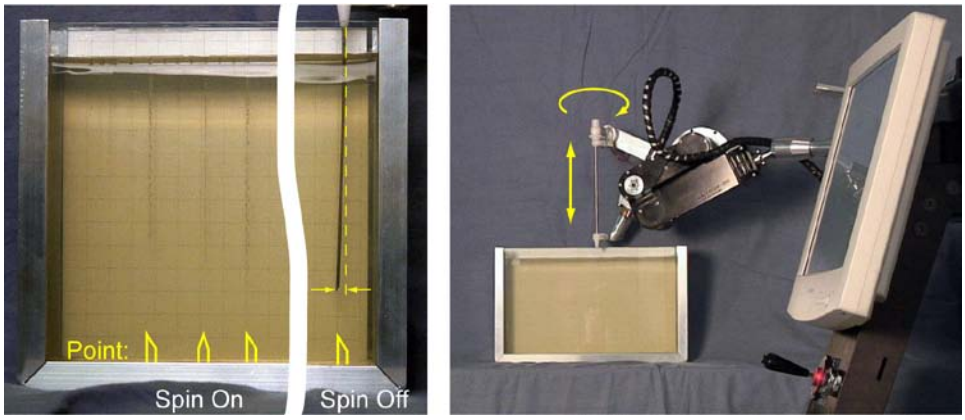

Figure 5: Right: Glass container with gelatin and AcuBot robot with Revolving Needle Driver. Left: Needle paths with and without spinning for bevel and diamond points.

Results: First: Lateral needle deflection experiments showed that bevel point needles pull laterally, as it is well known. Diamond point needles have less defection, unless they are imperfect. As it can be observed in Figure 1, spinning straightens the path. But spinning bevel point needles was also found to leave marks in the gelatin, raising concerns of tissue damage (see image). Yet, very slow spiral in motion showed marks that were similar to those without the spin. With a diamond point, marks were hardly observable. The second experiment showed that spinning may significantly reduce the deflection of the target. This was true when spinning while inserting or even when spinning afterwards. The movie in Figure 2 shows how targeting is improved by simply spinning the needle after reaching its target. Besides poking the needle this is also one of the techniques that physicians practice.

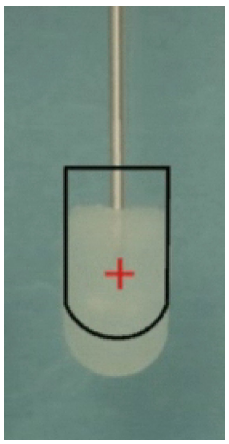

Conclusion: The study is an experimental validation of improving needle targeting. Most methods are known to experienced physicians, but the experiments offer an observable and controllable validation setup. The study also shows that needle driver mechanisms may offer capabilities that are manually difficult, such as needle "drilling" for example. Yet, their true potential is to be considered in conjunction with image-guided intervention systems.

*Figure 6: This is a **MOVIE**. Best viewed if this PDF document is opened with Adobe Acrobat 9.0 (Free download). The needle is first inserted in front of the box to show where is expected to hit the silicone target. Then, the needle is inserted at the target, without spin. As expected, the needle pushes the target away. Next, spinning is initiated. The movie shows that the target backs up over the needle reducing the initial error.*

ABSTRACT 32

IDENTIFICATION OF OPTIMAL LASER FIBER MOVEMENT FOR PHOTO-SELECTIVE VAPORIZATION OF THE PROSTATE IN AN *EX VIVO* ANIMAL MODEL

Eric C Kauffman[1], Wook Kang[2], Benjamin B Choi[1]

[1] New York Presbyterian Hosptial – Weill Cornell Medical Center, New York, NY
[2] American Medical Systems, Minnetonka, MN

Introduction: Photo-selective vaporization of the prostate (PVP) has emerged as an effective debulking procedure for prostatic urinary obstruction. However, technique for most efficient vaporization has received little scientific investigation. We used an *ex vivo* bovine prostate model to investigate how variation in the angle and speed of laser fiber rotational movement affects tissue vaporization.

Methods: PVP was performed on 100 freshly harvested bovine prostate specimens using the GreenLight™ HPS 120W laser. Each specimen was vaporized for a set time period in an ex-vivo chamber using computer-assisted axial movement of the laser fiber along the tissue. In experiment 1 (N= 40), PVP was performed at a fixed rotational sweeping angle (60 degrees) and variable rotational sweeping speeds (0.5, 1.0, 1.5, 2.0 sweeps/second). In experiment 2 (N= 60), PVP was performed at a fixed rotational sweeping speed (0.5 sweeps/sec) and variable rotational sweeping angles (0, 15, 30, 60, 90, 120 degrees). The volume of tissue vaporized for each specimen was calculated from ten 1-mm cross sections using an image processor. Volumes were compared by a two sample t-test.

Results: In experiment 1, vaporization at lower rotational sweeping speeds (0.5 and 1.0 sweeps/sec) removed significantly more tissue compared to higher sweeping speeds (1.5 and 2.0 sweeps/sec), with a nearly 2-fold decrease in tissue vaporization at the highest speed studied (2.0 sweeps/sec). In experiment 2, use of larger rotational sweeping angles generated wider but significantly more superficial vaporization defects, leading to smaller overall vaporized volumes (Figure). Specifically, vaporization volumes achieved with rotational angles of 0, 15 or 30 degrees were not significantly different, but were significantly greater than those achieved with rotational angles of 45, 60 and 90 degrees (~1.5-3.0X; $p < 0.05$)

Conclusions: Our findings support optimal vaporization at slower speeds (0.5-1.0 sweeps/sec) and narrower angles (0-30 degrees) of rotational laser-fiber movement in a bovine prostate *ex vivo* model. Given the similar vaporization efficiency using 0 and 30 degree angles, the latter may be preferable clinically due to the wider and better visualized surface area of exposed tissue, in contrast to the narrow groove created with 0 degrees. This study highlights that optimal PVP laser fiber movement can be tested in a scientific manner, identifying parameters to aid urologists in maximizing tissue vaporization efficiency.

ABSTRACT 33

ROBOTIC LAPAROENDOSCOPIC SINGLE SITE SURGERY USING GELPORT AS THE ACCESS PLATFORM

Robert J. Stein, Wesley M. White, Raj K. Goel, Brian H. Irwin, Monish Aron, Georges-Pascal Haber, Jihad H. Kaouk

Glickman Urologic and Kidney Institute, Cleveland Clinic, Cleveland, OH, USA

Introduction: Laparoendoscopic single site surgery (LESS) allows for the performance of major Urologic procedures with a single small incision and minimal scarring. The da Vinci Surgical System provides advantages of easy articulation and improved ergonomics, yet an ideal platform for these procedures has not been identified. We aimed to evaluate the GelPort® laparoscopic system as an access platform for robotic LESS (R-LESS) procedures.

Methods: Since April 2008, 11 R-LESS procedures have been completed successfully in a single institutional referral center. For the last 4 consecutive cases the GelPort has been used as an access platform through a 2.5 to 5cm umbilical incision. R-LESS cases performed with the GelPort included pyeloplasty (n=2), radical nephrectomy (n=1), and partial nephrectomy (n=1). Perioperative data were obtained for all patients including demographic data, operative indications, operative records, length of stay, complications, and pathological analysis.

Results: For both pyeloplasty cases, average operative time (OR time) was 235 minutes and estimated blood loss (EBL) 38cc. For the patient undergoing radical nephrectomy for a 5.1cm renal tumor, OR time was 200 min. and EBL 250cc. The final patient underwent partial nephrectomy without renal hilar clamping for an 11cm angiomyolipoma with OR time 180 min. and EBL 600cc. All R-LESS procedures attempted with the GelPort were completed successfully and without complication. Average length of hospital stay was 1.75 days (range 1-2). The partial nephrectomy patient required transfusion of 1 unit packed red blood cells.

Conclusion: Use of GelPort as an access platform for R-LESS procedures provides adequate spacing and flexibility of port placement and acceptable access to the surgical field for the assistant, especially during procedures that require a specimen extraction incision. Additional platform and instrumentation development will likely further simplify R-LESS procedures as experience grows.

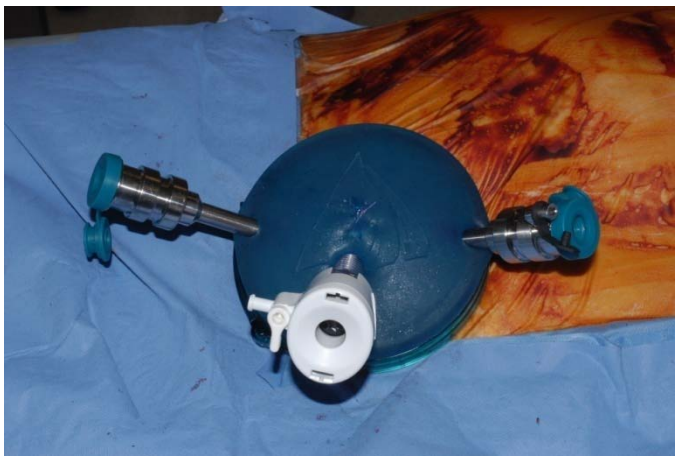

ABSTRACT 34

PRELIMINARY INVESTIGATIONS OF IRREVERSIBLE ELECTROPORATION (IRE) IN *IN VIVO* PORCINE KIDNEYS: ABLATION WITHOUT HEAT

Raymond J. Leveillee[1], Nelson Salas[1,2], Merce Jorda[3], Charles Moore[1], Maria E Sierra[3]

[1] Joint Bioengineering and Endourology Developmental Surgical Laboratory, Division of Endourology, Laparoscopy, and Minimally-Invasive Surgery, Department of Urology, University of Miami Miller School of Medicine, Miami, FL
[2] Biomedical Optics and Laser Laboratory, Department of Biomedical Engineering, University of Miami, Coral Gables, FL
[3] Department of Pathology, University of Miami Miller School of Medicine, Miami, FL.

Introduction: Irreversible Electroporation (IRE) has recently been investigated as a new minimally-invasive treatment modality for solid tumors. The use of high voltage direct current creates an electrical field resulting in nanopores in the cell membranes. This leads to permanent disruption of homeostasis of the cells, resulting in cell death. Unlike other ablative modalities which rely on temperature (hot or cold), electricity is utilized with minimal to no heat. Prior pre-clinical IRE studies have demonstrated that the IRE ablation effect spares connective tissue thus potentially sparing nerves and blood vessels. Because the mechanism of injury is not thermal there should be no circulatory "heat sink" or "heat source" effects. Unlike other organs such as liver, which are considered electrically isotropic, the kidneys are considered electrically anisotropic due to large variation in salt and fat content between the cortex and the medulla. Due to this electrical heterogeneity, we theorized that ablation results at different locations within the kidney will differ under similar parameters. The purpose of this preliminary investigation was to determine the feasibility of IRE for the minimally-invasive treatment of renal tissue utilizing an in-vivo porcine model.

Methods: Six Yorkshire pigs ranging from 40-60 kgs were used in this study: Four pigs were survived up to 18 days ; two pigs were sacrificed immediately. Each kidney was treated with the Nanoknife™ IRE system (Angiodynamics®, Queensbury, NY) and with either 2, 3, or 4 monopolar probes per lesion while directing the needles parallel or perpendicular to the longitudinal axis of the kidney. Each monopolar probe consists of a metallic tip that can be exposed from its insulating sheath between 0.1 and 4.0 cm in length. A spacer, specifically designed for IRE by the manufacturer, was used to maintain the distance between the monopolar probes constant. Ablations were performed under general anesthesia with muscular blockade utilizing a voltage range of 1800 – 3000 V, probe exposure lengths of 1.5 and 2.0 cm, and an inter-probe distance range of 1.5 - 3.0 cm. After euthanasia, the kidneys were harvested and evaluated for gross and histological differences.

Results: All lesions on gross examination appeared to have a hemorrhagic zone. Ablation sizes were estimated grossly by the size of this hemorrhagic zone. The range of lesion sizes for two, three, and four probe ablations were (0.5-2.5) x (0.3-2.0) x (0.3-1.5) cm, (1.0-2.0) x (0.5-1.5) x (0.7-0.8) cm, and (1.5-2.0) x (1.9-2.0) x (1-1.1) cm, respectively. Upon histological examination, congestion, hemorrhage, and coagulative necrosis were observed both within and up to 5 mm outside of the grossly observed lesion. Within 11 to 18 days of survival time, dystrophic calcification was observed within the lesion. Renal micro-architecture and preservation of glomeruli with "ghosting" was observed.

Conclusion: IRE is a novel ablation modality that can create lesions of various sizes in renal tissue under a variety of parameters. These lesions yield demonstrable cell necrosis and short term calcification, signifying cell death within 18 days with preservation of gross architecture. Continued investigation is warranted to attempt to achieve optimal treatment parameters in the kidney.

ABSTRACT 35 **OUTSTANDING PAPER AWARD**

A COMPARATIVE STUDY BETWEEN NOVEL AIR-CUSHION PROBE AND WHEELED PROBE FOR MIS

Dinusha Zbyszewski[1], Hongbin Liu[1],Oussama Elhage[2], Ben Challacombe[2], Prokar Dasgupta[2], Kaspar Althoefer[1], Lakmal Seneviratne[1]

[1] *Department of Mechanical Engineering, King's College London, London, U.K*

[2] *Department of Urology, Guy's Hospital & King's College London, Medical School, London, UK*

Introduction: This paper describes a comparative study between two novel tactile sensors used during minimally invasive surgery (MIS). The aim of these sensors is to provide tactile feedback concerning organ tissues in MIS that is not readily available due to the restrictions of MIS. The first sensor is an air-cushion tactile probe and the other is a wheeled indentation probe. The air cushion tactile probe (see Fig.1) consists of a 9mm sphere at the tip of a shaft that "floats" on a cushion of air when it is rolled over the tissue under inspection. The sensing element consists of an optical scheme that monitors the motion of the sphere along the longitudinal axis of the shaft. The wheeled indentation probe (see Fig.2) consists of a wheel of dimensions: 8mm in a diameter and 8mm wide. The sensing element is a Force/Torque sensor mounted above the wheel.

Methods: The experiments carried out to evaluate the capabilities of each probe consisted of establishing whether the probes could detect 3 embedded nodules in similar silicon phantoms. The air cushion tactile probe was attached to a Mitsubishi manipulator and was rolled over a silicone phantom under inspection along 13 individual parallel paths. The wheeled indentation probe was also rolled using the manipulator in parallel paths along a silicone phantom.

Results: The results of the air cushion tactile probe and the wheeled indentation probe are illustrated in Fig.3 and Fig.4, respectively.

Conclusion: It can be seen from Fig.3 and Fig.4 that both probes successfully detected the 3 embedded nodules in their respective silicone phantoms. The results are promising as these probes could be used in minimally invasive robotic surgery to provide haptic information on the mechanical properties of the tissues. This would permit surgeons to make well informed decisions on the dimensions and position of significant abnormalities such as tumours allowing for a reduction of the positive error margins during MIS.

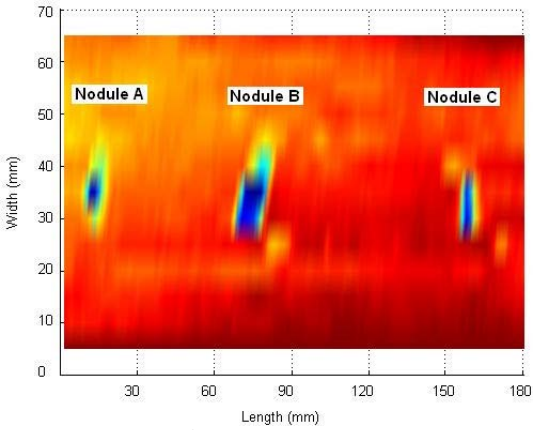

Fig. 3. Map of silicone block using air cushion probe

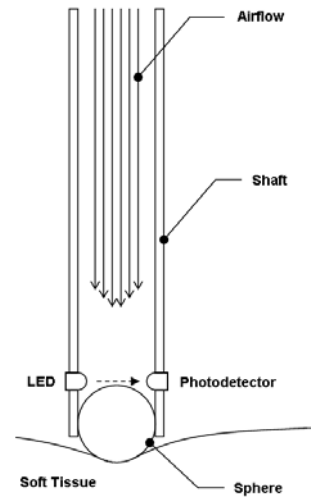

Fig. 1. Structure of the novel air-cushion sensor

Fig. 2. Structure of the cylindrical wheel-based force sensor.

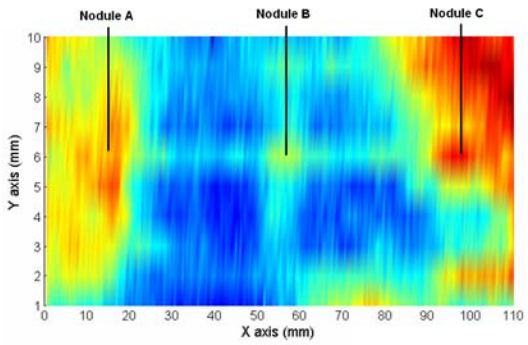

Fig. 4. Map of silicone block using wheel indentation probe

ABSTRACT 36

ENZYMATIC DISSOLUTION OF CALCIUM AND STRUVITE CRYSTALS: AN *IN VITRO* EVALUATION OF BIOCHEMICAL REQUIREMENTS

Nabil K. Thalji , Nigel G. Richards , Ammon B. Peck, Benjamin K. Canales

University of Florida, Gainesville, FL, USA

Introduction: Enzymatic digestion of renal calculi into more water-soluble salts could enhance lithotripsy, provide a painless alternative for poor surgical candidates, or be incorporated into stent materials for stone dissolution. We performed a preliminary evaluation of the factors affecting enzymatic dissolution rate of the mineral components of calcium oxalate monohydrate (COM), calcium phosphate (CaP), and magnesium ammonium phosphate (struvite) stones.

Methods: Oxalate decarboxylase (ODC) from *Bacillus subtilis* was used to dissolve 25 mg of COM crystals by converting sparsely soluble calcium oxalate to highly soluble calcium formate. Bacterial purine nucleoside phosphorylase (PNP) was used to dissolve 100 mg of CaP and struvite by catalyzing the phosphorolysis of inosine by mineral-derived phosphate. Dissolution of calcium-based crystals was monitored by measuring the increase in solution calcium concentration using a calcium ion selective electrode, while dissolution of struvite crystals was monitored by changes in the mass of insoluble mineral.

Results: For COM, a maximum dissolution of 6% was seen, and this did not vary when ODC levels were changed from 50 mcg to 200 mcg. On addition of the formate-catabolizing enzyme formate dehydrogenase (FDH) and nicotinamide adenine dinucleotide (NAD+), dissolution increased to 30%, suggesting that product inhibition by formate limits dissolution of COM crystals by ODC. Phosphate-containing minerals underwent 3% dissolution by 10 units of PNP, corresponding with literature values for the equilibrium constant of the reaction
Conclusion: Product inhibition and equilibrium position are two primary limitations to enzymatic stone dissolution. Both can be overcome by coupling the primary dissolution reactions to other enzymatic reactions whose equilibria favor product formation, reducing product concentration while driving equilibrium towards mineral dissolution. Future tests on human pure and mixed stones are needed to validate this preliminary work.

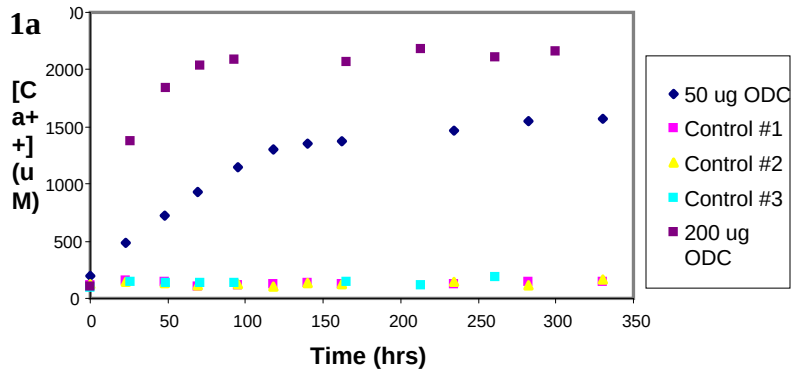

***Figure 1a**: Plot of calcium concentration over time as a measure of CaOx crystal dissolution by ODC. Both amounts of enzyme led to nearly the same dissolution level (2000 μM Ca++ corresponds to 6% of the total CaOx or 1.5 mg). Higher amounts of ODC led to faster initial dissolution rates.*

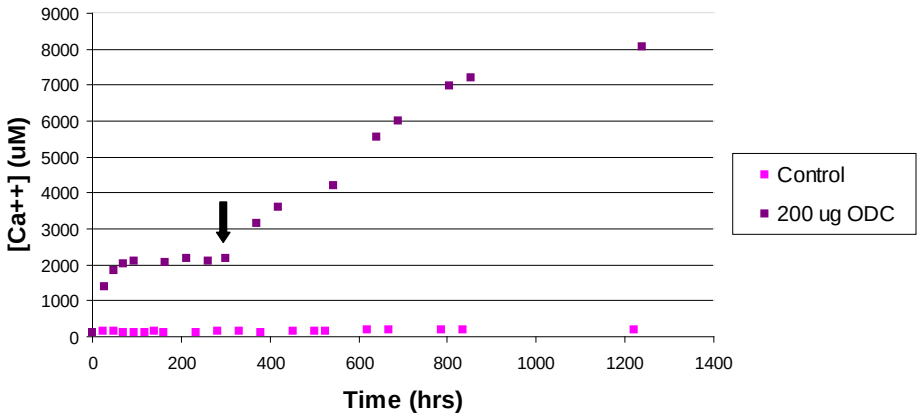

***Figure 1b**: Plot of dissolution of CaOx crystals by ODC before and after addition of FDH and NAD+ (bold arrow indicates addition of coupling reagents). The rise in Ca++ ion concentration suggests that formate inhibits ODC and that dissolution levels near 30% can be achieved by this coupling reaction.*

ABSTRACT 37

STEREOTACTIC PERCUTANEOUS CRYOABLATION FOR RENAL TUMOR: INITIAL CLINICAL EXPERIENCE

Haber GP, Crouzet S, O'Malley C, Remer E, Kamoi K, White W, Goel R, Kaouk J
Section of Laparoscopic and Robotic Surgery, GUKI, Cleveland Clinic, OH, USA

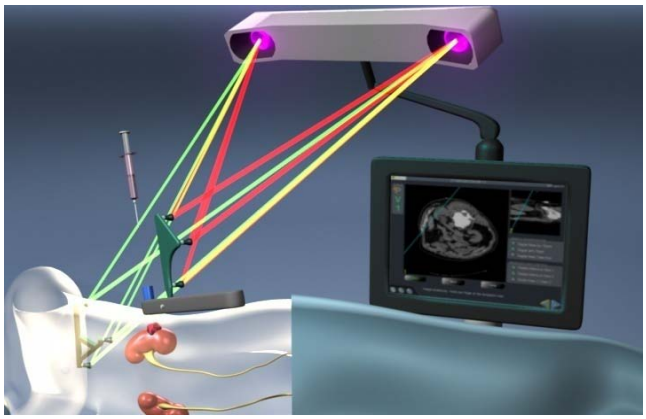

Introduction: Percutaneous image guided needle ablation is assuming an increasingly prominent role in the minimally invasive treatment of renal tumors. Precise needle placement is essential for successful ablation. CT-Nav® developed in collaboration with Koelis (Grenoble, France) is a novel stereotactic surgical navigation system that has the potential to achieve precise percutaneous needle placement while reducing radiation exposure compared to conventional CT-guided procedures.

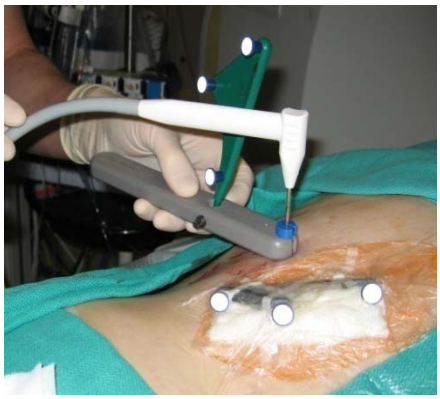

Methods: The system comprises a tracking sensor, targeting handle, stereoscopic infrared camera, and a personal computer. Using a point/area matching and registration protocol, the tracking sensor is automatically recognized in the 3D CT volume data. The infrared camera detects the tracking sensor and localizes it 3-dimensionally. Any movement of the patient is detected by the movement of the tracking sensor allowing real-time readjustment of the CT volume coordinates. The targeting handle is then used to navigate through the CT scan and guide the needle pecutaneously to the targeted tumor. The optimal trajectory is subsequently saved by the CT-Nav® system. A prospective pilot study was performed to evaluate the technical feasibility, safety, and accuracy of the CT-Nav® system during renal cryoablation. Demographic and perioperative data were obtained prospectively. Needle placement accuracy was measured in the 3 axes.

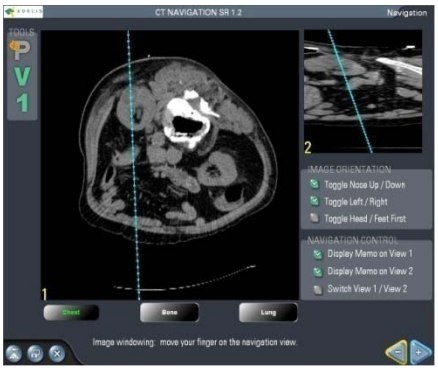

Results: A total of 13 tumors in 10 patients successfully underwent cryoablation using the novel navigational system. Mean tumor size was 2.2 cm. Tumors were located in various renal locations. Preoperative biopsy demonstrated RCC in 6 cases. Mean operative time was 155 min. No intraoperative or postoperative complications were noted. Mean length of stay was 9.5hrs. A mean decrease in CT fluoroscopy duration of 18.3 sec was noted for each probe placed. Mean targeting registration error was 4.2mm.

Conclusion: Based on our experience, stereotactic percutaneous cryoablation of renal tumors offers safe and precise needle placement while simplifying the procedure and reducing radiation exposure compared to traditional CT guidance.

ABSTRACT 38

ROBOTIC VERSUS LAPAROSCOPIC PARTIAL NEPHRECTOMY: A SINGLE SURGEON MATCHED COMPARISON OF 100 CASES

Georges-Pascal Haber, Wesley M. White, Raj K. Goel, Sebastien Crouzet, Kazumi Kamoi, Jihad Kaouk
Section of Laparoscopic and Robotic Surgery, GUKI, Cleveland Clinic, OH, USA

Objective: To compare a single-surgeon experience of Laparoscopic Partial Nephrectomy (LPN) and Robotic Partial Nephrectomy (RPN) in matched populations.

Materials and Methods: Between 06/2006 and 02/2009, 50 patients underwent RPN for radiographic evidence of an enhancing renal mass. Outcomes were then compared retrospectively to 50 matched patients who underwent LPN. Patients were matched for demographics, comorbidities, tumor specifications, and clamping technique. Preoperative, intraoperative and postoperative data were measured and compared. A learning curve for the RPN group was formulated.

Results:

	LPN (n=50)	RPN (n=50)	*p*
Preoperative Data			
Male/ Female	26/24	28/22	*0.84*
Age (yrs)	48	52	*0.57*
BMI(Kg/m2)	28	29	*0.64*
ASA	2.4	2.4	*0.89*
CCI	0.68	0.74	*0.7*
Side R/L	30/20	23/27	*0.16*
Tumor size (cm)	2.3	2.6	*0.24*
Inter/Lower/Upper Pole (n)	10/18/22	13/20/17	*0.56*
Preoperative eGFR (ml/mn)	78	83	*0.33*
Early/Conventional/Unclamped(n)	26/14/10	26/12/12	*0.84*
Intraoperative Data			
OR time (mn)	184	202	*0.04*
EBL (cc)	218	334	*0.09*
WI time (mn)	19.1	16.5	*0.25*
LOS (days)	4.3	4	*0.54*
Intraoperative Complications (n)	0	0	-
Conversion to laparoscopy (n)	-	2	-
Conversion to open	1	0	*0.31*
Postoperative Data			
% eGFR Change	-8.51%	-8.91%	*0.98*
Postoperative Complications (n)	6	8	*0.56*
RCC (n)	43	46	*0.34*
Positive Surgical Margin (n)	0	0	-

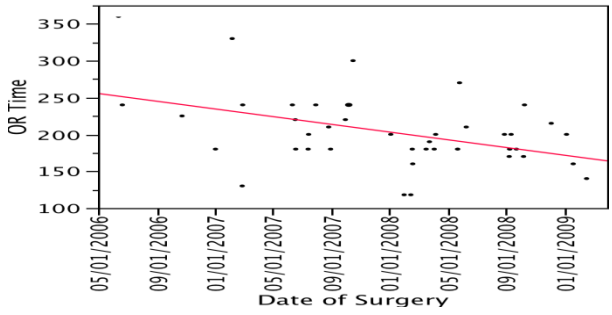

RPN: Learning Curve OR time *(p=0.002)*

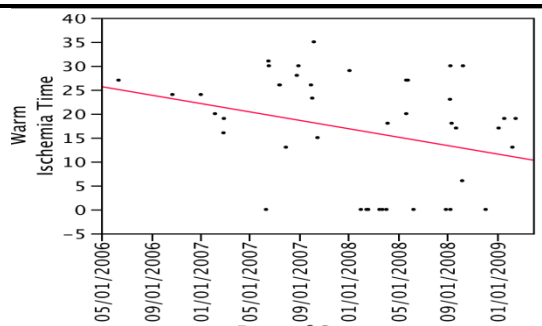

RPN: Learning Curve WI time *(p=0.04)*

Conclusion: Based on our experience, RPN offers comparable outcomes to LPN with an acceptable learning curve. With improved technique and burgeoning robotic experience, we expect RPN to assume a prominent role in the management of small renal masses.

ABSTRACT 39

LAPAROENDOSCOPIC SINGLE SITE (LESS) SURGICAL TOOLBOX: INSTRUMENTS, SCOPES, AND PORTS

Haber GP, White WM, Crouzet S, Kamoi K, Goel RK, and Kaouk JH
Glickman Urological and Kidney Institute, Cleveland Clinic, Cleveland, OH

Objective: To offer a practical summary of the available tools used during LESS surgery.
Methods: With over 100 LESS urologic procedures completed at our institution, we provide an experience-based synopsis of the available LESS equipment.
Results: See Table.
Conclusions: Despite evolving and ever improving surgical equipment for use during LESS surgery, there exists a continued and pressing need for more ergonomic, adaptable, and reliable purpose-built instruments.

Ports	Specifics	Advantages	Disadvantages
R-Port 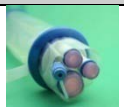	Multichannel valve (one 12mm, two 5mm) covered with an elastomer which maintains pneumoperitoneum.	-Flexible -Adapts to size of incision	-Fragile -Requires lubrication
Uni-X 	Cone-shaped plastic outer unit converging on three separate 5mm inlets.	-Venting -Curved instruments	-Fascial sutures -5mm ports only -Rigid
GelPort 	A wound protector, base plate and an external gel piece (unique soft gel-like material) that allows instrument passage.	-Ease of instrument exchange -Hand access	-Larger incision -Must use ports in addition to GelPort -Expense
SILS 	The flexible port accepts (3) 5mm cannulas or (2) 5mm cannulas and a 5mm-12mm port.	-Improved instrument spacing	-Suture passage difficult during robotic LESS
AirSeal 	Oval cannula with invisible pressure barrier	-No valves -Stable CO_2 pressures	-Rigid -Air pump -Only 2 instruments
Scopes	**Specifics**	**Advantages**	**Disadvantages**
EndoEYE HD 	Digital videoscope: 5mm, 30° All-in-one construction CCD chip at the distal tip	-Low profile -Image quality	-Inadvertent activation of functions
EndoEYE LTF 	Articulating Digital videoscope: 5mm All-in-one construction CCD chip at the distal tip	-Can position image off-axis	-Unstable image -Requires skilled assistant
Standard Scopes 	Conventional 5mm, 30° scope	-Ease of access -Cost	-External bulk
Instruments	**Specifics**	**Advantages**	**Disadvantages**
Roticulator 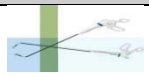	Hand-held articulating operating instruments with 80 degrees of freedom	- Not Tested	-Not Tested -No hook cautery
Pnavel 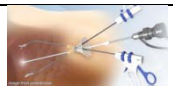	Hand-held fixed instrument with rotating tip	-Stability -Rigidity	-Lack of articulation -Poor tissue control
RealHand 	Hand-held instruments with full range of motion mirroring hand movement	-Low profile handle	-Locking mechanism not intuitive
Cambridge 	Hand-held articulating instruments with locking handle	-Wide array of products	-Bulky handles lead to external clashing

ABSTRACT 40 **OUTSTANDING PAPER AWARD**

IN VITRO TEST OF AN AUTOMATED CYSTOSCOPIC PROCEDURE FOR BLADDER SURVEILLANCE

W. Jong Yoon[1], Sangtae Park[2], Per G. Reinhall[1], Eric J. Seibel[1]
[1]*Department of Mechanical Engineering, University of Washington, Seattle, WA*
[2]*Section of Urology, Department of Surgery, University of Chicago Pritzker School of Medicine*

Introduction: We report an *in vitro* experiment of a highly flexible and pre-programmable cystoscopy system designed to automatically scan the interior surface of the bladder to increase the completeness of the examination, primarily for cancer detection and surveillance.

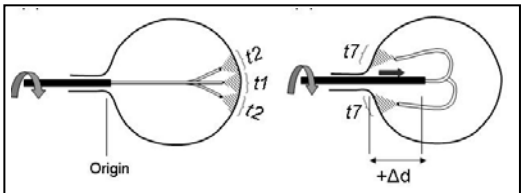

Fig. 1. Manipulations of the position and orientation of the imaging probe in the bladder use a controlled shaft arc, insertion depth, and rotation. Rigid portion of the shaft is black while flexible part is gray. Shaded areas illustrate the portion being imaged at times *t1*, *t2*, and *t7*.

Methods: An automated active steering mechanism is integrated with an extremely flexible 1.6-mm outer diameter imaging probe. The scanning fiber endoscope (SFE) developed at the University of Washington Human Photonics Lab provides > 70° field-of-view and a large range of depth of focus and uses red-green-blue low-power laser scanning to generate 500-line color images at video rate (30Hz). In order to manipulate the position and orientation of the imaging probe to ensure that the entire inner surface of a distended bladder is scanned to produce images, two independently controllable series of three shape memory alloy (SMA)-based segmental actuators are designed. The fully removable actuator set is disposed adjacent to the distal end of the imaging probe and they are selectively activated to produce a deflection of the imaging probe in a prescribed configuration. As depicted in Fig. 1, the probe is inserted straight and images the distal bladder, then the tip is actively deflected, followed by a 360° rotation. A second bending occurs followed by another complete rotation, which is repeated over 5 more times to examine the entire urothelium. A highly flexible polyurethane outer sheath reduces the flexural rigidity of the probe shaft which enables imaging of the bladder neck vicinity. A computed tomography (CT) cystogram of a female patient's bladder filled with 300cc fluid was used to construct a 3-D plastic phantom bladder which was used as a proof-of-concept *in vitro* model for testing the distal imaging tip trajectory (Fig.2a). This test was conducted in an open-air environment. Future testing will be in a saline environment and the addition of fluorescence imaging is straightforward using SFE.

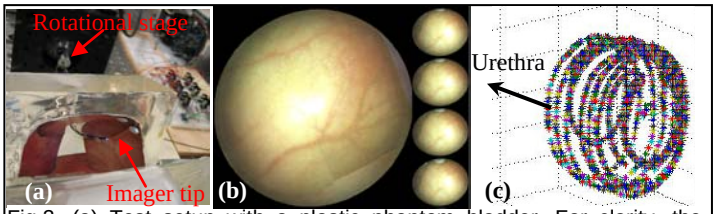

Fig.2. (a) Test setup with a plastic phantom bladder. For clarity, the plastic model is cut in half and the deflected SFE actuating part is shown. (b) A captured SFE sample image from the low-contrast/resolution printout surface of the phantom bladder and exemplary video frames out of seven videos captured from the phantom bladder (c) 3-D tracked tip locations of a mock-up SFE probe[1]

Results: This flexible bench-top imaging system provided more than 180º of tip bending with 10-mm bend radius compared to the previous prototype and commercial flexible ureteroscopes which have a minimum bend radius of 15-mm and 20-mm, respectively. Fig.2b shows an exemplary image of the phantom surface captured by the SFE during the automated imaging procedure. The object is a low-contrast/resolution printout mosaic from a cystoscopy procedure. Seven separate video clips were taken from parametrically defined 3-D imaging trajectories obtained from the seven optimal tip locations and rotational motion. We acquired a 5.1 % tip positioning error compared to the simulation trajectory using the 2-D coordinate data from the electromagnetic tracking system[1]. To verify full coverage of the bladder surface, the 3-D tracked tip trajectory of the mock-up probe was collected and the results support that the proposed configuration covered the entire surface of the bladder (Fig.2c). The design requirements used for the optimal trajectory included the minimal number of tip positions, imaging coverage overlap (20 ~ 30 %), distance from the wall (10 ~ 15-mm), and viewing angle (> 60º). The independently controllable segmental actuators resulted in more selection of tip locations for orthogonal viewing. For example, some shaft configurations that are not possible from the conventional wire pulling bending system have been observed.

[1] W. Jong Yoon, Sangtae Park, Per G. Reinhall, and Eric J. Seibel, Development of an automated steering mechanism for bladder urothelium surveillance (on-line), *ASME Journal of Medical Devices*, Volume 3, Issue 1, March 2009.

ABSTRACT 41

A THERM-SENSITIVE REMOVABLE METALLIC PROSTATE STENT FOR THE MANAGEMENT OF BLADDER OUTFLOW OBSTRUCTION (BOO)— EXPERENCE FROM THREE CENTERS IN TWO COUNTRIES

[1]Papatsoris AG, [2]Sawada Y, [3]Takahashi T, [1]El-Husseiny T, [1]Maan Z, [1]Moraitis K, [1]Masood J, [1]Junaid I, [1]Buchholz N

Departments of Urology: [1]Barts and The London NHS Trust, London, UK; [2]Sawada Clinic, Yoshiaki Sawada, Japan; [3]Kitamurayama Hospital, Tsutomu Hamazaki, Japan

Objective: We present our long-term experience with the use of a novel thermo-sensitive metallic prostate stent for the management of bladder outflow obstruction (BOO).

Material and Methods: Since 2001, 88 patients aged 47 to 92 years old (mean 76.2) with BOO due to benign prostatic hyperplasia (77 patients) or prostatic carcinoma (11 patients) were treated with the insertion of a thermo-sensitive metallic prostate stent (Memokath 028®, PNN Medical, Copenhagen/ Denmark). This prostate stent is a coil of a nickel-titanium alloy and has shape memory with the proximal end expanding when flushed with heated (~55°C) normal saline (a deformed piece of alloy is restored to its original shape by increased temperatures). The Memokath stent has a tight spiral structure which prevents urothelial in-growth between the coils. The lack of outward pressure lessens the risk of secondary ischemic injury to the urethra.
Local anesthesia and flexible cystoscopy were used in the majority of the procedures (71.6%), which were performed as day cases. In the majority of patients (n=63; 72%), an indwelling catheter was present prior to the stent insertion. In 50.7% of the patients the American Society of Anesthesiologists (ASA) score was 3, while in 40.8% the ASA score was 2. In case patients were on anticoagulation medication this did not need to be discontinued. Follow up consisted of flow rate studies and measurement of the residual urine volume (RUV).

Results: Follow up ranged from 11 to 92 months (mean 59.3). During the follow up the mean maximum flow rate increased by 7 ml/sec (mean pre-op: 7.6; post-op: 14.6), while the mean RUV decreased by 97.6 ml (mean pre-op: 120.5; post-op: 22.9). There were no statistically significant differences between outcomes in patients with benign prostatic hyperplasia and prostate cancer. The mean stent indwelling time was 9 months. At the time of data analysis 64.3% of patients had a stent in situ. In 53.7% of cases the stent had been removed and/or exchanged due to stent migration (15.1%), penile pain (10.1%), BOO symptoms recurrence (8.5%), encrustation (7.5%), urinary incontinence (3.8%), tissue granulation (2.8%), recurrent urinary tract infections (2.8%), or urethral stricture (2.8%). Removal and/or exchange were found easy and quick in all cases.

Conclusions: The thermo-expandable metallic prostatic stent (Memokath®) is an effective minimally invasive treatment of BOO. Flow rate study parameters and RUV were significantly improved after the stent insertion. However, in all centers there was a negative selection of patients given the high risk score and the high number of patients with urinary retention and indwelling bladder catheters. Not surprisingly, in nearly half of the patients the prostatic stent had to be removed and/or exchanged due to long-term complications at some stage during follow-up. This should however not discourage its use. We are currently developing a standardized treatment protocol which together with a refinement of indications will certainly improve results further.

ABSTRACT 42

ROBOTIC INSTRUMENT INSULATION FAILURE: INITIAL REPORT OF A POTENTIAL SOURCE FOR PATIENT INJURY

Adam C. Mues, Geoffrey N. Box, Ronney Abaza
The Ohio State University, Department of Urology

Introduction: At this time there is a reportedly low rate of mechanical failure for the da Vinci robotic surgery system. Similarly, there is no data in the literature regarding failure of robotic instruments or associated equipment. In order for failure to be identified, a high case volume is necessary. As a high-volume robotic surgery center and an institution with an experience of over 2,000 robotic cases, we identified a previously unreported defect in a robotic instrument accessory with the potential for serious patient injury. We report our experience with failures in the insulating robotic cautery instrument tip cover reviewing both the incidence of failure and patient complications that have resulted.

Methods: All da Vinci robotic procedures performed at our institution since the first report of failure were reviewed. This included procedures done in urology, gynecology, cardiothoracic surgery, general surgery, otolaryngology, and neurosurgery. All failures were documented in writing at the time of the incident by the surgeon and collected by a designated member of the robotic surgery team. All failures were recorded regardless of whether or not a surgical or post-operative complication occurred and all tip covers were collected and inspected.

Results: Our database identified 454 robotic assisted cases performed after the first reported failure in July 2008 through January 2009. The majority of procedures were performed by urology (59.7%) followed by gynecology (30.0%). There were a total of twelve accessory tip cover failures that occurred over this time period for a failure rate of 2.6%. All failures involved burn defects in the insulating cover (image below) that were identified by inadvertent cautery of tissue by the shaft of the instrument. All cases in which failures were identified involved urologic and gynecologic procedures, such that the failure rate within these specialties alone was 2.9%. Three out of twelve failures (25%) led to significant patient injuries including bowel injury, external iliac vein injury, and ureteral injury requiring reimplantation.

Conclusion: Robotic accessory tip cover failures occur at a significant rate of 2.6% and lead to patient injury in 25%. Additional testing is required to identify the cause of failure and to ensure patient safety. Evaluation for the cause of failures is currently being investigated at our institution, including in the laboratory setting, in order to provide preventative measures to other institutions performing robotic surgery.

ABSTRACT 43

MICROFABRICATION OF HEAT-SENSITIVE MICROBUBBLES FOR ABLATION MARGIN ASSESSMENT

Jiwei Huang[1], Jeff Xu[2], Ronald Xu[2*]

[1]Biophysics Graduate Program, [2]Biomedical Engineering Department
The Ohio State University, Columbus, OH 43210, USA
** xu.202@osu.edu*

Thermal ablation processes hold the promise of less invasive cancer management with outpatient treatments, minimal trauma to the patient, and improved recovery time to normal activities. However, broader acceptance of cancer ablation processes is hindered by controversial issues and concerns related with clinical safety, efficacy, and long-term local recurrence. These concerns are due to the lack of intraoperative assessment of the ablation margin.

We developed a heat-sensitive microbubble contrast agent for intraoperative imaging of ablation margin. The contrast agent was fabricated by encapsulating low boiling point compounds such as perfluorocarbon (PFC) into poly (lactic-co-glycolic acid) (50:50) (PLGA) microbubbles. At the temperature threshold for tissue coagulation, the volume of heat-sensitive microbubbles will expand significantly, allowing for intraoperative assessment of the ablation margin by clinical ultrasound and other imaging tools. Technical feasibility of using heat-sensitive microbubbles for ablation margin assessment was demonstrated by microscopic and ultrasound imaging results in Figure 1.

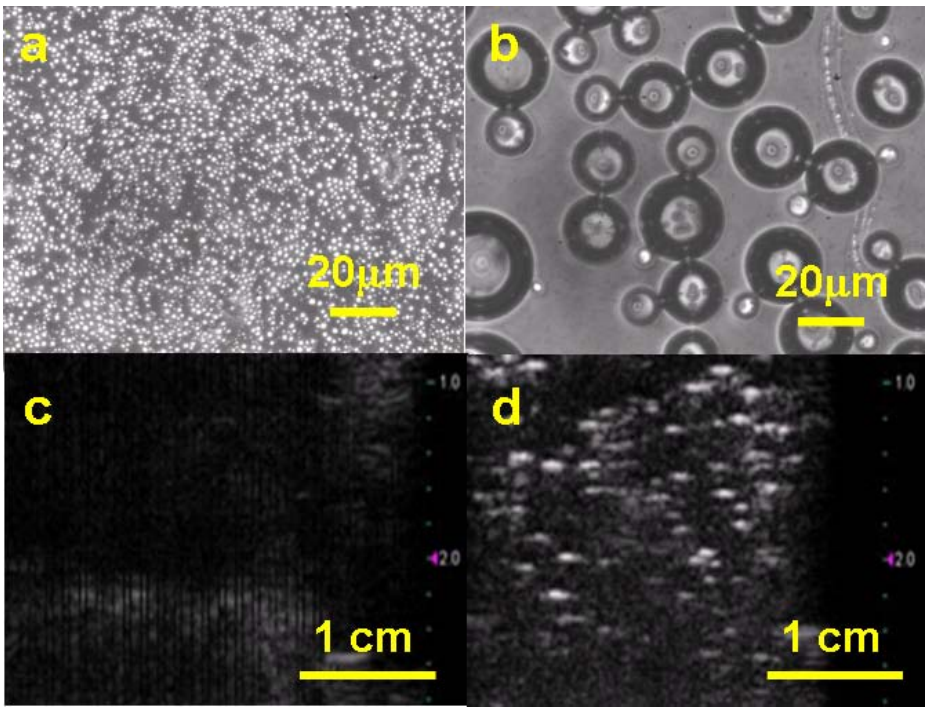

Figure 1. Images of heat-sensitive microbubbles: (a) microscopic image at 25°C, (b) microscopic image at 55°C, (c) ultrasound image at 25°C, (d) ultrasound image at 55°C.

ABSTRACT 44

ICE BURN: PROTECTING THE FLANK DURING RENAL CRYOTHERAPY

Jennifer L. Young, Surendra B. Kolla, Donald L. Pick, Petros Sountoulides, Oskar G. Kaufmann, Victor B. Huynh, Adam G. Kaplan, Cervando G. Ortiz-Vanderdys, Kathryn E. Osann, Lorena A. Andrade, Elspeth M. McDougall Ralph V. Clayman

University of California, Irvine, USA

Introduction and Objective: Cryoablation is being used more commonly to treat small renal masses in situ. The most common complaint after renal cryotherapy is pain and paresthesias at the cryoprobe insertion site (Figure 1). We investigated the protective effects of a 14 gauge angiocatheter as a possible insulating sheath during renal cryotherapy (Figure 2).

Methods: Six Yorkshire pigs underwent laparoscopic-guided percutaneous cryoablation of the upper and lower pole of each kidney. Cryolesions were created with a single 1.47 mm IceRod using a Precise cryoablation unit (Galil Medical, Plymouth Meeting, PA) with pressurized argon at 4,300 psi. Each site underwent two ten minute freeze cycles separated by a five minute active thaw with pressurized helium at 2,200 psi. Each trial was randomized with a random number generator to either a bare probe or probe placement through a preplaced 14 gauge angiocatheter. Flank temperatures were recorded at 5 and 15 mm using a multithermal sensor.

Results: Twelve trials were completed with a sheath; twelve trials were done without a sheath. There was a trend toward statistical significance of sheath insulation ranging from 3 to 10ºC at freeze 2 at both the 15 mm (p=0.07) and 5 mm (p=0.08) temperature sensors (Table I).

Conclusions: A 14 gauge angiocatheter provides some insulation and thereby might help protect against "ice burn" during renal cryotherapy.

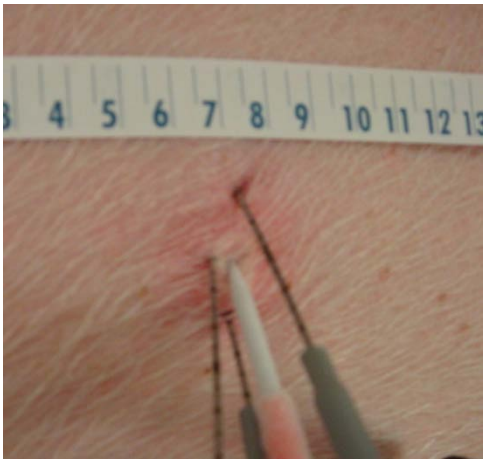

Figure 1. Freeze in progress without sheath, "ice burn" is visible.

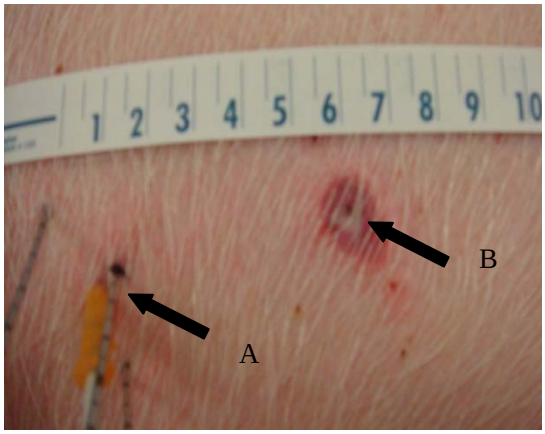

Figure 2. Freeze in progress with angiocatheter (A), no "ice burn" noted; where a bare probe was used (B), "ice burn" is present.

Table I. Flank Temperatures with and without a 14 Gauge Angiocatheter

	Outer sensor				Inner sensor			
	Baseline	**Freeze 1**	**Thaw**	**Freeze 2**	**Baseline**	**Freeze 1**	**Thaw**	**Freeze 2**
No sheath (^{o}C) Mean (range)	37 (29-40)	18 (7-31)	32 (27-36)	11 (-5-21)	37 (34-40)	18 (-2-34)	33 (30-38)	11 (-26-30)
Sheath (^{o}C)	37 (30-39)	22 (14-36)	32 (26-38)	17 (7-36)	38 (34-40)	21 (-21-36)	33 (25-38)	21 (3-35)
p value	0.59	0.15	0.95	0.07	0.74	0.57	0.85	0.08

ABSTRACT 45

ANALYSIS OF INFECTIOUS STONES: VARIABILITY OF LABORATORY ANALYSIS

Amy E. Krambeck[1], Naseem F. Khan[2], Molly E. Jackson[2], James E. Lingeman[1], James C. Williams, Jr.[2]

[1]Methodist Hospital Institute for Kidney Stone Disease [2]Indiana University School of Medicine
Indianapolis, Indiana

Introduction: Medical and surgical treatment of patients with urolithiasis can greatly vary depending on the reported stone composition. Specifically, a more diligent approach to surgical removal of all fragments and prolonged administration of antibiotics will be undertaken if an infectious component is identified. Furthermore, the co-existence of struvite with calcium oxalate implies an underlying metabolic disorder. The goal of this study was to determine the accuracy of infection stone composition analysis by major commercial laboratories.

Methods: Forty-six human renal stones with known compositions determined by infrared spectroscopy (IR) were hand fragmented into six aliquots and studied with micro computed tomography (CT) to ensure similar fragment compositions. Only 26 stones had fragments similar enough to be considered identical. The identical fragments were submitted to 1 research and 5 commercial laboratories for blinded analysis.

Results: Of the 26 stone submitted for analysis, 5 (19.2%) had an original IR interpretation of struvite (magnesium ammonium phosphate) mixed with either carbonate apatite (CA) or ammonium acid urate (AAU) prior to fragmentation. Of these 5 stones, only 2 (40%) were identified as having struvite as a component by all blinded laboratories; however, in none of the stones did all labs identify struvite as the main component ($\geq$ 50% of the composition). Of the 5 stones, 3 (60%) were also reported as having a metabolic calcium oxalate monohydrate (COM) component: 2 labs for 1 stone and 1 lab for the 3rd stone. Furthermore, struvite was reported as a component by some, but not all, labs for 4 stones not thought to contain struvite pre-fragmentation: 3 apatite and 1 atazanavir. The atazanavir was reported as a mixed stone by all labs with a total of 7 different crystal components and only 1 lab identified the atazanavir component. Overall, there was disagreement among the labs over the presence or absence of struvite in 7/26 (26.9%) stones.

Conclusion: This study demonstrates a tremendous variability in analysis of infection stones. In this study the presence of struvite was not agreed upon by all the labs in over 1/4 of the overall cohort. Furthermore, the presence of a metabolic component mixed with struvite was also not agreed upon in 10%. Such variability of laboratory results has important implications for the long-term management of these patients.

ABSTRACT 46

DRILLING THROUGH THE IMPACTION: POSSIBLE USE OF AN ATHERECTOMY DRILLING DEVICE FOR UROLITHIASIS

David A. Lifshitz, Sergey Shikanov, Arieh L. Shalhav, Kevin C. Zorn
Section of Urology, Department of Surgery, University of Chicago Medical Center, Chicago, Illinois, USA

Introduction and objectives: The Rotablator® (Boston Scientific) is an angioplasty device which is passed over a wire. It uses a high speed rotational "burr" (2 mm in diameter) that is coated with microscopic diamond particles and cooled by saline . It rotates at high speed (approximately 200.000 rpm) breaking up blockage into minute (smaller than red blood cells) fragments. We investigated, *in vitro,* the possible use of the Rotablator® for urinary stone disease.
Methods: Human stones of different sizes and composition were used for the experiment. Stone impaction in vitro was modeled by wedging the stones into the proximal part of a silicon Foley catheter (Fig. 1a,b). Likewise, an *ex vivo* study was performed on stones placed into a freshly harvested swine ureter using a nitinol basket (Fig 2). Data regarding the drill time, remaining stone size, and ureteral damage were collected.
Results: Overall 15 stones were treated (10 *in vitro* and 5 *ex vivo*). The device drilled through all the stones allowing complete passage of the burr. The pre-treatment mean stone size for the silicon and ureteral testing was 65 mm^2 and 34 mm^2, respectively. The post-treatment size was 54 mm^2 and 24 mm^2, respectively. No change, but the drilled hole, was noted in 4 stones. Average treatment time was 100 seconds. No visual macroscopic ureteral damage was observed.
Conclusions: *In vitro* the Rotablator® is capable of drilling through stones with minimal damage. However, stone fragmentation is minimal. Further studies are required to investigate the use of the Rotablator® for the fluoroscopic-guided passage of ureteral impaction in difficult clinical settings.

Figure 1a: Rotablator® in vitro model

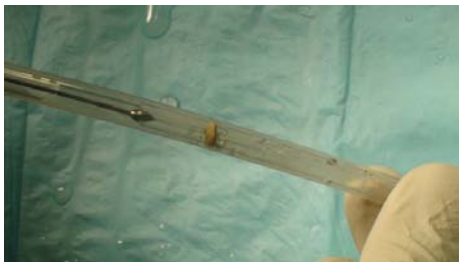

Figure 1b: View of a drilled stone

Figure 2: View a drilled ureteral stone after the ureter was incised open

ABSTRACT 47

SHOCK WAVE ADMINISTRATION RATE - IS SLOWER REALLY BETTER ?

Thorsten Bergsdorf, Christian Chaussy, Stefan Thueroff

Department of Urology, Klinikum Harlaching, Munich, Germany

Introduction: Most users perform ESWL with a fixed shock wave administration rate of 90 or 120 SW/min., to achieve a short treatment time. In-vitro experiments and clinical studies suggest that a lower shock wave frequency results in a better disintegration due to a reduction of cavitation in the shock wave propagation path. It was aim of our in-vitro setup, to evaluate the quantitative effect of a reduction of shock wave administration rate in regard to disintegration efficacy.

Methods: Artificial stones (AST 0118), located in a basket with 2 mm mesh were positioned in a water tank on a commercially available lithotripter (SIEMENS Lithoskop®) and exposed to shock waves until complete disintegration. The total number of shock wave impulses, required for complete stone comminution was assessed with different shock wave administration rate (30, 45, 60, 90, 120 SW/min.). All experiments were performed with the same shock wave energy (E+12 mm: 31 mJ) and performed three times for every shock wave frequency.

Results: The *in vitro* experiment displayed a linear correlation between shock wave frequency and required number of shock wave pulses for complete stone fragmentation (regression analysis, CI 95 %, R-Sq (ad) 87,7 %). A reduction of the shock wave administration rate (SW/min.) leads to an increase of the disintegration effect. 60 SW/min. instead of 90 SW/min. showed a 10 % reduction of shock wave pulses required for complete stone breakage.

Conclusion: The reduction of shock wave administration rate is an easy and effective measure, to improve the efficacy of ESWL. The decreased number of shock wave pulses, needed for stone comminution will compensate the longer treatment time partially and will be beneficial in regard to tissue injury. Main goal should be an efficient and not a fast ESWL.

ABSTRACT 48

BOVINE SERUM ALBUMIN GLUTARALDEHYDE FOR COMPLETELY SUTURELESS LAPAROSCOPIC PARTIAL NEPHRECTOMY IN A UNIQUE SURVIVAL PORCINE MODEL

Michael K. Louie[1], Aldrin J. Gamboa[1], Rachelle J Lin[1], Adam G Kaplan[1], Amanda Khosravi[1], Hung P Truong[1], Reza Alipanah[1], Lorena A Andrade[1], Cervando G Ortiz[1], David McCormick[1], Geoffrey N Box[2], Hak J Lee[1], Leslie A Deane[3], Robert A Edwards[1], Elspeth M McDougall[1], Ralph V Clayman[1]

[1] *University of California, Irvine Medical Center, Orange, CA*
[2] *Ohio State University Medical Center, Columbus, OH*
[3] *University of Illinois, Chicago Medical Center, Chicago, IL*

Introduction: Due to technical challenges, laparoscopic partial nephrectomy (LPN) has yet to receive widespread clinical application. Bovine serum albumin glutaraldehyde (BSAG) is a hemostatic agent that crosslinks albumin to tissue surface proteins. We created a unique sagittal heminephrectomy as a worst case scenario for partial nephrectomy to test BSAG as the sole agent for parenchymal and collecting system closure during LPN in a survival porcine model.

Methods: 18 Yorkshire pigs, after hilar clamping, underwent LPN by sagittal cold excision of the lateral one-third to one-half of the entire right kidney as developed by Deane. The opened collecting system was covered with oxidized cellulose to prevent BSAG seepage into the urinary tract. BSAG was applied onto the dried wound surface and allowed to set for 10 minutes. BSAG only closure of the LPN defect was performed in 12 animals; 6 control pigs were acutely studied in the same manner as the BSAG kidneys but with saline as the sole closure method. Urinary extravasation was evaluated by parenteral furosemide and indigo carmine injection. A bleeding score (from 0 to 3) was assigned after removal of the hilar clamps. At 6 weeks, BSAG closed kidneys were harvested for burst pressure testing and histological analysis.

Results: All 12 LPN pigs undergoing BSAG closure survived to 6 weeks. A second BSAG application was needed in 5 of 12 LPN pigs to achieve a bleeding score of 0 or 1. All 6 control pigs bled with saline only closure, followed by BSAG closure and nephrectomy. In all pigs, application of BSAG effectively sealed the arterial and collecting system, and exceeded physiological arterial and collecting system pressures, respectively. At 6 weeks, harvested BSAG kidneys had a pseudocapsule covering the excision site. Histology showed inflammatory giant cell reaction to BSAG, but organized scar on the renal parenchyma.

Mean Percentage of Kidney Removed by LPN by Weight	27% (10 - 70%)
Mean Total Clamp Time	29 min (22 – 41 min)
Mean Bleeding Score (0=no bleeding, 1=mild, 2=moderate, 3=severe)	1.1 (0 – 3)
Mean Estimated Blood Loss	10.5 mL (0 – 50 mL)
Extravasation after initial BSAG closure	0
Median Arterial Burst Pressure	270 mmHg (210 – 420 mmHg)
Median Collecting System Burst Pressure	178 mmHg (60 – 610 mmHg)

Conclusion: Bovine serum albumin glutaraldehyde for completely sutureless laparoscopic partial nephrectomy is feasible in a worst case scenario survival porcine model.

ABSTRACT 49

INTRAVESICAL PROSTHETIC MATERIALS: *IN VITRO* AND *IN VIVO* (RABBIT) ENCRUSTATION AND BIOCOMPATIBILITY

D. Pick[1], A Khosravi[1], MK Louie[1], AJR Gamboa[1], W Chu[1], A Lau[1], R Lin[1], H Truong[1], R Alipanah[1], L Andrade[1], C Ortiz[1], DR Tyson[2], JF Borin[3], AF Yee[1], FG Shi[1], JC Earthman[1],EM McDougall[1], and RV Clayman[1].

[1] *University of California – Irvine, Departments of Urology and Earth Sciences*
[2] *Vanderbilt University School of Medicine*
[3] *University of Maryland Medical Center*

Introduction: In searching for the optimal inert material for prosthetic bladder reconstruction, we noted the resistance of titanium to encrustation when placed in the bladder. As such we tested 6 substances, 3 containing titanium, *in vitro* and *in vivo* for both biocompatibility and encrustation. *In vivo* rabbit studies were completed using a technique originally developed by Borin *et al.*

Methods: Medical grade silicone (MS), titanium alloy, stainless steel, proprietary silicone (PS) (F. Shi), PS impregnated with high concentration titanium oxide, and PS impregnated with low concentration of titanium oxide were tested as 8 mm discs strung with 2-0 monofilament suture and fixed in randomized positions along the strand. Medical grade silicone acted as the control material in the center of each strand. Strands were sterilized and placed in constantly stirred artificial urine at 37°C for 7 days. At harvest, strands were air-dried for 48 hours prior to weighing individual discs. In vivo, similar strands were implanted, and then harvested at 7 days from the bladders of 12 rabbits. Biocompatibility of each of the materials was evaluated using Teu-2 (human ureteral epithelium) cell culture and colorimetric cytotoxicity assay (MTT assay).

Results: *In vitro* results showed the least encrustation for PS ($p < 0.01$), over the other materials compared to the MS control. *In vivo* results showed encrustation equivalence of PS to MS control ($p=0.63$), but showed a trend of decreased encrustation compared to titanium ($p=0.33$). Biocompatibility testing using MTT assay revealed strong composite-cell adhesions and colonization of cultured cells for all materials except stainless steel and titanium alloy which exhibited significant cytotoxicity ($p < 0.05$).

Conclusion: A newly developed proprietary silicone resisted early encrustation more than medical grade silicone or titanium based materials both *in vitro* and *in vivo*. Furthermore the silicone materials were more biocompatible than the titanium constructs.

ABSTRACT 50

VESICAL MICTURITION MODIFIED CYSTOMETRY: AN INNOVATIVE WAY TO DECREASE PAIN ON CATHETER REMOVAL

Michael Eufemio Macalalag, Rafael Lising, Karl Marvin Tan, Leslie Rafanan,
Pompeyo Nolasco, Alfredo Uy

Introduction: Insertion of Foley catheters is a very common hospital procedure that patients are unwelcome to the idea of because of catheter-associated pain. Catheter pain is subdivided into pain experienced as the catheter is inserted (passed), while *in situ*, and upon removal. Relating to the pain felt on insertion, different techniques have been utilized to decrease pain, ranging from local anesthetic, antiseptic gel and/or generous lubricating jelly. Different studies have been made addressing the catheter. This is the first study wherein it aims to decrease the pain with Foley catheter removal.

Methodology: All male patients who were catheterized were enrolled in the study. Patients with no history of prior catheterization were randomized into a "control" group or an "experimental"/"Vesical Micturation Modified Cystometry" group. The control group patients would undergo conventional Foley catheter removal, which is merely pulling out the catheter. The experimental group contained patients who utilized the "Vesical Micturition Modified Cystometry" technique of Foley catheter removal. This is done by filling of the bladder with saline/water through the patient's Foley catheter. When the patient has the urge to void, filling is discontinued and one waits as the patient is able to push the Foley catheter out and void spontaneously. A third group was assigned to those with previous experience of catheterization and who were asked to recall the previous experience of catheter removal and give a VAS score.

Results: A total of 181 male patients who underwent urologic procedures were included in this study. A total of 139 patients had no previous history of catheterization. Sixty-seven (67) patients were assigned into the control group and 72 patients into the "Vesical Micturition Modified Cystometry" group. The experimental group had significantly less pain compared to the control group. The VAS of control patients was significantly higher than the experimental group, with means of 3.36 and 0.31, respectively, with p-values of 0.00. The mean VAS score of the third group or "recall" group was 3.88 as compared to experimental group's mean VAS score of 0.31, which showed a statistically significant result ($p<0.05$). The other statistical tests used in this study were Wilcoxon-Machted-Pairs Signed Ranked test, and Mann-Whitney U-test.

Conclusion: Comparing the "control" group and "Vesical Micturition Modified Cystometry" group for patients with no history of catheterization showed that the "Vesical Micturition Modified Cystometry" offered a significantly less painful experience compared to the group undergoing conventional pulling of the Foley catheter. For patients with previous history of catheter removal, "Vesical Micturition Modified Cystometry" congruently offers a less painful experience. It is recommended by the authors that "Vesical Micturition Modified Cystometry" technique be offered and applied to our patients in the aim of alleviating their pain during catheter removal.

ABSTRACT 51

ULTRASOUND TO FACILITATE CLEARANCE OF RESIDUAL STONES

Anup Shah[1], Mathew D. Sorensen[1], Marla Paun[2], Barbrina Dunmire[2], John Kucewicz[2], Bryan W. Cunitz[2], Frank Starr[2], Peter J. Kaczkowski[2], Oleg A. Sapozhnikov[2,3], and Michael R. Bailey[2]

[1] *Department of Urology, University of Washington School of Medicine, 1959 NE Pacific Street, Seattle, WA, 98195 USA*

[2] *Center for Industrial and Medical Ultrasound, Applied Physics Laboratory, University of Washington, 1013 NE 40th Seattle, WA, 98105 USA*

[3] *Department of Acoustics, Physics Faculty, Moscow State University, Moscow, Russian Federation*

Introduction: Residual kidney stone fragments often remain after extracorporeal shockwave lithotripsy, ureteroscopic laser lithotripsy, and percutaneous nephrolithotomy due to suboptimal position within the collecting system. New stones may grow from these fragments and contribute to a 50% recurrence rate within 5 years. We describe the use of radiation pressure and streaming created by transcutaneous focused ultrasound to manipulate the location of stone fragments within the collecting system and to facilitate passage of residual stone fragments.

Methods: A research focused ultrasound device was used to generate stone motion. Natural and artificial stones were placed in a transparent kidney phantom consisting of gel surrounding a water-filled space and in cadaveric porcine kidneys. Stone motion was observed visually in the kidney phantom and using diagnostic ultrasound in the porcine kidneys. The ultrasound device was created by combining a commercial ultrasound imaging system with a research focused ultrasound therapy system. The imaging probe was placed within and oriented down the axis of the therapy probe which consists of an 8-element annular array of 2.75 MHz elements with an outer diameter of 6 cm. This configuration allowed ultrasound energy to be focused at depths ranging from 4.5-8.5 cm. Longer bursts of higher amplitude ultrasound were applied than are used in diagnostic ultrasound (30-ms, 10-MPa bursts repeated at 10 Hz).

Results: Stones in the kidney phantom were seen to move as shown in Fig. 1. Stone velocities were on the order of 1 cm/s and quickly moved out of the ultrasound focus. Operators could generally control the direction of stone movement.

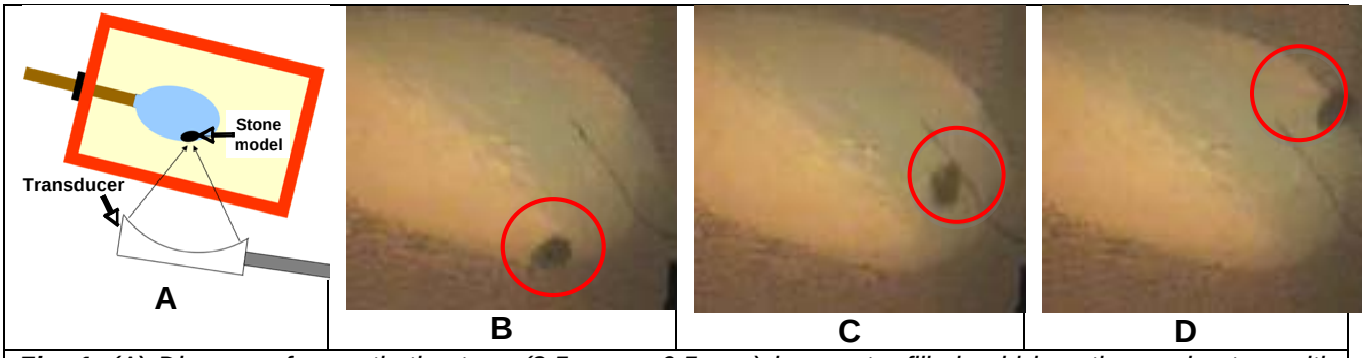

Fig. 1*. (A) Diagram of a synthetic stone (8.5 mm x 6.5 mm) in a water-filled void in a tissue phantom with ultrasound transducer shown at the bottom. (B-D) The stone traveled 2 cm in approximately one second within the "collecting system" of the kidney phantom.*

A sonographer using Doppler ultrasound and what is known as "twinkling artifact" visualized stones as small as 1 mm in the kidney. When focused ultrasound was applied these stones jumped at ~1 cm/s before falling back down. No evidence of thermal necrosis of kidney tissue was observed on gross examination.

Conclusion: Focused ultrasound can be used to move stones within the collecting system in order to optimize rates of stone clearance. Further studies are required to assess minimum ultrasound exposures necessary to move stones, bio-effects caused by the ultrasound, and whether passage of fragments is facilitated.

Work supported by NIH DK43881 and NSBRI SMST001601.

ABSTRACT 52

PRIMARY FIXATION OF MINI SLINGS: A COMPARATIVE STUDY *IN VIVO*

Paulo Palma, Cassio Riccetto, Rodrigo Siniscachi, Luiz Maciel, Alessandro Prudente, Maria B Soares, Inácio Dal Fabbro.

Division of female Urology, Universidade Estadual de Campinas - Unicamp - São Paulo, Brazil

Introduction and objectives: The minisling concept for stress urinary incontinence is an anatomical approach that involves placing a midurethral low-tension tape anchored to the obturator internus muscles bilaterally. They overcome the blind passage of long needles and all the related complications. There are many different devices available and because these are out patient procedures, primary fixation plays an important role in the outcome.

Methods: A total of 60 wistar rats were divided in 2 groups of 30 rats each. They underwent 5 subcutaneous implantation of 6 different minislings, TVT-Secur (Gynecare, USA), Unitape and Ophira mini sling system (Promedon , Argentina), Tissue Fixation System (TFS PTYAustralia), Zipper sling and mini sling (Prosurg USA) Fig. 1

Fig. 1- Equipment used in the study.

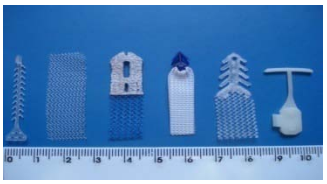

The abdominal wall was removed *en bloc* and each anchoring system underwent five evaluations using a precision tensiomenter to access the primary fixation. Force was applied to the extremity of the fixation system or mesh, until it was completely removed from the tissue (Fig. 2). The force was measured in Newton (N) and Kruskal-Wallis test was used for statistical analysis.

Fig. 2- Experiment

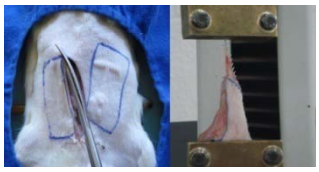

Results: There were significant differences in the resistance to extraction between the different fixation systems. At 7 days the Ophyra fixation system presented the best fixation and mini sling the worst. There was no difference between TVT-Secur and mesh alone. At 2 weeks Ophyra and TFS were equally good with no differences in the other fixation system when compared to the results after 7 days of the implant (Fig. 3).

Fig. 3 – Results

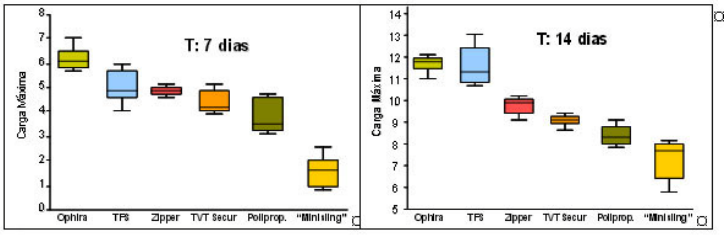

Conclusion: The Ophira minisling system presented the best primary fixation at 7 days. At 14 days Ophira and TFS were equally good. On the other hand the TVT-Secur and Zipper slings, because they depend on tissue integration, presented less than optimal primary fixation. These findings may have implication in the clinical setting for outpatient procedures do require reliable primary fixation systems.

ABSTRACT 53

SINGLE-PORT VERSUS STANDARD LAPAROSCOPIC DONOR NEPHRECTOMY: MATCHED-PAIR COMPARISON

David Canes, Andre Berger, Ricardo Brandina, Monish Aron, Georges-Pascal Haber, Jihad H. Kaouk, David A. Goldfarb, Mihir M. Desai, Inderbir S. Gill*

Department of Urology, Glickman Urological and Kidney Institute
Cleveland Clinic, Cleveland, Ohio, USA

Purpose: To present the initial experience with laparoendoscopic single site (LESS) donor nephrectomy (LESS-DN), retrospectively comparing perioperative outcomes with patients undergoing standard LDN.

Materials and Methods: Between 11/07 and 11/08, 18 consecutive patients underwent LESS-DN through an intra-umbilical novel multi-channel port. The kidney was extracted through a slightly extended umbilical incision in all cases. A contemporary matched-pair cohort of 18 patients undergoing standard LDN was selected for comparison.

Results: Baseline demographics, operating time, blood loss, and hospital stay were comparable between groups. No patient in the LESS group was converted to standard laparoscopy. Mean warm ischemia time was longer in the single-port group (3.2 vs 6 minutes, p=0.0001); however, allograft function was immediate and comparable between groups. Analgesic requirements (102 vs 100 mg) and mean visual analog score at discharge (1.5 vs 2.6) were statistically equivalent. Patient-reported convalescence was faster in the single-port group, including days on oral pain medication (18 vs 4, p=0.009), days off work (40 vs 14, p=0.003), and days to 100% physical recovery (85 vs 25, p=0.005). Regardless of laparoscopic approach, patient global satisfaction with kidney donation and willingness to recommend their procedure to others were favorable and equivalent between groups.

Conclusions: Matched-pair comparison between LESS and standard LDN suggests the single-port approach is associated with quicker convalescence. Early allograft outcomes are comparable. Although single-port LDN is associated with longer warm ischemia times in this initial series, this is expected to decrease with experience.

ABSTRACT 54

USE OF A NOVEL ANTIRETROPULSION DEVICE REDUCES STONE FRAGMENT MIGRATION AND SIGNIFICANTLY INCREASES THE EFFICIENCY OF PNEUMATIC LITHOTRIPSY: AN *IN VITRO* STUDY

Brian H. Eisner, Witsanu Pengune, Marshall L. Stoller

Department of Urology, University of California, San Francisco

Introduction: Prevention of stone retropulsion during ureteroscopic lithotripsy leads to decreased operative times and secondary procedures secondary to cephalad calculus migration. It has been theorized that an antiretropulsion device may increase the level of stone fragmentation due to the device maintaining the stone in a position that is optimal for lithotripsy. The objective of this study was to document any effect on the efficiency of stone fragmentation during pneumatic lithotripsy when using a novel antiretropulsion device, the Accordion Stone Management Device (PercSys, Palo Alto, CA).

Methods: Stone phantoms molded from Ultra-Cal 30 (size 5 mm diameter by 5 mm length) were placed in a model ureter constructed of silicone which had an inner diameter of 5 mm and submerged in a bath of normal saline. Pneumatic lithotripsy was performed continuously on 10 stones for 20 seconds (generating 200 strikes) without the Accordion device in place (control group) and on 10 stones with a 10 mm Accordion device engaged immediately proximal to the stone (experimental group). The distance of retropulsion during lithotripsy was monitored. The stone phantoms were weighed before and after pneumatic lithotripsy. Significance between mean values was determined using Student's *t*-Test.

Results: Mean retropulsion distance for control stones was 6.4 cm (range 4-8.5 cm); no stone retropulsion occurred when the Accordion device was in position. After 20 seconds of continuous pneumatic lithotripsy, the stones in the experimental group lost significantly more weight (53%) than did those in the control group (16%) when calculated as a percentage of weight change ($p < 0.001$).

Conclusion: The Accordion device successfully prevented stone retropulsion and increased fragmentation efficiency during i*n vitro* pneumatic lithotripsy in a silicone model ureter. Use of an antitretropulsion device to prevent stone retropulsion and increase fragmentation efficiency should lead to decreased overall treatment costs by not only reducing the incidence of secondary procedures necessary to capture migrated stone fragments and but also by shortening operative times.

ABSTRACT 55

IS ROBOTIC PROSTATECTOMY SAFE IN ASIAN ELDERLY PERSONS OVER 75 YEARS OLD? COMPARISION OF PERIOPERATIVE DATA

Wooju Jeong, Seung Ryeol Lee, Enrique Ian S. Lorenzo, Cheol Kyu Oh, Young Seung Lee, Woong Kyu Han, Seung Choul Yang, Koon Ho Rha

Department of Urology, Yonsei University Health System
Urologic Science Institute, Seoul, Korea

PURPOSE: Prostate cancer in Korea tends to be a high stage and diagnosed in old age; especially since age-related diseases, such as cardiovascular disease and diabetics, are prevalent in the elderly and they have risk factors of post-operative morbidity from anesthesia and surgery. We examined the peri-operative data of robotic laparoscopic radical prostatectomy (RARP) in patients over 75 years old.

MATERIALS AND METHODS: Between July 2005 and July 2008, 326 patients had RARP and 277 out of the 326 did not have any suspicious metastatic lesions in their lymphatics or bone or a history of hormonal therapy preoperatively. Group 1 contained patients younger than 74 years old (n=266), and Group 2 had patients older than 75 (n=11). We examined age, body mass index (BMI), prostate volume on transrectal ultrasound, serum PSA, Gleason's score on preoperative biopsy and post-operative pathology, and clinical and pathological stage. Between the groups we compared ASA scores, intra-operative complication, transfusion as peri-operative risk factors and operation time, estimated blood loss and positive surgical margin as peri-operative factors.

RESULTS: The mean age of Group 1 was 62.4±7.2 and of Group 2 was 77.5±3.3. There were no significant differences with BMI (p=0.819), TRUS prostate volume (p=0.562), PSA (p=0.545), preoperative and postoperative Gleason's score (p=0.907; p=0.448), and the ratio of localized prostate cancer (p=1.000) in the two groups. Neither operative time (Group 1 = 206.8±44.3 vs. Group 2 = 206.1±40.6; p=0.960) or EBL (Group 1 = 337.0±278.7 vs. Group 2 = 380.0±256.3; p=0.631) were significantly different between the groups. The median ASA score preoperatively was 1 in Group 1 and 2 in Group 2 (p=0.019). The incidence of intra-operative complications, transfusion and PSM in the groups, however, did not show any difference significantly (p>0.05). Also the date to general diet was 1 day in both groups (p=0.950), and the length of a hospital stay was 5.1 days in Group 1 and 5.0 days in Group 2 (p=0.934).

CONCLUSIONS: Although patients over 75 had higher ASA scores, morbidity in elderly patients was not significantly different from that in younger patients. Robotic prostatectomy is safe and feasible even in an old patient with prostate cancer.

ABSTRACT 56 **OUTSTANDING PAPER AWARD**

FUTURE PROSPECTS IN PERCUTANEOUS ABLATIVE TARGETING: COMPARISON OF A ROBOTIC AND COMPUTER-ASSISTED NAVIGATION

Richard Pollock[1], Pierre Mozer[1], Thomas Guzzo[1], Jonathan Marx[2], Brian Matlaga[1], Doru Petrisor[1], Bogdan Vigaru[1], Dan Stoianovici[1], Mohamad E. Allaf[1]

[1]*Urology Robotics, Department of Urology, Johns Hopkins Medicine, Baltimore, MD*

[2]*Department of Radiology, Johns Hopkins Medicine, Baltimore, MD*

http://urobotics.urology.jhu.edu/

Introduction: Image-guided therapies are becoming an increasingly utilized approach in treating the urologic patient. Precise targeting is essential for effective outcomes but the majority of these procedures are performed manually. New technologies such as robotic and computer-assisted navigation systems have the potential to increase the accuracy and efficiency of needle targeting. The objective of this study is to assess these technologies and compare their performance to standard manual needle placement in an anatomical phantom model.

Methods: A previously described synthetic anatomical torso (Lapman) was filled with agar gel. Metal beads (2mm) were placed in the gel at varying angles and acted as targets. Half the targets in any given experimental arm were placed underneath ribs and required an oblique angled approach (>20°). A minimum of 12 attempts per arm were performed. The computer-assisted navigation system (Koelis, La Tronche, France) used with a Polaris® infrared camera system (Northern Digital Inc, Ontario, Canada) to localize the needle tip was tested using 3 operators: an interventional radiologist and 2 endourologists. AcuBot is a novel and completely automated image-guided robot capable of needle placement. DICOM data were acquired after each attempt and images were reconstructed and analyzed using a specialized software package (Amira, Visage Imaging, Carlsbad, CA; USA). Accuracy was assessed by measuring proximity of the tip of the needle to the metal bead on CT-guided imaging. Accuracy and time to target were also quantified and compared.

Results: All modalities allowed for eventual accurate targeting of the beads. The time between target selection and needle placement was fastest for the AcuBot system and slowest for standard manual placement (37sec vs. 234sec, $p<0.05$). The robotic system was significantly faster than the navigational system which was in turn significantly faster than the manual attempts ($p<0.05$). Manual targeting required on average 1.9 attempts (range 1-4) to achieve adequate accuracy (within 1.5cm of the bead) while only one attempt was necessary using AcuBot and the navigational system. Overall accuracy and precision were statistically superior for AcuBot compared to the navigational system and manual attempts ($p<0.05$). Mean distance between needle tip and target for the robotic system was 1.2mm with no attempt resulting in a targeting error greater than 2.8mm. In contrast, the mean distance to target for the navigational system and manual attempts was 5.8mm (range 1.8-11.8mm) and 8.7mm (range 2.2-15.0mm) respectively. Additionally, the angle of entry needed to reach the target had no impact on overall accuracy for the AcuBot attempts. However, targeting beads placed at oblique angles (>20°) resulted in significantly longer times and lower accuracy than non-oblique attempts for both the navigational system and manual approaches ($p<0.05$).

Figure 7: Needle targeting with Koelis navigation system (left) and AcuBot robot (right)

Conclusion: Emerging technologies hold promise for increased accuracy during percutaneous targeted procedures. Both the AcuBot and the Koelis computer-assisted navigation system were accurate and efficient in a phantom targeting model. AcuBot was significantly more accurate, faster and less user or target dependent than the navigation system. Further studies in animal and clinical studies are warranted to further advance this promising technology.

ABSTRACT 57

LAPARO-ENDOSCOPIC SINGLE SITE (*LESS*) SURGERY: FIRST 100 CASES

Mihir Desai, Andre Berger, Ricardo Brandina, Monish Aron, Brian Irwin, Mahesh Desai, Rene Sotelo, David Canes, Robert Stein, Inderbir Gill

Department of Urology, Glickman Urological and Kidney Institute, Cleveland Clinic, Cleveland, Ohio, USA

Introduction: Laparo-endoscopic single site (*LESS*) surgery is a novel minimally invasive approach that has recently been used to perform various urologic procedures. To our knowledge, we report our experience with the initial 100 *LESS* procedures in urology.

Materials and methods: Between October 2007 and December 2008, we performed *LESS* urologic procedures in 100 patients for various indications. These included nephrectomy (N=34; simple 14, radical 3, donor 17), nephroureterectomy (N=2), partial nephrectomy (N=6), pyeloplasty (N=17), transvesical simple prostatectomy (N=32) and others (N=11). Data were prospectively collected in an IRB approved database. All procedures were performed using a novel single port device (r-Port) and a varying combination of standard and specialized bent/articulating laparoscopic instruments. Robotic assistance was used to perform *LESS* pyeloplasty (N=2) and simple prostatectomy (N=1). In addition to standard peri-operative data, post-discharge analgesia requirements, time to complete convalescence, and time to return to work were obtained.

Results: In the study period, *LESS* procedures accounted for 15% of all laparoscopic cases by the authors for similar indications. Conversion to standard multi-port laparoscopy was necessary in 2 cases, addition of a single 5 mm port was necessary in 4 cases, and conversion to open surgery was necessary in 4 cases. There was one mortality following simple prostatectomy in a Jehovah's Witness due to patient refusal to accept transfusion following hemorrhage. Intra- and post-operative complications occurred in 5 and 9 cases, respectively. Mean operative time was 145, 230, 220, and 113 minutes and hospital stay was 2, 2.9, 2, and 3 days for simple nephrectomy, donor nephrectomy, pyeloplasty and simple prostatectomy, respectively.

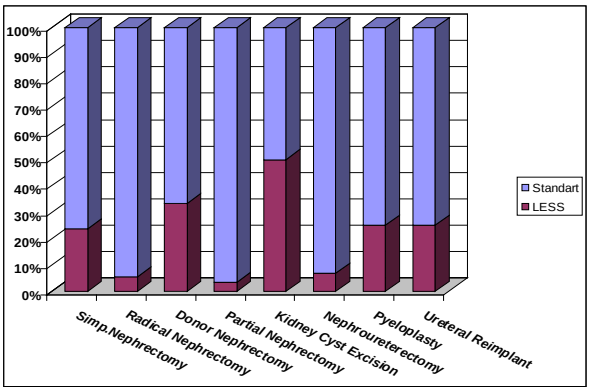

Figure 1. Number of LESS and standard laparoscopic procedures since September 2007.

Conclusions: Laparoendoscopic single site (*LESS*) surgery is technically feasible for a variety of ablative and reconstructive applications in urology. With proper patient selection, conversion and complications rates are low. Improvement in instrumentation and technology is likely to expand the role of *LESS* in minimally invasive urology

ABSRACT 58 **OUTSTANDING PAPER AWARD**

THE IMPACT OF A URETERAL STENT AND A FOLEY CATHETER ON RENAL PELVIC PRESSURES IN THE *IN VIVO* PORCINE MODEL

Michael K Louie, Aldrin J Gamboa, Hung P Truong, Rachelle J Lin, Amanda Khosravi, Victor B Huynh, Kevin Sohn, Adam G Kaplan, Reza Alipanah, Lorena A Andrade, Cervando G Ortiz, Elspeth M McDougall, Ralph V Clayman

University of California, Irvine Medical Center, Orange, CA

Introduction: The widely accepted use of a ureteral stent and a Foley catheter after ureteral reconstruction has not been proven to decrease renal pelvic pressures, and therefore prevent urine leakage after surgery. We performed manometric assessment of renal pelvic pressures (RPP) and urine flow rates in the in vivo porcine model at bladder pressures from 0 – 20 cmH2O, with and without a ureteral stent, with and without a Foley catheter, and with and without a diuretic challenge.

Methods: 6 large domestic pigs underwent an initial gravity cystogram at 40cmH2O to exclude renal units with vesicoureteral reflux. If neither renal unit exhibited reflux, a laparoscopic right nephrectomy was performed to isolate flow from the left kidney; conversely the opposite kidney was chosen if reflux was present. A 6F nephrostomy tube and 16F Foley catheter were placed and connected to water manometers. RPP measurements were noted without a stent every three minutes until three consecutive readings were within 10% of each other at bladder pressures of 0, 5, 10, 15, and 20cmH2O. RPP and urine flow rate were measured at 0cmH2O bladder pressure and following a furosemide injection of 1mg/kg after a 10cc/kg fluid bolus of normal saline. The RPP and urine flow rate measurements were repeated following the insertion of a 6F x 22cm double pigtail ureteral stent.

Results: With or without a stent, an increase in bladder pressure causes an increase in renal pelvic pressure ($p=0.56$). A stent and a Foley catheter significantly reduced renal pelvic pressure ($p<0.05$). In multivariate analysis, a Foley was more important than a stent for reducing renal pelvic pressures ($p<0.05$). During a diuretic challenge, a stent maintains renal pelvic pressure at baseline compared to increasing pressures developed without a stent ($p=0.01$). Urine flow rates at baseline with a stent were increased compared to without a stent ($p=0.02$). However, with a diuretic challenge, the urine flow rates were not significantly different with or without a stent ($p=0.2$). Multivariate analysis showed significant interaction between the stent and diuretic ($p=0.02$), but not with the stent alone ($p=0.57$) indicating the urine flow rates behave differently with the stent when presented with a diuretic challenge.

Conclusion: Our study confirms that the lowest renal pelvic pressure and maximum drainage are achieved when both a ureteral stent and a Foley catheter are used. Interestingly, increasing bladder pressure increased renal pelvic pressure regardless of the presence of a stent, and a diuretic challenge changes the drainage characteristic of a stent.

ABSTRACT 59

AirSeal™ VALVE-LESS TROCAR FOR UROLOGIC LAPAROSCOPY: AN INITIAL EVALUATION

Amin S. Herati, Mohamed A. Atalla, Soroush Rais-Bahrami, Sero Andonian, Ardeshir R. Rastinehad, Louis R. Kavoussi

Smith Institute for Urology, New Hyde Park, NY, USA

Introduction: Laparoscopic surgery is typically performed using trocars that maintain pneumoperitoneum using trap door valves and silicone seals. However, valves and seals hinder passage of instruments, cause lens smudging, trap specimens and needles being removed from the abdominal cavity, and lose their seal with repeated instrument exchange. The aim of the present study was to evaluate the feasibility of the newly designed AirSeal™ valve-less trocars.

Methods: AirSeal™ (SurgiQuest; Orange, CT) creates a curtain of forced CO_2 gas, which maintains pneumoperitoneum. Gas escaping from the abdomen is collected at the top of the trocar, filtered and returned to the peritoneal cavity through openings at the bottom of the trocar. The inner diameter is 12mm, thus allowing the passage of 10 mm laparoscopes and instruments up to 12mm in diameter. Removing physical seals allows for an unobstructed direct view into the operative site. The first generation of AirSeal™ trocars were prospectively used in 9 patients undergoing laparoscopic renal surgery at our institution. Patient demographics, operative time, amount of CO_2 gas used, perioperative parameters, and postoperative complications were analyzed for the first 9 patients undergoing urologic laparoscopic surgery using this device.

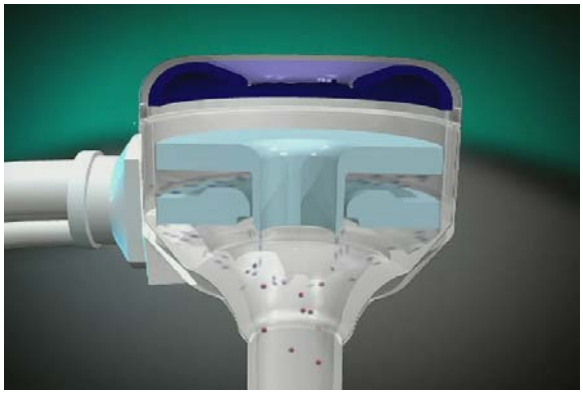

Results: Nine patients with a mean age of 65.6 years (range 47-81) underwent laparoscopic renal surgery by a single surgeon (LRK). The new AirSeal™ trocars were used in laparoscopic radical (n =5) and partial (n=4) nephrectomies maintaining a stable pneumoperitoneum pressure of 11-15 mmHg throughout the procedure. The mean volume of CO_2 used to maintain insufflation during laparoscopic radical and partial nephrectomy was 93.4 L (range 37–156) and 71 L (range 47-114), respectively. The mean operative time for laparoscopic radical and partial nephrectomy was 143.2 and 126.2 minutes with a mean body mass index of 28.7 Kg/m^2 and 38.3 Kg/m^2, respectively. The surgeon noted that during electrocautery, smoke was evacuated automatically with clearing of vision simultaneously. Furthermore, it allowed unhindered removal of surgical specimen and needles and obviated the need for frequent laparoscope cleaning. Pneumoperitoneum was maintained even during continuous use of a suction device. Although no perioperative complications were noted in any of these cases, pneumoperitoneum was lost completely during one case when neuromuscular blockade wore off and the patient contracted abdominal muscles. This occurred due to an automatic shut-off feature in response to the sudden increase in pneumoperitoneum. The smoke evacuator was considered noisy during initial use. The surgical team got accustomed with the noise after repeated use.

Conclusion: The new AirSeal™ trocar decreased smudging of laparoscopes, automatically evacuated smoke during cauterization leading to improved visualization, maintained pneumoperitoneum even while suctioning, and allowed for multiple instruments to pass through a single trocar when compared to conventional trocars. These advantages may translate into decreased operative times. However, AirSeal™ should be compared with conventional trocars in a randomized fashion to confirm these results. Second generation smoke evacuators should be able to generate higher pneumoperitoneum pressures and reduce the noise level.

ABSTRACT 60 **OUTSTANDING PAPER AWARD**

REGIONAL HYPOTHERMIA DURING ROBOTIC RADICAL PROSTATECTOMY USING AN ENDORECTAL COOLING BALLOON TO IMPROVE URINARY CONTINENCE

David S. Finley[1], Kathryn Osann[2], Douglas Skarecky[1], Alexandra Chang[1], Thomas E. Ahlering[1]

[1]Departmenst of Urology and [2]Medicine, University of California Irvine, Orange CA

Introduction: Acute inflammation secondary to the trauma of surgical excision of the prostate is probably a major contributing factor to incontinence and impotence after radical prostatectomy. Downstream sequelae of inflammation have been linked to muscle and nervous tissue damage and dysfunction. We hypothesized that pre-emptive local hypothermia to the pelvis would attenuate inflammation caused by excision of the prostate resulting in earlier return to continence. To achieve locoregional hypothermia of the pelvis during robotic-assisted laparoscopic radical prostatectomy (RLP), we created a novel endorectal cooling balloon. Herein we present feasibility and early outcomes data.

Methods: An endorectal cooling balloon (ECB) was designed to distend at low pressure and conform to the rectal wall, extending from the membranous urethra to just above the bladder neck to effect loco-regional hypothermia of the prostate, urethra, cavernous nerves, urogenital diaphragm and surrounding structures (**Fig. 1).** 47 of 50 consecutive patients undergoing nerve-sparing hRLP (case #668-717, 3 were excluded: 2 radiation, 1 withdrawn due to balloon failure) were prospectively compared to standard RLP (control group case #1-667). Loco-regional pelvic cooling was achieved utilizing 4°C intracorporeal irrigation and an ECB cycled with 4°C saline. Intracorporeal temperatures (T) were measured. Continence was defined as zero urinary pads. Kaplan-Meier analysis of time to zero pads and multivariate Cox Proportional Hazards Regression was used to examine group differences in continence after adjusting for baseline characteristics.

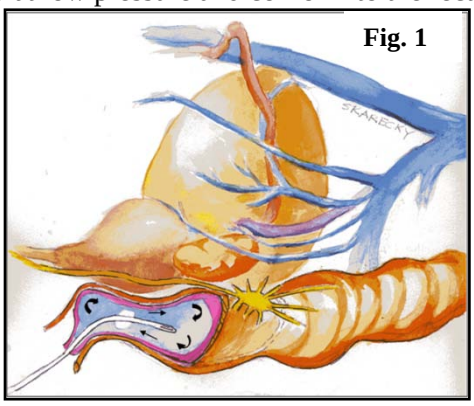

Results: Median T=29.0°C (ECB,range: 24.4-35.9°C) and 25.5°C (ECB+irrigation, range:19.4-34.0°C), respectively. Time to zero-pad status was determined in 590 of 667 controls (88%). Three month hRLP zero-pad rates were 86.8%±5.8% vs controls 68.6%±2.0%. Return to continence was faster for hRLP vs. controls: median 39days (range:0-110) vs. 59days (range:1-720), respectively (p=0.002, log-rank test, **Fig 2**.). Multivariate analysis adjusting for factors including age, AUAss, IIEF-5, BMI, prostate weight, stage, Rocco modification, nerve-sparing and learning curve demonstrated faster return to continence for the hRLP group relative to controls (HR=1.66,95%CI:1.11-2.49 p=0.014).

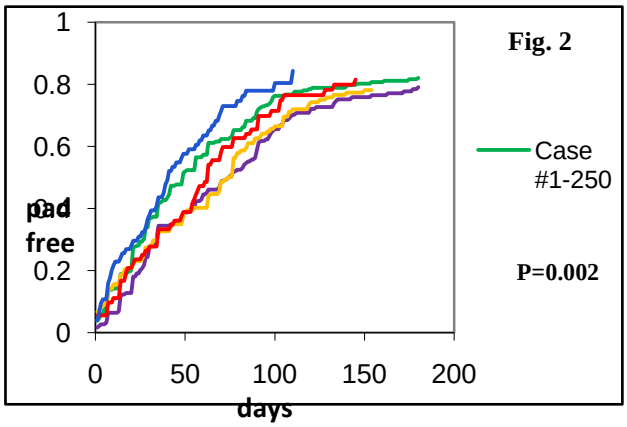

Conclusion: We successfully induced moderate to deep local hypothermia during RLP using an ECB. Hypothermic radical prostatectomy resulted in a statistically significant increase in early post-operative continence rates.

ABSTRACT 61

IMPACT OF PNEUMOPERITONEUM ON ICEBALL SIZE IN RENAL CRYOTHERAPY

Jennifer L. Young, Cervando G. Ortiz-Vanderdys, David W. McCormick, Victor B. Huynh, Adam G. Kaplan, Nick S. Jain, Donald L. Pick, Michael K. Louie, Lorena A. Andrade, Kathryn E. Osann, Lorena A. Andrade, Elspeth M. McDougall and Ralph V. Clayman

University of California, Irvine, USA

Introduction and Objective: Cryotherapy has allowed small renal masses to be treated in situ with minimal morbidity and mortality. However, many questions remain regarding the optimal administration of cryotherapy in the kidney. As pneumoperitoneum is known to decrease blood flow to the kidney, we sought to define the effects of pneumoperitoneum pressure on the iceball, and the resulting cryolesion, at four commonly used pneumoperitoneum pressures. Our hypothesis is that increased pneumoperitoneum pressure would lead to decreased renal vein blood flow and hence a possibly larger cryolesion.

Methods: Twelve Yorkshire pigs underwent laparoscopic-guided percutaneous cryoablation of the upper and lower pole of each kidney at four randomized pneumoperitoneum pressures (10, 15, 20, 25 mmHg). Cryolesions were created with a single 1.47 mm IceRod using a Precise cryoablation unit (Galil Medical, Plymouth Meeting, PA) with pressurized argon at 4,300 psi. Each site underwent two 10 minute freeze cycles separated by a 5 minute active thaw with pressurized helium at 2,200 psi. At the end of each freeze cycle, the iceball volume was measured with intraoperative laparoscopic ultrasound. The kidneys were then harvested and the cryolesion surface area was calculated. The lesions were fixed in 10% buffered formalin and then excised with a 1 mm margin to obtain a volume measurement.

Results: Twelve trials were completed at each experimental pressure. There were no intraoperative complications. There was no statistically significant difference for iceball volume by ultrasound for freeze 1 or 2, cryolesion volume by graduated cylinder or cryolesion surface area by macroscopic measurement for any of the pneumoperitoneum pressures (Table I).

Conclusions: Pneumoperitoneum pressures between 10 and 25 mm Hg did not affect iceball size as measured by intraoperative ultrasound, cryolesion surface area or volume during laparoscopic-guided percutaneous renal cryotherapy. This finding implies that pneumoperitoneum pressure can be adjusted according to the individual patient or operative needs without concern about any alterations in iceball size.

Table I.

	10 mm Hg	15 mm Hg	20 mm Hg	25 mm Hg	p value
Iceball volume freeze 1 (cm^3) Mean (range)	3.41 (1.00-5.90)	2.85 (0.62-4.94)	3.44 (1.18-6.25)	2.36 (0.57-2.73)	0.156
Iceball volume freeze 2 (cm^3)	3.67 (2.29-6.31)	3.34 (1.64-5.94)	4.88 (1.11-10.3)	3.95 (0.89-9.61)	0.195
Cryolesion volume (cm^3)	4.06 (1.80-5.90)	3.77 (2.50-5.80)	3.97 (2.30-5.70)	3.93 (2.80-5.90)	0.859
Cryolesion surface area (cm^2)	4.55 (291-661)	4.38 (3.12-6.16)	4.39 (3.14-5.72)	4.20 (2.75-5.80)	0.707

ABSTRACT 62

THE NEW Invisio® DUR-D "chip-on-the-tip" URETEROSCOPES—EVALUATION OF CHANGES IN PHYSICAL PROPERTIES OVER TIME

El-Husseiny T, Papatsoris AG, Moraitis K, Maan Z, Masood J, Buchholz N, Birch M*
*Endourology & Stone Services and *Dept. of Medical Physics, Barts and The London NHS Trust, London/ UK*

Background and Purpose: Flexible ureteroscopes have become an essential tool in endourological practice. Recently, a new generation of digital flexible ureteroscopes has been marketed (Invisio® DUR-D, ACMI, USA) with which a new optical technology was introduced. The tip houses dual Light Emitting Diodes (LED) driven light carriers. A 1mm digital camera at the tip eliminates the need for fragile low-resolution fibre-optics and provides superior resolution. In addition, the image quality is digitally enhanced. It was claimed that not only should this markedly increase the image quality, but also make the instrument more durable in the whole. We have therefore compared both, light intensity and deflection angles with and without indwelling instruments between identical scopes after different number of uses.

Materials and Methods: On three identical Invisio® DUR-D digital flexible ureteroscopes of different usages we measured and compared the light intensity at a given setting of the light source using an Ocean Optics optical spectrometer at 20mm distance from the tip. Measurements were taken three times each with the ureteroscopes in straight position and upwards/ downwards deflection, respectively. The first scope was brand new; the second had been used 30 times while the third had been used 44 times. We also measured and compared the deflection angles without and with instruments - a 0.035" Cook guidewire, a 200 µm laser fibre and a 3F zero-tip nitinol basket - inside the working channel in four identical scopes after 0, 10, 30, and 44 uses, respectively.

Results*:* Light intensity for each scope showed slight differences in relation to deflection angles, which is within the experimental error and did not significantly differ. Light output remained stable after many uses:

	Straight	**upwards**	**Downwards**
0 uses	**5.5**	**4.36**	**4.84**
30 uses	**6.19**	**6.30**	**6.25**
44 uses	**5.05**	**5.25**	**5.15**

(unit: Lux x10^3)

In contrast, the deflection angle is shown to deteriorate with instruments inside the working channel. This is relatively independent of the type of micro-instrument used, but the decrease is directly proportional with advanced age of the scope:

	No instruments	.035'' guidewire	200µm laser fibre	3F nitinol basket
0 uses upwards	218º	196º	205º	204º
10 uses upwards	216º	194º	203º	203º
30 uses upwards	197	173º	174º	174º
44 uses upwards	163º	148º	155º	152º
0 uses downwards	216º	194º	209º	191º
10 uses downwards	199º	191º	192º	190º
30 uses downwards	230º	139º	151º	147º
44 uses downwards	170º	123º	141º	158º

Conclusions: As an advantage over earlier generation scopes, light output remains constant due to the avoidance of the fragile low-resolution fibre-optics, further helped by digital enhancement. Similarly to the earlier generation scopes, there remains a decrease in deflection capability over time with the new Invisio® DUR-D digital flexible ureteroscopes.

ABSTRACT 63

ACOUSTIC RADIATION FORCE IMPULSE (ARFI) IMAGING OF HUMAN PROSTATE *IN VIVO*

Vladimir Mouraviev[1], Liang Zhai[2], Matvey Tsivian[1], John Madden[3], Thomas J. Polascik[1], Kathryn Nightingale[2]

[1]Division of Urologic Surgery, Department of Surgery, Duke University Medical Center, [2]Department of Biomedical Engineering, Duke University, and
[3]Department of Pathology, Duke University Medical Center, Durham, NC , 27710

Introduction: Tissue elasticity changes with pathological processes, thus providing opportunities for elasticity imaging techniques to detect abnormalities inside the prostate. Acoustic radiation force impulse (ARFI) imaging is a novel elasticity imaging technique capable of visualizing structures with different stiffnesses with high resolution. ARFI imaging uses high intensity, focused acoustic beams to mechanically excite, or push, on tissue, and ultrasonic correlation based methods to monitor the tissue displacement response. The 'push' arises from the absorption of acoustic energy, which results in both a net force, and some minimal tissue heating.

Materials and Methods: In this study, ARFI techniques were developed and implemented to image human prostates *in vivo*. A modified Siemens Antares™ Scanner and a 3D, end-firing, curvilinear mechanical wobbler endo-cavity transducer (EV9F4, Siemens Medical Solutions USA, Inc., Ultrasound Division, Issaquah, WA) were used for this study. ARFI push pulses use a center frequency of 4.0 MHz, F# 3.0, focal depth 20 mm and duration 0.1 ms. The tracking beams use a center frequency of 8.89 MHz. To scan the entire 3D prostatic volume, 2D ARFI images are acquired in sequential planes. For this preliminary investigation, a full 3D data acquisition takes 2.5 minutes. Under the IRB approval, 4 patients expecting robotic prostatectomy were consented for the study in Duke Medical Center. 3D ARFI datasets were obtained transrectally under general anesthesia, immediately prior to surgery.

Results: ARFI imaging was able to visualize the internal anatomical structures, benign prostatic hyperplasia (BPH) and focal cancerous lesions in prostates. The central zone was found to be stiffer than the peripheral zone; BPH nodules presented with softer centers and stiffer boundaries; focal prostate cancer (PCa) lesions were stiffer than normal tissue and created bilateral asymmetries.

Conclusion: The results suggest ARFI imaging is a promising new tool for providing image-guidance for targeted prostate needle biopsies and focal therapy. The *in vivo* images visualized the anatomical structures, calcifications, BPH, and PCa, as determined by correlation with histological analysis. We conclude that *in vivo* 3D ARFI imaging of the prostate is feasible, and has the potential for targeting prostate biopsy procedures.

ABSTRACT 64

MOLECULAR IMAGING OF PROSTATE CANCER IN VIVO USING A TARGETED CONTRAST AGENT IN INTERMOLECULAR MULTIPLE-QUANTUM COHERENCES MRI EXPERIMENTS

Vladimir Mouraviev[1], Rosa T. Branca[2], Rahila Andrews[1], Matvey Tsivian[1] , Daniel S. Sullivan[3] , Carola Leuschner[4], Challa Kumar[4], Warren S. Warren[2], Thomas J. Polascik[1]

[1]Duke Prostate Center, Duke Medical University Center, [2]Duke University, NC, [3] Duke Comprehensive Cancer Center, NC; [4]Louisiana State University, LA.

Introduction: The recent emergence of molecular imaging tools should be used in the near future to give alternative diagnostic options to men with localized prostate cancer. This study explores a fundamentally different source of MRI signal (intermolecular multiple quantum coherences-iMQCs) coupled with a novel molecular probe, supeparamagnetic iron oxide nanoparticles (SPION) conjugated to luteneizing hormone releasing hormone (LHRH), that improve the detection of early stage prostate cancer.

Material & Methods: PC-3 xenografts were established in 24 athymic Hsd-nu male nude mice (4 weeks of age). At a tumor volume of 70–100 mm^3, the animals were injected with LHRH-SPION a day before imaging by tail vein injections. A high resolution (Tesla 7) animal MRI animal device was used to image the tumor. Mice were imaged once a week for 3 weeks and euthanized 7 days after the last treatment. At the end of the study, a complete necropsy was performed.

Results: Our *in vivo* data demonstrated the effects of the large susceptibility changes induced by nanoparticles in proton iMQC experiments (Fig.1). LHRH-SPION dramatically increases the local anisotropy of the magnetic field because SPION particles create extra magnetic field that locally perturb the resonance frequency of nearby spins. For this reason, they are remarkably sensitive targets for detection via iMQCs, specifically by measuring differences between images taken with gradients in different directions.

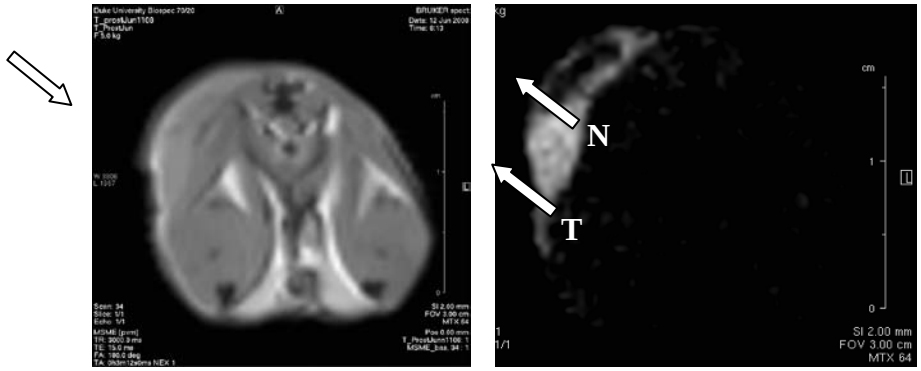

Fig. 1. A. Spin-echo image of a PC-3 xenograft of prostate tumor (arrow) in the right hind leg. B. iMQC anisotropy map image of the same area differentiating viable tumor cells (arrow T), actively targeted by the LHRH-SPION, from untargeted necrotic tumor tissue (arrow N).

Conclusion: iMQC signal used in conjunction with a novel molecular probe (LHRH-SPION) may be an accurate diagnostic tool to image early stage prostate cancer with MRI if further *in vivo* experiments and a phase 1 clinical study support feasibility of this technique

ABSTRACT 65

ANTI-RETROPULSION DEVICES INCREASE STONE FRAGMENTATION EFFICIENCY WITH HOLMIUM:YAG LASER LITHOTRIPSY

Lee M. Jonat, Ben H. Chew, Dirk Lange, Ryan F. Paterson, Joel M. Teichman

The Stone Centre at Vancouver General Hospital, Department of Urologic Sciences, University of British Columbia, Vancouver, BC.

Introduction: Stone fragmentation efficiency is proportional to the power applied with Holmium:YAG laser lithotripsy; however, increased power leads to increased retropulsion that may result in higher failure rates, prolonged procedures, and necessitate lower power lithotripsy. We hypothesized that anti-retropulsion devices would increase stone fragmentation efficiency for a given amount of total energy by holding the stone in place during lithotripsy even at high power settings.

Methods: One hundred eighty UltraCal 30 stones of similar size were divided into 6 groups, including a control group (no backstop device), the 7mm and 10mm Stone Cone (Boston Scientific), the N-Trap (Cook Urological), and the 7mm and 10mm Accordion (PercSys). Each group was further divided into 3 power setting groups: 0.5J/10Hz, 1J/20Hz, and 2J/40Hz to yield groups with sample sizes of 10. During each trial, a total of 500 joules of energy was delivered. Stones were placed in a horizontal 8.5mm diameter acrylic tube immersed in saline. The primary endpoint was stone fragmentation efficiency as defined by stone mass change for a given unit of energy.

Results: At the lowest power setting, only the 7mm Accordion and 10mm Stone Cone increased stone fragmentation efficiency over control ($p<0.05$). At the higher power settings (20W and 80W), all devices increased efficiency over controls ($p<0.001$). Stone fragmentation efficiency was not improved with increasing power deployment in the control group. In all devices, however, stone fragmentation efficiency significantly increased as the power settings were raised. Stone retropulsion increased significantly with higher power settings in the absence of any devices ($p<0.01$).

Conclusion: This trial demonstrates that anti-retropulsion devices increase stone fragmentation efficiency and facilitate high power lithotripsy compared to controls. No device was shown to be clearly superior to any other. Presumably, the improved efficiency was a result of preventing retropulsion and increasing the contact time between the laser fiber and stone. Migration of stone fragments was uncommon when using the devices and no fragments larger than 2mm migrated past any device. These results may have application in the clinical setting in that it may decrease procedural times and increase stone free rates.

ABSTRACT 66

IN VIVO URETERAL AND VESSEL SEALING ACHIEVED WITH ENERGY BASED SEALING DEVICES IN THE ACUTE PORCINE MODEL

Michael K Louie[1], Hung P Truong[1], Aldrin J Gamboa[1], Rachelle J Lin[1], Amanda Khosravi[1], Victor B Huynh[1], Kevin Sohn[1], Reza Alipanah[1], Lorena A Andrade[1], Cervando G Ortiz[1], Geoffrey N Box[2], Hak J Lee[1], Joben Abraham[1], Robert A Edwards[1], Elspeth M McDougall[1], Ralph V Clayman[1]

[1] *University of California, Irvine Medical Center, Orange, CA*
[2] *Ohio State University Medical Center, Columbus, OH*

Introduction: Energy-based vessel sealing devices have been recently developed to speed dissection by rapid occlusion and cutting of small veins and arteries. To date, these devices have not been applied for ureteral occlusion. Using an acute porcine model, the ability of the Ligasure V® (Covidien, Mansfield, MA) and the Harmonic ACE® (Ethicon Endo-surgery, Cincinnati OH) to seal both the ureter and blood vessels is characterized. To the best of our knowledge, this is the initial report on the use of bipolar energy to seal the ureter.

Methods: 6 Yorkshire pigs during laparoscopic and open abdominal exploration, had arteries (1-6.3 mm), veins (3.4-11 mm), and ureters with periureteral tissue (2.28-7.86 mm) sealed in vivo using the Harmonic and Ligasure. The Harmonic was used on the "minimum" setting. The Ligasure was tested using both a single seal (seal – cut) and a double seal (seal-seal immediately next to the previous seal-cut) technique. Tissue seals were subjected ex-vivo to burst pressure testing and histological evaluation.

Results: For arteries up to 3mm, both the Harmonic and the Ligasure 1 seal withstood pressures >300 mmHg, however for sealing arteries from 3mm to 5mm, only the Ligasure 1 seal was effective. For venous sealing, Ligasure 1 and 2 seals performed similarly for vessels up to 8mm by withstanding pressures >100 mmHg, while the Harmonic was significantly less effective (p=0.02). Neither of the devices could seal veins >8mm reliably. The ureteral sealing results showed no difference between the devices, but the Harmonic had the higher mean burst pressure.

Ureteral Sealing - Ligasure V vs. Harmonic ACE

	Harmonic ACE	Ligasure 1 seal	*p-value*	Ligasure 2 seal	*p-value*
Mean Burst Pressure (mm Hg)	128.3	100.0	0.39	63.00	0.44
Mean Ureteral Diameter (mm)	4.5	3.7	0.64	5.12	0.78
Mean Time to Seal (sec)	8.0	5.0	0.20	9.8	0.46
Mean *Char* Score (0 = no charring, 1 = mild charring, 2 = moderate and severe charring)	1.0	1.3	0.23	1.20	0.61
Mean *Sticking* Score(0 = no sticking, 1 = mild sticking, 2 = moderate and severe sticking)	0.5	1.0	0.37	1.20	*<0.05*
Mean *Tissue Separation* Score (0 = no separation, 1 = some resistance to separation, 2 = cleanly separated	2.0	0.7	*<0.05*	1.00	*<0.05*

Conclusion: The Harmonic ACE seals arteries up to 3mm, while the Ligasure 1 seal will seal arteries up to 5mm. The Ligasure is effective for sealing veins up to 8mm, but neither device is effective for veins >8mm. Either device seals the ureter well, but the Harmonic ACE had a higher mean burst pressure and less tissue injury. The Ligasure 2 seal is less effective and causes more tissue damage than the Ligasure 1 seal.

ABSTRACT 67

SEMI-AUTOMATIC SEGMENTATION OF PROSTATE ULTRASOUND IMAGES USING SHAPE PRIORS

Kevin Dowlut[1], Michael Baumann[1,2], Sébastien Martin[1], Jocelyne Troccaz[1]
[1] *TIMC Laboratory – School of Medicine – Domaine de la Merci – 38700 La Tronche – France*
[2] *KOELIS – 5, Avenue du Grand Sablon – 38700 La Tronche – France*

Introduction: Several systems have been developed for computer-assisted localization of ultrasound-guided prostate biopsies. Some of them integrate reconstructed volumes from sets of 2D ultrasound images. The system developed in Grenoble [1,2], in collaboration with the urology department of La Pitié Salpétrière Hospital, registers 3D ultrasound volumes. Segmenting the prostate capsule in these ultrasound data is useful for (1) surface registration with MRI segmented images, (2) visualization of the executed biopsies, and (3) precise evaluation of the ability to reach the target zones.

Methods: In a previous project for computer-assisted prostate brachytherapy developed in collaboration with Grenoble University Hospital (radiation oncology and urology departments), we have constructed a prostate atlas [3] based on 18 MRI exams segmented by experts. This atlas includes, among other information, a statistical shape of the prostate computed from the 18 patients. The statistical shape consists of the average shape obtained after registration of the 18 exams and the principal modes of variations obtained by PCA. The software that we developed is based on the deformation of this average prostate surface to points defined by the user on the ultrasound data. In a first stage the operator has to define three landmarks for initial registration of the model to the patient volume. Then, the operator navigates in the images and clicks on points that are clearly visible on the prostate capsule. Each time a point is defined, the algorithm adapts the model in order to match the points. The operator may navigate again in the data and verify that the resulting contour matches the images, modify or remove one point, add another point until he/she is satisfied.

Results: One can see on the figure the interface presenting the three orthogonal images slices reconstructed from the US volume; each image shows the user-defined points and the contours resulting from the deformation of the model. A surface representation also displays in 3D the deformed model and the user-defined points (bottom right). In general, about thirty to forty points are necessary for a good segmentation. The force of the algorithm is that it yields a statistical shape in image regions without signal (noise, regions outside US beam), which is in general a good prediction of the real shape. The semi-automatic process takes about 5 minutes where a manual segmentation of comparable quality takes 20 to 30 minutes.

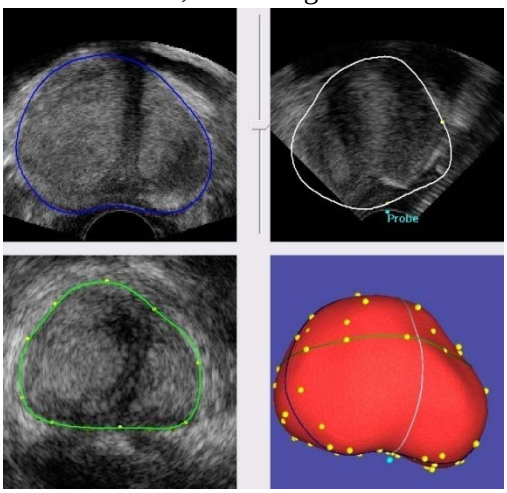

Conclusion: We have developed an efficient tool for semi-automatic segmentation of ultrasound prostate volumes. Extensive evaluation is about to start to precisely evaluate the performance of the system in clinical routine.

References:

[1] M. Baumann, P. Mozer, V. Daanen, and J. Troccaz, *"Towards 3D ultrasound image based soft tissue tracking: A transrectal ultrasound prostate image alignment system"*, MICCAI'2007, vol. 4792, pp. 26–33, Springer, LNCS.
[2] P.Mozer, M. Baumann, G. Chevreau, A. Moreau-Gaudry, J. Troccaz. *Mapping of Transrectal Ultrasound Prostate Biopsies: Quality Control and Learning Curve Assessment by Image Processing.* Accepted in Journal of Ultrasound in Medicine, forthcoming
[3] S. Martin, V. Daanen, J. Troccaz. *Atlas-based prostate segmentation using a hybrid registration.* International Journal of Computer Assisted Radiology and Surgery, Springer Verlag, December 2008, 3:485-492

ABSTRACT 68

SYRINGE WITH SPIRAL TIP USED IN BOTULINUM TOXIN A INJENCTON FOR TREATING LOWER URINARY TRACT DYSFUNCTION

Chung Cheng Wang[1], Chien-Yu Lin[2], Weng-Pin Chen[2]

[1]*Department of Urology, En Chu Kong Hospital, Taipei, Taiwan*
[2] *Department of Biomedical Engineering, Chung Yuan Christian University, Taoyuan, Taiwan*

Introduction: An operative room nurse noted that cone-tip syringe was easily disconnected from cystoscopy during botulinum toxin A injection (BoNT-A) to lower urinary tract. We compared cone-tip syringe and spiral-tip syringe (fig.1) used in the BoNT-A injection for lower urinary tract dysfunction.

Methods: Sixty-three male patients underwent transurethral BoNT-A 100U ~ 200 U injection to urethra, bladder and prostate for treating various lower urinary tract dysfunctions. Cone-tip syringe and spiral-tip syringe were used in 27 and 36 patients respectively. Mechanical pullout test was measured by using materials testing machine Instron® 8511(Instron Corporation, Canton, MA, USA).

Results: Injection to urethra, bladder and prostate was performed in 35, 17 and 11 patients, respectively. Disconnection rate using cone tip and spiral tip syringe was 22.2% (6/27) and 0% (0/35) respectively. Pullout test showed that the separated strength using spiral tip syringe was significantly greater than that using cone tip syringe (185 ± 10N versus 25 ± 2N, $p<0.01$).

Conclusion: Our preliminary experiences suggested that a syringe with spiral tip was a more reliably tool used in the transurethral injection route to treat lower urinary tract dysfunction.

Fig.1 Syringe with cone tip (left) and syringe with spiral tip (right)

Fig. 2 Mechanical pullout test

ABSTRACT 69

LAPAROSCOPIC VERSUS PERCUTANEOUS RENAL CRYOABLATION

Sebastien Crouzet, Raj K. Goel, Georges-Pascal Haber, Kazumi Kamoi, Wesley White, Inderbir S. Gill and Jihad H. Kaouk

Section of Laparoscopic and Robotic Surgery, Glickman Urological and Kidney Institute
Cleveland Clinic, Cleveland, Ohio

Introduction: Cryoablation of small renal masses is an emerging treatment alternative for select patients with compromised renal function or multiple co-morbidities. Herein we present a comparison between laparoscopic renal cryoablation (LRC) and percutaneous renal cryoablation (PRC).

Methods: Retrospective analysis of all renal cryoablations performed at a single institution between 1997 and 2008 was reviewed. Patient demographics, perioperative data and oncological outcomes were evaluated. Variation in renal function as determined by estimated glomerular filtration rate (eGFR) and absolute creatinine was also assessed.

Results: A total of 307 renal cryoablations have been performed (LRC: 244 and PRC: 63). Patient and tumor characteristics were similar in both cohorts although PRC tended to have either solitary kidney or prior renal surgery: LRC 11.8% vs. PRC 30.2%, p=0.0012 and LRC 21.9%, vs. PRC 55.6%, p<0.0001, respectively. Functional outcomes were similar for LRC and PRC: Creatinine (1.5 vs. 1.4 mg/dl, p=0.97) and eGFR (59.2 vs. 57.3mL/min/1.73m^2, p=0.94). Intra-operatively, more probes were used in PRC (1.4 2.2 probes, p<0.0001). A higher incomplete treatment rate was seen in PRC (1.6% vs. 7.6% p=0.0055) but all other operative data was similar. Hospital stay was shorter in the PRC group (59.1 vs 22.0 hours, p<0.0001). Two-year overall, cancer-specific and recurrence-free survival was similar between groups.

Conclusion: Although PRC is performed as an outpatient procedure, it is associated with higher incomplete treatment rates compared to LRC despite more probe use. Comparative follow-up is currently limited, however cryoablation performed either laparoscopic or percutaneously provides equivalent cancer control at two years.

	Laparoscopic	**Percutaneous**	*p*-value
Tumor size (cm)	2.6±0.9	2.5±0.9	0.59
Cryolesion day 1 (cm)	3.8±1.0	4.1±1.4	0.4
Cryolesion 6 months (cm)	2.7±1.2	2.9±1.2	0.27
Incomplete treatment	4 (1.6%)	5 (7.6%)	**0.018**
Recurrence	15 (6.2%)	2 (3.0%)	0.31
Mean Follow up (Months)	51.4±34.8	15.5±6.9	**<0.0001**

	Creatinine		**eGFR**		**eGFR decrease post ablation**	
	Preoperative	**Postoperative**	**Preoperative**	**Postoperative**	**Absolute**	**%**
	(mg/dl)		(mL/min/1.73m2)			
Laparoscopic	1.4±0.7	1.5±0.9	64.6±29.2	59.2±28.9	-1.5±23.3	4.7±26.9
Percutaneous	1.3±0.4	1.4±0.6	60.1±18.7	57.3±20.3	-2.8±11.0	4.9±17.8
p-value	0.35	0.97	0.4	0.94	0.85	0.92

ABSTRACT 70

SINGLE PORT – SINGLE SURGEON ROBOTIC-ASSISTED LAPAROSCOPIC UROLOGIC SURGERY

Sebastien Crouzet, Georges-Pascal Haber, Kazumi Kamoi, Raj Goel,
Wesley White, and Jihad H. Kaouk

Section of Laparoscopic and Robotic Urology, Glickman Urological and Kidney Institute
Cleveland Clinic, Cleveland, Ohio

Introduction: Herein we present the initial experience with single-port robotic-assisted laparoscopic surgery in reconstructive urology performed by a single surgeon.

Methods: We performed on 5 males farm pigs, 10 dismembered pyeloplasties (5 right and 5 left) and 10 partial nephrectomies (5 right and 5 left) followed by 10 radical nephrectomies (5 right and 5 Left). The animal was placed in lateral flank position. The single port (TriPort, ASC, Bray, Ireland) was inserted through a 2cm incision in the umbilicus. The scope was held using a novel low profile Light Endocopic Robot (LER) (Viky, EndoControl, Grenoble, France) fixed to the OR table and controlled using voice-command or foot-control. We used articulated instruments with deflectable and 360° rotatable tips that provide 7-degrees of freedom (CambridgeEndo, Framingham, USA).

Results: All procedures were performed without any addition of laparoscopic port or open conversion by a single surgeon. The mean incision size after closure was 2.6cm (range 2.3 to 3 cm). The robotic endoscope holder with foot control provides a stable image with easy movements. Mean operative time for pyeloplasty was 110 min (range 95 to 130 min), 120 min for partial nephrectomy (range 100 to 150 min) and 20min radical nephrectomy (15 to 30min). The partial nephrectomies were performed without hilum clamping. The mean estimated blood loss was 240mL (range 200 to 280mL). When analyzing the learning curve, the preparation time decrease with the increasing number of case without reaching statistically significant value (p=0.08).

Conclusion: The combination of a single-port, a robotic scope holder and articulated instruments has the potential of a single surgeon procedure. With a single port access, the robot gives more room to the surgeon than an assistant.

Fig 1. Operative view of the system.

Fig. 2. Robotic scope holder on the Single-Port

Fig 3. Pyeloplasties with articulated instruments

ABSTRACT 71

3D ULTRASOUND IMAGE GUIDED FIXED PLATFORM TRANS-RECTAL PROSTATE BIOPSY

Sijo J. Parekattil, Drew Palmer, Rikin Patel, Hany N. Atalah, Philipp Dahm, Johannes W. Vieweg, Li-Ming Su

University of Florida, Gainesville, FL

Introduction: Previous studies have shown that 3D ultrasound image guided trans-rectal prostate biopsy devices may provide a higher accuracy in tumor localization compared to standard 2D ultrasound systems. Our goal was to assess if the use of 3D ultrasound with a fixed platform needle delivery system would not only provide enhanced accuracy in tumor localization, but also improve biopsy reproducibility and decrease inter-surgeon variation compared to standard manual 2D ultrasound guidance.

Methods: A prospective randomized control trial of standard 2D (GE Inc, Piscataway, NJ) versus 3D fixed platform biopsies (TargetScan Touch, Envisioneering Inc, St.Louis, MO) was conducted on a prostate phantom model. A single surgeon performed eight prostate biopsies (128 cores - 16 per biopsy) randomized into two groups of four (2D versus 3D) on the same prostate phantom. The phantom was designed with six different color regions (figure below) to identify the region being biopsied. These regions could not be differentiated by ultrasound imaging and the surgeon was blinded to them during the biopsy. Accuracy in correctly localizing the regions (color detected in the biopsy core) and the reproducibility of the biopsy scheme were assessed. Inter-surgeon reproducibility of the 3D technique was assessed by having two novice surgeons perform 3 prostate biopsies each (16 cores per biopsy) on the phantom.

Results: For the experienced surgeon, accuracy in correctly localizing all the regions of the prostate was 100% (64 cores) using the 3D technique and 78% (64 cores) using standard 2D technique ($P < 0.001$). The reproducibility of the cores (ability to get the same region on repeat biopsies) was 100% for the 3D technique and 80% with the 2D technique ($P < 0.001$). For the two novice surgeons using the 3D technique, the localization accuracy was 98% and 100%; the reproducibility was 98% and 100%.

Conclusion: Trans-rectal prostate biopsy using the 3D ultrasound with a fixed platform needle delivery system appears to be superior to standard 2D technique in localization accuracy and reproducibility. The outcomes with the 3D technique appear to be reproducible across surgeons with different levels of training. These findings may have implications on improving cancer mapping, clinical staging and planning for focal therapy.

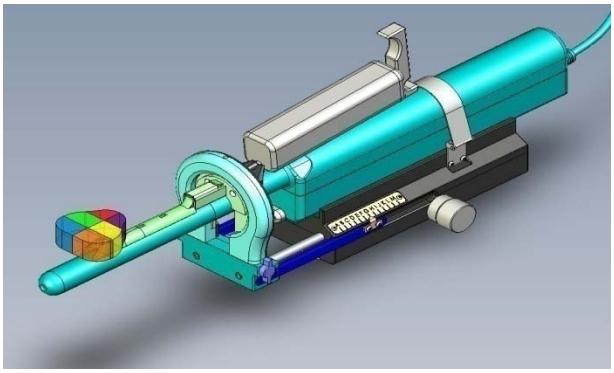

ABSTRACT 72 **OUTSTANDING PAPER AWARD**

ANALYSIS OF ACOUSTIC ACCESS TO THE PROSTATE THROUGH THE PERINEUM FOR NON-INVASIVE HISTOTRIPSY THERAPY

Timothy Hall[1], Brian Sabb[2], Christopher Hempel[1], William Roberts[1]

[1]*Department of Urology, University of Michigan Health System, Ann Arbor, MI*
[2]*Department of Radiology, University of Michigan Health System, Ann Arbor, MI*

Introduction: Histotripsy is a method of non-invasive, non-thermal ultrasound therapy for the ablation of soft tissues. Intense pulses of focused ultrasound from an extra-corporeal transducer generate a cloud of oscillating, cavitating microbubbles that cause cell disruption and mechanical fragmentation of tissue at the focus without damage to overlying tissue. The therapeutic process is easily imaged with standard diagnostic ultrasound due to the high reflectivity and dynamic nature of the microbubbles created. We are developing this technique for application in the treatment of BPH. Disrupted prostate tissue will be reduced to a liquid consistency where it is flushed with normal urination relieving symptoms. Experimental studies to date have required a large therapy transducer (10 cm diameter or larger) with an f-number ≤ 1 (ratio of focal length to diameter) to produce adequately intense ultrasound pulses. The location of the prostate in the pelvis surrounded by acoustically opaque bones could preclude the use of histotripsy. This study seeks to test the hypothesis that acoustic access to the prostate for histotripsy is possible through the perineum.

Methods: Image data from randomly selected patients undergoing arterial contrast enhanced CTs were used to create high resolution 3-D reconstructions of the pelvis. Subjects less than 56 years of age or with very small prostates were excluded leaving a set of 16 (mean age 66.4). Target locations at the base and apex of the prostate were marked. From these points 881 uniformly spaced rays (up to 56° from the cranial-caudal axis) were back-projected to outside the body. Rays encountering high density tissue (bone) were considered to be blocked. The remaining rays defined the useful therapeutic window in terms of solid angle. A 20 mm diameter cylindrical mask simulating a transrectal imaging probe (GE model ERB) was also placed in the reconstruction blocking therapy propagation along certain paths. The fraction of unblocked rays within a 60° solid angle circular aperture (f-number = 1) placed to maximize the fraction then represented the percentage of a transducer surface area available for that target. The process was repeated for apex and base locations in each subject.

Results: For all 16 subjects, the available transducer aperture was 100% for apex target locations. For base targets, the average aperture was 76% (low = 52%, high = 98%) with obstructions primarily caused by the pubis, the caudal ends of the ischial tuberosities, and the imaging probe in the rectum. The free aperture for the base targets was a triangular shaped region.

Conclusion: A significant acoustic window exists through the perineum to access the prostate with extra-corporeal ultrasound therapy. The apex of the prostate is easily accessed without obstruction. The base of the prostate is partially blocked by bones of the pelvis, but a large fraction of a typical therapy transducer aperture is still available for many subjects suggesting that this approach is feasible. Additional studies of patients in a lithotomy position (the optimal position for trans-perineal prostate histotripsy) with ultrasound imaging should provide the skin to target distances needed to construct an effective therapy transducer.

ABSTRACT 73

PHYSICAL CHARACTERISTICS OF FOLEY CATHETERS

Kari Hendlin, Manoj Monga

University of Minnesota

Introduction: The Foley catheter is one of the most common medical devices placed in medicine today. This in vitro study evaluated physical properties of Foley catheters including advancement, buckling and friction forces.

Methods: Testing of 11 Bard Lubri-Sil® (16 Fr, Bard) and 10 Kendall Dover™ (16 Fr, Kendall) Foley catheters was performed using a linear motion stage driven by a stepper motor with a resolution of 5 microns/step or by hand. Force was measured at a sampling rate of 5Hz with a Wagner FDIX digital force gauge. Friction force was measured by pulling each Foley catheter at a rate of 2.5mm/s through a 5.2 mm (15.6 F) hole drilled in 36mm thick biological material (Oscar Meyer Beef Light bologna 12 oz. package). Advancement force was measured by the force necessary to bend the catheter tip around a 90 degree turn in a urinary tract modeled by 5/16 inch inner diameter silicone tubing and lubricant. Buckling force at the tip (8 mm), from the distal end of the balloon to the tip (30 mm), and of a 20 cm section of the shaft were measured using the appropriate size force gauge.

Results: No significant difference was noted for friction force. Kendall (0.0686±0.102 lb_f) took more force to advance than Bard (0.602±0.110 lb_f, p=0.003). Buckling force along the shaft and from the balloon to the tip were significantly greater for the Bard (0.051±0.02 lb_f, p<0.001 and 0.892±0.166 lb_f, p<0.001) compared to the Kendall (0.027±0.007 lb_f and 0.803±0.129 lb_f) Foley catheters. Buckling force at the tip was significantly greater for the Kendall (2.644±0.552 lb_f, p<0.001) compared to the Bard (2.101±0.437 lb_f) Foley catheters.

Conclusion: Traumatic catheterization is a major cause of urethral stricture. Catheter stiffness may increase the risk of urethral injury and subsequent stricture formation. The Kendall catheters being stiffer at the tip relative to the Bard catheters coincide with our institution's observations of a 70% increase in the difficulty of Foley catheter placement with the recent conversion of our catheter from Bard to Kendall.

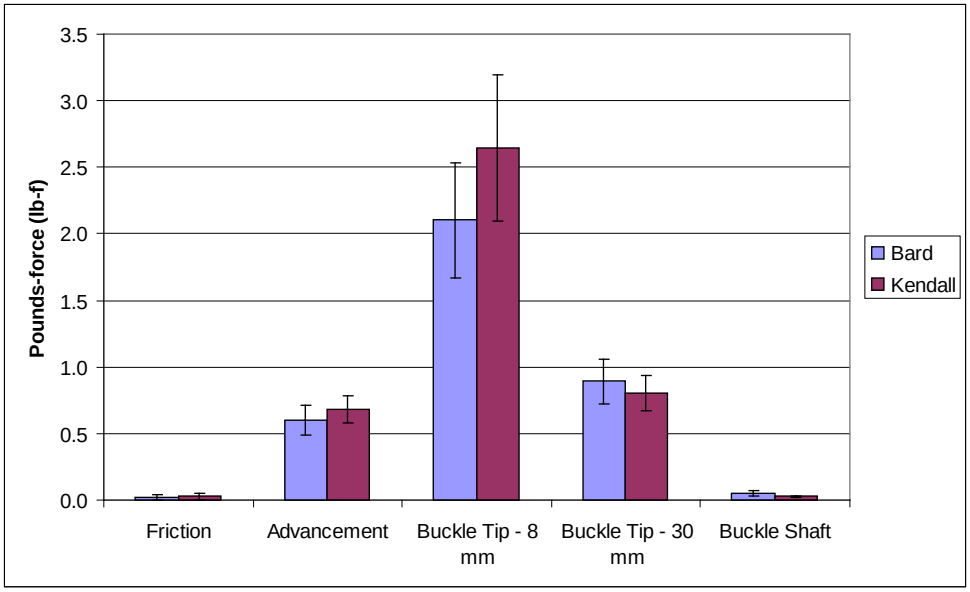

ABSTRACT 74

ROBOTIC ASSISTED MICROSURGICAL DENERVATION OF THE SPERMATIC CORD

Sijo J. Parekattil, Hany N. Atalah, Marc S. Cohen, Johannes W. Vieweg.
University of Florida, Gainesville, FL

Introduction: Previous studies have shown that microsurgical denervation of the spermatic cord (MDSC) can treat select patients with chronic testicular pain. There is recent work to suggest that robotic assistance may provide technical advantages in microsurgery. Our goal was to develop a robotic assisted microsurgical approach for the denervation of the spermatic cord (RMDSC) and present our initial results.

Methods: Nine patients with the following criteria were selected: chronic testicular pain (at least 6 months), failed antibiotics, anti-inflammatory medications and conservative pain management, negative neurology workup, negative testicular ultrasound and upper tract imaging, and complete temporary resolution of pain with local anesthetic mapped spermatic cord block. A 2-3 cm subinguinal incision approach was utilized. The ilioinguinal and genitofemoral nerve branches were ligated, and the spermatic cord was then elevated. A robotic microsurgical platform was utilized (DaVinci S with high magnification). All the arteries, 1-2 veins, 1-2 lymphatics and the vas deferens were spared (figure below). The cremasteric fibers and remaining vessels were ligated. The vas deferens was stripped (to incise any nerve fibers along the vas). Post-operative follow-up ranged from 1-4 months (mean 2 months).

Results: Mean operative duration for all cases was 54 mins (25-75). No complications occurred. Postoperatively, 78% (7/9) patients have had complete resolution of their pain, have stopped all their pain medications and have pain scores of 0/10. In the 2 patients with continued pain: one patient had resolution of pain for only 1 month, the other has had resolution of his original type of pain, but now has scrotal discomfort on that side. The robotic platform appeared to offer technical advantages over the microsurgical technique in terms of ergonomics and tissue handling. The 4th robotic arm allowed the surgeon to control one additional instrument (Potts scissors or Doppler probe for arterial localization) during the cases. This enabled improved surgeon efficiency and less reliance on the microsurgical assistant.

Conclusion: Robotic assisted microsurgical denervation of the spermatic cord appears to be a safe procedure. The preliminary results appear promising. However, longer follow is needed. Further evaluation is needed to assess its clinical potential and to quantify if there are any benefits over the pure microsurgical technique.

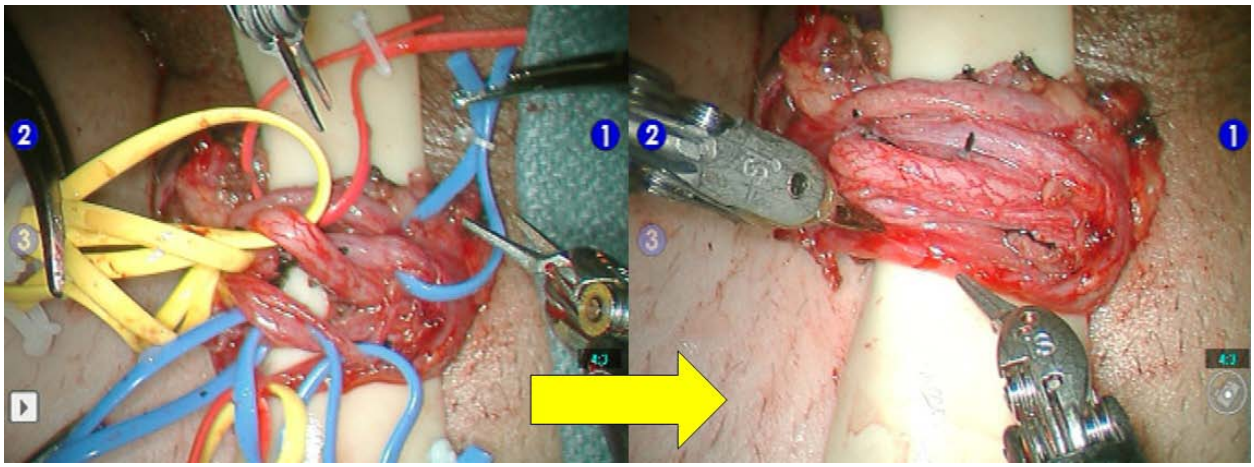

ABSTRACT 75

6-DOF HAPTIC MASTER FOR ROBOTIC LAPAROSCOPIC SURGERY

Felix Schäfer, Matteo Zoppi, Rezia Molfino
Department of Mechanics and Machine Design, University of Genoa, Italy

Introduction: Minimally invasive robotic surgery can overcome the difficulties of the manual approach by providing a higher manipulability with additional DOF inside the patient's body and by making the handling of the instrument easier and more intuitive. This requires a suitable haptic master, which allows the desired motions and gives force feedback to the surgeon for all six DOF. The motion of the instrument is constrained by the incision, which allows only three rotations around this center point of rotation (CPR) and one translation along the trocar axis. Further a micro-wrist orienting the tool with two DOF is commonly used. The master architecture shown in the figure does already integrate all these constraints. The spherical submechanism provides three rotations around the CPR and the wrist submechanism, actuated by three prismatic joints provides the translation along the trocar axis and the two tilts of the micro wrist. As low inertia is an important requirement for haptic interfaces this architecture allows to place already three actuators in the base, driving the spherical submechanism. Further the parallel architecture will provide high stiffness and thus a good force transmission and high bandwidth.

Methods: Inverse and velocity kinematics have been computed using screw theory and the Jacobian for both submechanisms as well as for the overall mechanism has been derived. Based on the condition number of the Jacobian matrices of the submechanisms a dexterity and singularity analysis has been performed, assuring that all the workspace is singularity free. Further the geometrical parameters of the spherical submechanism have been optimized applying a sensitivity analysis, which considers the link angle, the global conditioning index (GCI) and the average deviation from the GCI that allows discovering bad conditioned areas in the workspace. Finally static forces have been computed.

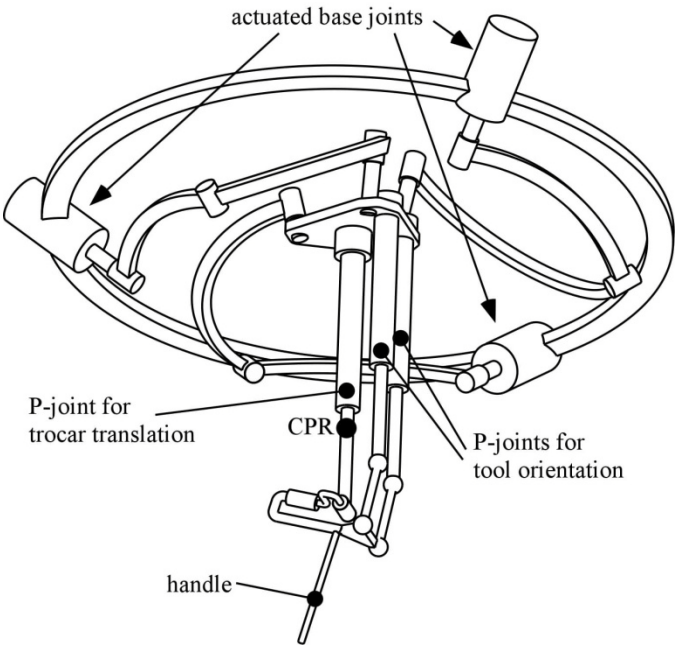

Figure: Proposed Architecture

Results: Based on the dexterity analysis using the optimized geometry the haptic master provides a singularity free conic workspace with a vertex angle of 60 degrees, a torsion angle around the trocar axis of 160 degrees, a translational motion of 100 mm along the trocar axis and 120 degrees for both tilting angles of the micro wrist. A static force of 5 N can be applied on the handle at a distance of 100mm from the microwrist all over the workspace with acceptable joint torques/forces.

Conclusion: A 6-DOF haptic master has been proposed, which provides a huge singularity-free workspace and does already contain all environmental constraints. The dexterity and static forces analysis showed positive results.

ABSTRACT 76

IN VITRO EVALUATION OF THE EFFECT OF COLOR ON IDENTIFICATION OF URINARY TRACT CATHETERS IN A HEMORRHAGIC ENVIRONMENT

Zhamshid Okhunov, Harmanmeet Singh, Daniel Lee, Alberto Pérez-Lanzac de Lorca, Diana Lee, Juan Carlos Rosales, Mantu Gupta, Ketan Badani, Jaime Landman

Department of Urology, Columbia University Medical Center, New York, NY

Introduction: Endoscopically deployed stents, such as ureteral stents, are very common in clinical practice. Identification and manipulation of these stents in a hemorrhagic environment can be challenging. To date, the endoscopic visibility of different color stents has not been evaluated.

Methods: Videos of eight different colored stents in a bladder model were created. The videos were created using a flexible cystoscope in a clear saline, mildly bloody (1cc of blood in 600cc of saline), moderately bloody (2 cc), and severely bloody (3 cc) environments. Participants reviewed the videos, and were asked to identify the color of each stent, and rate the visualization on a 10 point scale. The videos were presented in a random sequence. Logistic regression models were used to model the relationship between visualization, stent color, environment, and experience.

Results: Forty-seven participants reviewed the videos. The mean visualization scores for all the environments were significantly higher for blue and green stents compared to other colors (one way ANOVA p=0.004) (Fig 1). For the clear saline and mildly blood environments, blue stents had the highest visualization (p<0.06 and p=0.001 respectively). In the moderately environment, yellow stents had the highest visualization (p<0.01), and silver stents had the highest visualization in the severely blood setting (p=0.004) (Fig 2). After adjusting for environment, experience with endoscopy, stent color, and level of training, the environment and stent color remained independent predictors of correct stent identification. Regarding actual color identification, participants were able to correctly identify only blue and green stents more than 50% of the time (68.5% and 56.8%, respectively, p<0.001).

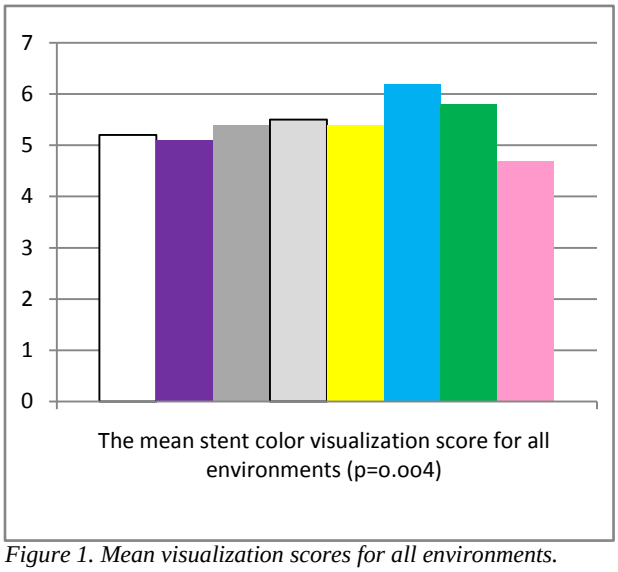

Figure 1. Mean visualization scores for all environments.

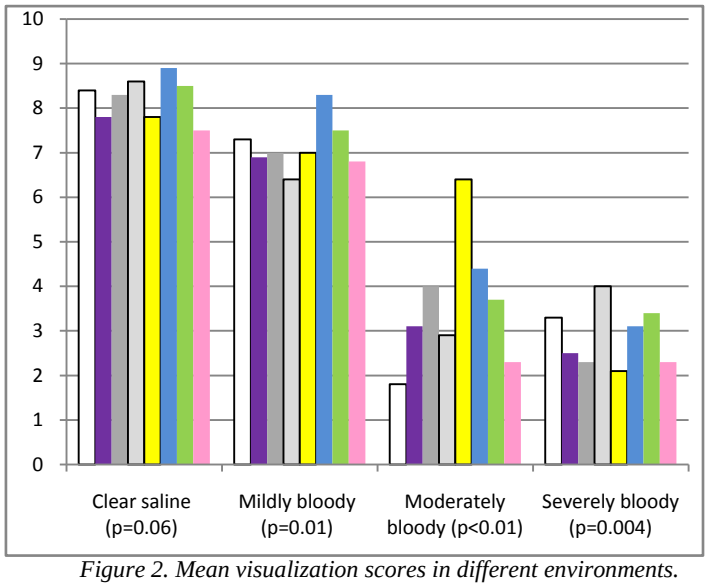

Figure 2. Mean visualization scores in different environments.

Conclusions: Stent color plays an important role in endoscopic visualization; blue stent color offers superior visibility in both clear and hemorrhagic environments. In a very blood environment, a silver color may be advantageous.

ABSTRACT 77

THE SOLO-SURGEON VAMS DONOR NEPHRECTOMY

Young Seung Lee, Seung Ryeol Lee, Young Hoon Lee, Wooju Jeong, Woong Kyu Han, Koon Ho Rha, Seung Choul Yang

Department of Urology, Urologic Science Institute, Yonsei University Health System, Seoul, Korea

PURPOSE: Human assistance needs costs and often does not fulfill surgeon's needs. VAMS donor nephrectomy, first introduced by Yang *et al.*, could be performed by solo-surgeon without an assistant, using Unitract® (Aesculap Surgical Instrument, Germany). We examined the results of the solo-surgeon VAMS donor nephrectomy and the human-assisted VAMS donor nephrectomy.

MATERIALS AND METHODS: Between July 2007 and April 2008, a series of 82 VAMS donor nephrectomies were performed by 2 surgeons and randomized with the approval of IRB. All the VAMS donor nephrectomy procedures were done in the same manner described in the literatures by Yang et al. The roles of a first assistant were substituted by Unitract® (Fig. 1). We prospectively collected the perioperative data.

RESULTS: There were no significant differences in age, sex, the laterality and operation time between two groups (Table I).

CONCLUSIONS: The solo-surgeon VAMS donor nephrectomy showed similar operative outcomes compared to the human-assisted VAMS donor nephrectomy. It could be performed safely with economical benefits.

Table I. Comparison of patient demographics & operative data between solo-surgeon VAMS donor nephrectomy (Solo-surgeon) and human-assisted VAMS donor nephrectomy (Human-assisted)

Variables	Solo-surgeon (n=35)	Human-assisted (n=47)	p-value
Mean age (yrs)	40.89±10.57	39.17±10.52	0.665
Laterality (Lt : Rt)	28 : 7	38 : 7	
Sex (M : F)	22 : 13	27 : 20	
Mean operative time (min)	201.86±32.90	202.40±48.26	0.082

Figure 1. Configuration of the assembly of instuments for solo-VAMS nephrectomy.

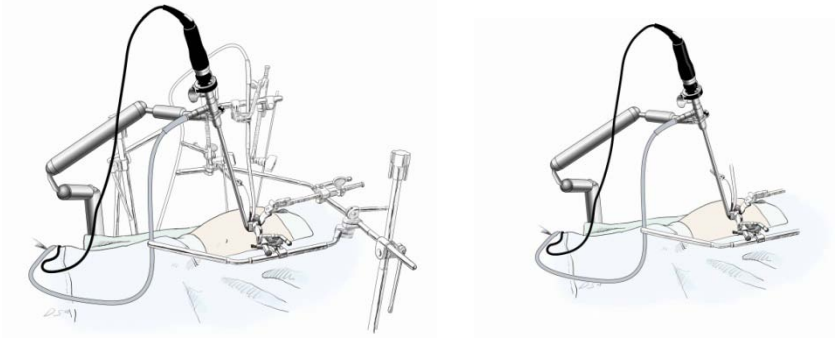

ABSTRACT 78

ROBOTIC RADICAL PROSTATECTOMY: TRANSVESICAL APPROACH

Andre Berger, Monish Aron, Ricardo Brandina, Rene Sotelo, Brian Irwin, Robert Stein,
David Canes, Inderbir Gill, Mihir Desai
Department of Urology Glickman Urological and Kidney Institute, Cleveland Clinic, Cleveland, Ohio, USA

Objectives: To report the technical feasibility of performing transvesical robotic radical prostatectomy

Methods: Transvesical robotic radical prostatectomy was performed in 2 fresh male cadavers (prostate volume 46 and 30 cc) and in 1 live patient (61 years, PSA 4.6, Gleason 6 in 2 cores). The first procedure was performed using 4 laparoscopic transvesical trocars and the 2 following procedures using one single port device placed percutaneously into the bladder. Pneumovesicum was established in both cases and the da Vinci-S robotic system (Intuitive Surgical, Sunnyvale, CA) was used to perform transvesical radical prostatectomy. All steps of the procedure including dissection of the seminal vesicles and vas deferens, ligation of prostatic pedicles, release of neurovascular bundles, apical dissection, urethral transection, and urethro-vesical anastomosis were performed transvesically and robotically. Real time trans-rectal ultrasound (TRUS) monitoring was performed in case #1.

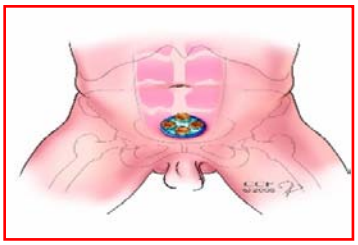

Figure 1. Actual photograph of the four-channel single-port device (cadaver)

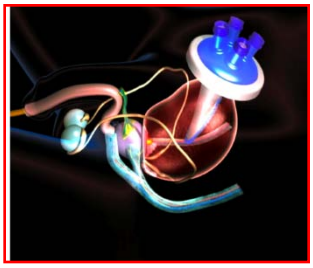

Figure 2. Sagittal view (cadaver)

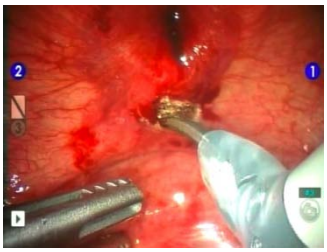

Figure 3. Incision along the bladder neck distal to the ureteric orifices

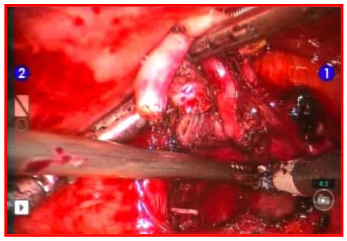

Figure 4a. The completely dissected seminal vesicles and dividing vasa

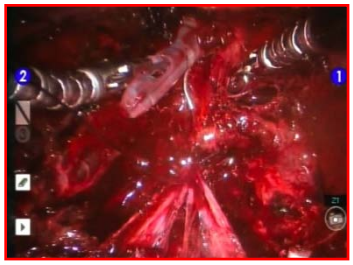

Figure 4b. Running vesico-urethral anastomosis (first stitch)

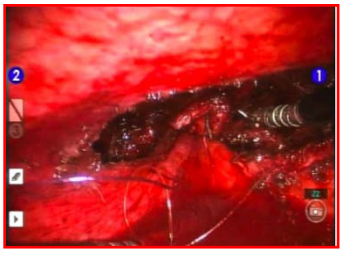

Figure 5.. Running vesico-urethral anastomosis

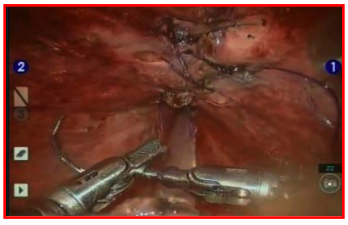

Results: All procedures were technically successful transvesically without need for additional ports or conversion to standard laparoscopy. In the cadaver, operative time for the multi-port procedure was 3 hours and the single-port procedure was 4.2 hours. Operative time in the live patient was 6 hours, estimated blood loss 200 cc, hospital stay 3 days. Pathological report confirmed a Gleason 6 prostate cancer with focal positive surgical margin. Clashing of the da Vinci arms was the primary technical difficulty with the single port procedure.

Figure 6. The redundant bladder neck opening is reconstructed in an anterior tennis-racket fashion.

Conclusions: Transvesical radical robotic prostatectomy under pneumovesicum is technically feasible using multiple ports or using a single port approach. Further refinement of technique and instruments may lead to an increasing role of percutaneous transvisceral surgery in various surgical disciplines.

ABSTRACT 79

A NOVEL UNIFIED SPATIAL FORMULATION METHOD FOR MODELING 1/2/3-DIMENSIONAL OBJECTS IN REAL TIME FOR SURGICAL SIMULATION

Nan Zhang[1], Yunhe Shen[1], Xiangmin Zhou[2], Kumar Tamma[2], and Robert Sweet[1]
[1] Center for Research in Education and Simulation Technologies (CREST), Department of Urologic Surgery,
[2]Department of Mechanical Engineering, University of Minnesota

Introduction: In order to create a laparoscopic transperitoneal nephrectomy simulator that exhibits realistic behavior in real time, we are using a variety of biophysical-simulation approaches. Due to the complexity and diverse nature of the structures of the renal hilum, traditional spatial discretization techniques such as finite element (FE) method are insufficient to achieve our objectives. As a solution, we have advocated the use of a variety of physical elements—solids (3D), thin shells (2D), and threads (1D), to model the physical behavior of underlying tissues. However, effective simulation algorithms for shells and threads are complicated and still under active research. In this study, two modeling challenges that need to be addressed involve complex deformations and damage of each of the critical anatomical structures. We propose a unified approach using a proposed 1D element called the ***gy***roscopic ***rod*** (gyrod) element to successfully meet these challenges. While the detailed derivation of the gyrod element is being described by our group in a separated paper, here we demonstrate a novel application of this element for modeling 1D, 2D, and 3D objects.

Methods: The gyrod element is a non-trivial extension of the classical spring element. In addition to the axial resistance, it additionally possesses the orientation-change resistance. The vertices of an object and their 1-ring neighboring vertices are used as the basic simulation elements. Each vertex, together with its immediate neighboring vertices, forms a star-like shape. To integrate the equation of motion, a rotation matrix is first computed via a polar decomposition of the deformation matrix of the star shape. All the neighboring vertices are rotated onto a reference coordinate using the computed rotation matrix. Then, for each edge of the star shape, elastic force from its corresponding gyrod element is computed. Finally, the forces are rotated back onto the global coordinate. In explicit time integration, the primary computational complexity is due to the forces evaluation. In implicit time integration, the stiffness matrices are computed accordingly. Due to the simplicity of the gyrod elements, the overall computation is efficient but with realistic physical behavior.

Results: The proposed formulation demonstrates good approximation results in comparison with FE based simulation results. Unlike the mass-spring based approximation methods, both the young's modulus and poisson ratio parameters can be utilized. Because of the orientation deformation energy, the dynamic behavior is close to FE methods, even when very large deformations are encountered. The simulation speed almost doubles that of the fastest corotational FE method. Similar effects can be observed in thin shell and net models. Figure 1 shows such a simulation environment where the kidneys are modeled in solids and the aorta is modeled as a thin shell. However, all objects are simulated using the same underlying star shaped elements. Speed and accuracy data with a live demonstration will be provided.

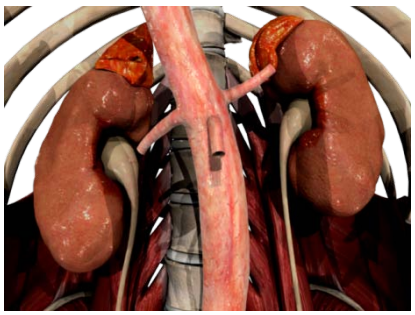

Conclusion: A simple yet efficient spatial formulation has been proposed for simulating 1D, 2D, and 3D objects in a unified approach. The objective is to ease the implementation of physically based deformation systems and their future development, such as parallelization using multi-threading or Graphics Processing Unit acceleration. We are integrating the above techniques in modeling urologic tissues relevant for a laparoscopic transperitoneal nephrectomy simulator.

ABSTRACT 80 **OUTSTANDING PAPER AWARD**

FREE HAND 3D-TRUS PROSTATE BIOPSY MAPPING

Pierre Mozer[1], Michael Baumann[2], Gregoire Chevreau[1,2], Vincent Daanen[3],Jocelyne Troccaz[2]
[1] *Department of Urology, Pitié-Salpêtrière Hospital, Pierre et Marie Curie University (Paris VI) Paris, France.*
[2] *TIMC Laboratory, IN3S, Faculté de Médecine, Domaine de la Merci, 38706 La Tronche Cedex, France.*
[3] *KOELIS© - www.koelis.com*

Introduction: We present a new prostate imaging assistant that intra-operatively displays and records the 3D spatial distribution of prostate biopsies with reference to an initial location of the prostate. The method is based on 3D transrectal ultrasound (3D TRUS). The system allows the clinician to perform regular or targeted biopsy sampling.

Methods: We use a 3D TRUS probe on a Sonoace X8 scanner (Medison, Korea), linked to the computer with a network cable (Fig 1). The 3D cartography is based on an automatic registration method described in [1]. The clinical workflow is unchanged. An initial "reference" 3D image of the prostate is recorded before starting the biopsy sampling. Although the registration method is robust to prostate motion and deformation to some extent, the operator sees to apply minimum force on the probe. The biopsy tract is guided by real time 2D TRUS. After every biopsy gun shot, the needle is left in the prostate less than 5s while a 3D TRUS image is transferred to the computer, and displayed in 3D on the reference prostate (Fig 2). The clinician may rotate, zoom or reslice the 3D prostate and biopsies using a trackball. Alternatively, a 3D TRUS image may be transferred before a biopsy shot in order to check the actual biopsy target that can be reached afterwards providing the probe is unmoved. Once histological results are known, one may eventually integrate them to the patient's data file to visualize the positive biopsy locations with respect to the patient's prostate (Fig 3).

Figure 8 - Left: Laptop, Middle: UltraSound

Results: The registration accuracy was validated on 237 3D images from 14 patients. Using fiducials (calcifications), the average error was 1.4mm and max error 3.8mm. The success rate of 800 registrations from 70 patients was 97%. No post-biopsy complication was reported.

Conclusion: In addition to being very useful to improve the biopsies distribution, the potential of this system is above all the possibility to create for each patient a precise map of sampled areas without significant change in routine clinical practice. That can be used in the near future in order to merge repeated biopsy sessions or to plan an accurate focal therapy treatment.

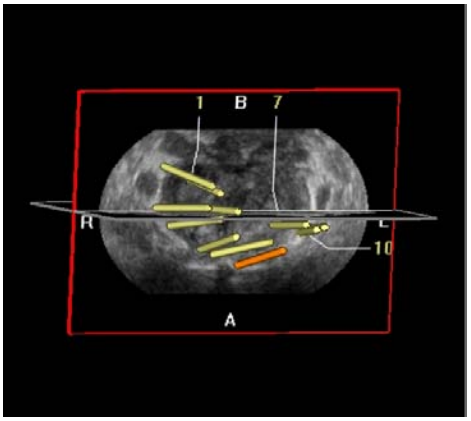

Figure 10 : Distribution of the biopsies inside a "reference" 3D TRUS image. B=Base, A=Apex, L=Left, R=Right. Yellow: biopsies performed. Orange: biopsy simulated.

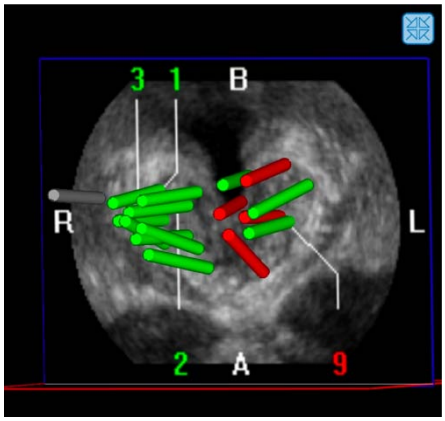

Figure 9 : Green: Negative biopsies. Red: Positive biopsies.

(1) Michael Baumann *et coll.*, "Towards 3D ultrasound image based soft tissue tracking: a transrectal ultrasound prostate image alignment system," Medical image computing and computer-assisted intervention 10, no. Pt 2 (2007): 26-33.

SOCIETY OFFICERS:

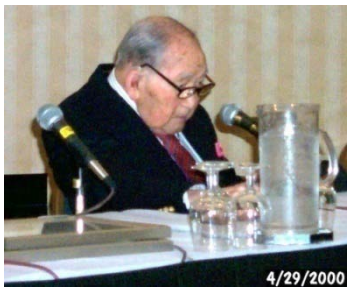

George Nagamatsu, M.D.
Founder

Jean de la Rossette, M.D., Ph.D.
President

Jens Rassweiler, M.D.
Vice-President

Jack Vitenson, M.D.
Secretary

John Denstedt, M.D.
Treasurer

Louis Kavoussi, M.D.
Councilor

Dan Stoianovici, Ph.D.
Executive Director

ADVISORY BOARD

Jeffrey Cadeddu, M.D.

Ralph Clayman, M.D.

John Denstedt, M.D.

Thomas Lawson, Ph.D.

Douglas Milam, M.D.

Stephen Y. Nakada, M.D.

Will Roberts , M.D.

Ihor S. Sawczuk, M.D.

Arthur Smith, M.D.

Li-Ming Su , M.D.

Hessel Wijkstra, Ph.D, M.Sc.

AWARDS:

Best Paper Award:

TANDEM-ROBOT ASSISTED LAPAROSCOPIC RADICAL PROSTATECTOMY: CLINICAL FEASIBILITY STUDY FOR NEUROVASCULAR BUNDLE VISUALIZATION
Misop Han, Chunwoo Kim, Pierre Mozer, Shadie Badaan, Bogdan Vigaru, Felix Schäfer, Kenneth Tseng, Doru Petrisor, Bruce Trock, Dan Stoianovici
Robotics Lab, Urology Department, Johns Hopkins Medicine, Baltimore, MD

Outstanding Paper Awards:

REGIONAL HYPOTHERMIA DURING ROBOTIC RADICAL PROSTATECTOMY USING AN ENDORECTAL COOLING BALLOON TO IMPROVE URINARY CONTINENCE: David Finley, Kathryn Osann, Douglas Skarecky, Alexandra Chang, Thomas Ahlering

ANALYSIS OF ACOUSTIC ACCESS TO THE PROSTATE THROUGH THE PERINEUM FOR NON-INVASIVE HISTOTRIPSY THERAPY: Timothy Hall, Brian Sabb, Christopher Hempel, William Roberts

DOES NEEDLE SPINNING IMPROVE TARGETING PRECISION?: Shadie Badaan, Pierre Mozer, Chunwoo Kim, Doru Petrisor, Felix Schaefer, Mohamad Allaf, Kevin Cleary, Dan Stoianovici

A NOVEL PROXIMITY-SENSING STENT TO ASSIST NON-UROLOGICAL SURGEONS WITH INTRAOPERATIVE IDENTIFICATION OF THE URETER: John Kefer, Mihir Desai, Monish Aron, Georges Pascal-Haber, Inderbir Gill

THE IMPACT OF A URETERAL STENT AND A FOLEY CATHETER ON RENAL PELVIC PRESSURES IN THE IN VIVO PORCINE MODEL: Michael Louie, Aldrin Gamboa, Hung Truong, Victor Huynh, Adam Kaplan, Lorena Andrade, Cervando Ortiz, Rachelle Lin, Elspeth McDougall, Ralph Clayman

FREE HAND 3D-TRUS PROSTATE BIOPSIES MAPPING: Pierre Mozer, Michael Baumann, Gregoire Chevreau, Vincent Daanen, Jocelyne Trocaz

FUTURE PROSPECTS IN PERCUTANEOUS ABLATIVE TARGETING: COMPARISON OF A COMPUTER-ASSISTED NAVIGATION SYSTEM AND THE ACUBOT ROBOT: Richard Pollock, Pierre Mozer, Thomas Guzzo, Jonathan Marx, Michelle Semins, Brian Matlaga, Bogdan Vigaru, Dan Stoianovici, Mohamad Allaf

MODELING AND SIMULATION FOR FLEXIBLE URETEROSCOPY: Vijay Rajagopal, Ravi Janardan, Ricardo Miyaoka, Manoj Monga, Robert Sweet

IN VITRO TEST OF AN AUTOMATED CYSTOSCOPIC PROCEDURE FOR BLADDER SURVEILLANCE: Jong Yoon, Sangtae Park, Per G. Reinhall, Eric J. Seibel

A COMPARATIVE STUDY BETWEEN NOVEL AIR-CUSHION PROBE & WHEELED PROBE FOR MIS: Dinusha Zbyszewski, Hongbin Liu, Oussama Elhage, Ben Challacombe, Prokar Dasgupta, Kaspar Althoefer, Lakmal Seneviratne

AWARDS:

Best Reviewer Awards:

Dr. Ernesto Arada

Dr. Mahesh Desai

Dr. Brian Eisner

Dr. Michael Gong

Dr. Hrishikesh Joshi

Dr. Kazumi Kamoi

Dr. Thomas Lawson

Dr. Kevin Zorn
(2007, 2008, 2008)

REVIEW COMMITTEE:

The paper review committee has been assembled by e-mail solicitation. One hundred reviewers from around the world accepted to participate. We gratefully acknowledge their contribution to the success of the meeting and thank them for taking the time to help in this process.

Ronney Abaza
Jose-Benito Abraham
Mutahar Ahmed
Joe Akornor
David Albala
Sero Andonian
Ernesto Iii Arada
Thorsten Bach
Shadie Badaan
Ketan Badani
Michael Bailey
Andre Berger
Vigaru Bogdan
Agnas BONVILAIN
Jorge A. Campos
Ben Challacombe
Ben H. Chew
Gary Chien
Philippe Cinquin
Sebastien Crouzet
Philipp Dahm
In-Cio Dal Fabbro
Carlos D'ancona
John Denstedt
Mahesh Desai
Brian Eisner
Matthew Gettman
Islam Ghoneim
Michael Gong
Georges-Pascal Haber
Nicholas Hellenthal
Thomas Herrmann
Ravi Janardan
Hrishikesh Joshi
Kazumi Kamoi
Daniel Kaplon
Mark Katz
Louis Kavoussi
Jason Kim
Surrendra B. Kolla
Amy E. Krambeck
David Kwartowitz
Dirk Lange
Thomas Lawson
Yi Chia Lin
Michael Louie
Michael Macalalag
Luiz Maciel
Andreas Melzer
Rezia Molfino
Manoj Monga
Oliver Moormann
Vladimir Mouraviev
Ayman Moussa
Pierre Mozer
Atsushi Nagai
Ricardo Natalin
Zhamshid Okhunov
Koji Okihara
David Ornstein
Cervando G. Ortiz-Vanderdys
Paulo Palma
Prabhakar Pandey
Athanasios Papatsoris
Alexandru Patriciu
Renato Pedro
Koenig Philippe
Donald Pick
Soroush Rais-Bahrami
Koon Ho Rha
William Roberts
Luiz Santos
Felix Schafer
Bradley Schwartz
Yunhe Shen
Aboseif Sherif
Bruce Shingleton
Mathew Sorenson
Petross Sountoulidis
Massimiliano Spaliviero
Robert Stein
Dan Stoianovici
Kazuo Suzuki
Robert Sweet
Joachim Thueroff
Matvey Tsivian
Chung-Jing Wang
Chung Cheng Wang
Graham Watson
Jeffery Wheat
Wesley White
James C. Williams
Anne B Wong
Ronald Xu
Jeff Xu
Daniel Yachia
W. Jong Yoon
Yingchun Zhang
Nan Zhang
Kevin Zorn

Special thanks to **Dr. Thomas Lawson** for his contributions to the review process and help with formatting and editing this program.